THE
PHYSICAL REVIEW
A Journal of Experimental and Theoretical Physics
VOL. 45, NO. 3 FEBRUARY 1, 1934 SECOND SERIES

The Three Types of Cosmic-Ray Fluctuations and Their Significance

ROBERT A. MILLIKAN, CARL D. ANDERSON AND H. VICTOR NEHER, *Norman Bridge Laboratory of Physics, California Institute of Technology*

(Received December 19, 1933)

A theory of cosmic-ray bursts is advanced with which the energy released in them is assumed to come not from the cosmic-rays themselves but from the battery which charges the electroscope. These bursts then represent, according to this theory, instrumental accidents which must be eliminated before the remaining fluctuations can be interpreted. The discovery that the remainder of the ionization observed in a cosmic-ray electroscope is due wholly to positrons and negatrons shooting through the chamber makes it possible to compute the fluctuations to be expected from a random distribution of these electron shots. The observed fluctuations, after the elimination of bursts, are found to be somewhat larger than the fluctuations thus computed. From the amount of this excess the percentage of cosmic-ray "showers" (two or more associated tracks) can be computed and is found by Evans and Neher to be in general agreement with the number directly observed in cloud-chamber experiments.

FOR the past six years, Millikan has been accumulating a large amount of data on cosmic-ray fluctuations as revealed by measurements made at high and low altitudes with a spherical electroscope 15 cm in diameter and about 1600 cc in capacity, visually observed, and Millikan and Neher have during the past two years used in similar observations a similar self-recording instrument, the records of which are now capable of statistical study.

However, a knowledge of the mechanism by which the ions are produced in such an electroscope has been necessary before an intelligent analysis of the accumulated data could be made. The first step in this knowledge was taken when in the fall of 1931 Bowen and Millikan[1] proved that in the case of cosmic rays, precisely as in the case of gamma-rays, the immediate agents that do practically all the ionizing are high energy electrons or beta-rays, since otherwise the parallelism which both they and Hoffmann had found to exist between cosmic rays and gamma-rays as a function of pressure was not to be expected.

But, the discovery of the free positive electron or positron by Anderson and the later proof, through the use of the Pasadena high energy measuring apparatus, that the positive particles that appear in a cosmic-ray cloud chamber are practically always positrons, still further simplifies the treatment of cosmic-ray fluctuations. For these fluctuations can now be said, with much assurance, to be due to three causes which we shall describe under the names, (1) bursts, (2) showers and (3) "free-electron shots."

The cloud-chamber experiments carried out at the Norman Bridge Laboratory have now shown that about 88 percent of all the cosmic-ray photographs taken reveal single "electron shots," 10 percent more show double electron shots, or pairs, while the other 2 percent consist of more complicated multiple tracks.

If all of the ionization were due to single elec-

[1] R. A. Millikan and I. S. Bowen, Nature, October 3, 1931; see also R. A. Millikan, Phys. Rev. **39**, 397 (1932).

tron shots, positrons or negatrons, the problem of fluctuations could be treated with much assurance and certainty by the Poisson-Bateman theory of random fluctuations in accordance with which if t is the duration of an observation and λ the average rate of appearance of ions in such an interval, so that λt is the average number of ions formed, then the probability P_l that l ions instead of λt ions will appear in that interval is given by:

$$P_l = (\lambda t)^l e^{-\lambda t}/l!$$

Treating the great mass of data which we now have reveals the fact that the observed fluctuations are somewhat larger than those thus computed and this, of course, means that other causes of fluctuations are superposed upon that of the single electron shots since each associated pair of tracks is the equivalent of a single track of double the ionizing power, and such bunching of the ionization must obviously increase the chance of divergence from the mean of the ionization produced by completely randomly distributed shots.

But, there is a further cause of departure from this mean. It is found in a phenomenon first noticed by Hoffmann, and usually known as "Hoffmann bursts." When the visible method of observation is used, one occasionally finds that the total discharge obtained during a period of, say, six hours is perhaps five or even six percent larger than the mean although more than 95 percent of the six hour observations fall within less than 2 percent of the mean; and, when the self-recording method is used the inclined line, the slope of which represents the rate of discharge, occasionally shows a sudden displacement which may correspond to a very sudden loss of charge of the electroscope which in extreme cases indicates the instantaneous loss of as much as a sixth, indeed in one instance a half, of the total charge of the electroscope. Such bursts occur in an electroscope of 15 cm diameter, shielded by 10 cm of lead, not oftener than two or three times a day at sea level, but on Pike's Peak, where the rate of discharge is three times as great, we have sometimes found them occurring three or even four times as frequently, They are found to occur very, very rarely when the electroscope is unshielded, but when it is surrounded with a lead shield 10 cm thick, their frequency is multiplied at least ten times by the shield.

This behavior clearly indicates that these bursts are in some way *conditioned* by the aforementioned showers. If the surrounding matter in which the incoming photons can produce showers is condensed about the electroscope, the center from which a shower starts is, on the average, brought close enough to the electroscope so that from the mere geometry of the situation two or more—sometimes many—of the elements of a shower can enter the electroscope, but if the matter from some point in which the shower starts is spread out to a remote distance from the electroscope, most of the elements of the shower will, or course, escape the electroscope. Reasoning in this way as to the distance from the electroscope of the point within the lead shield from which the showers must start, and assuming that the whole observed ionization within the electroscope is due immediately to the shower itself, Steinke[2] has computed that the total ionization produced in the lead on the way to the electroscope, plus that within the electroscope itself, is so great that the photon, which started off the shower, must have been endowed with an energy of 10^{11} or 10^{12} volts. The fact that no energies greater than about one-hundredth of these amounts have ever been found in our cloud-chamber work, indicates to us that Steinke's assumed mechanism of burst-formation cannot be the correct one.

But, there is a second mode of approach to the problem which fortifies this conclusion. The number of pairs of ions produced by a single cosmic-ray electron-shot traversing the average path which it must traverse in going through our electroscope is very close to 5000. This figure is obtained simply by multiplying the number of ions per cm of path, directly counted by Anderson and Neddermeyer at atmospheric pressure, namely 35, by the length of the average path, namely 10 cm, by the observed multiplying factor, namely 14, of our electroscope when the pressure within it has been raised to 30 atmospheres of air. But, we observed on Pike's Peak in the summer of 1932 one burst which corresponded in ion-pairs produced within our elec-

[2] E. G. Steinke and H. Schindler, Naturwiss. **20**, 491 (1932).

troscope to 25,000,000 and very recently in an airplane flight to a height of 21,000 feet we got, when using a 15 cm iron shield, another burst corresponding to 75,000,000 ion-pairs. Dividing 75,000,000 by 5000 shows that to account in Steinke's way for this burst requires that the electroscope be traversed at a single instant by 15,000 electron shots. But, not one-hundredth of this number has ever been observed, nor indeed could any such number be produced by the explosion of any known nucleus since even the uranium nucleus contains but 384 electrons, positive and negative all told. Furthermore, even in dense matter the distance between nuclei is so great relatively to their size that the collaboration of many nuclei is scarcely to be considered.

We think, therefore, that by far the simplest explanation of these bursts is found in the assumption that the energy released in the electroscope by them comes, not from the cosmic rays themselves, but rather from the energy supplied by the battery in charging the electroscope. This amounts in our case to 5 billion (10^9) volt-electrons. The energy released in the largest burst we have ever observed—the one that released the 75,000,000 ion-pairs—is about one-half of this amount. The battery energy is, therefore, amply sufficient to produce the quantity of ions involved.

The mechanism which we suggest to account for these bursts is the following: a cosmic-ray shower produces in one side of the electroscope a large number of ions. This swarm of ions by its motion toward the central electrode causes a concentration of the field near this electrode exactly similar to the concentration of field in the cathode dark space in an ordinary discharge tube. An incipient arc is thus formed (i.e., a multiplication of ions by collision) which discharges a considerable portion of the charge on the electroscope before the field falls so low as to stop further ionization by collision. This theory, then, makes these bursts merely "instrumental accidents" which have little to teach about the mechanism of the ionizing action of the cosmic rays themselves.

Accordingly, for the study of fluctuations, we simply discard all those very infrequent records of electroscope discharge-rates in which such bursts appear, and compute the fluctuations from the slopes of all the discharge-rate lines which reveal only an essentially continuous rate of discharge without noticeable sudden breaks. The fluctuations so obtained are a little larger than those computed from the Poisson-Bateman law and because of this difference yield some indication of the number of showers which must be superposed upon the electron shots to account for them. These indications are in pretty good agreement with the percentage of showers found directly in Anderson's and Neddermyer's studies on cloud-chamber tracks. The character of this agreement is shown in the following paper by Robley Evans and H. Victor Neher.

All of the data which have made these studies possible has been obtained through the aid of funds provided by the Carnegie Corporation of New York, administered through the Carnegie Institution of Washington.

The Nature of Statistical Fluctuations with Applications to Cosmic Rays

ROBLEY D. EVANS,* *Department of Physics, University of California, Berkeley,*
AND
H. VICTOR NEHER, *Norman Bridge Laboratory, California Institute of Technology, Pasadena*

(Received November 27, 1933)

I. The square of the mean deviation D of the combined effect of several random processes releasing an average of $x, y, z \cdots$ particles per unit time and producing $a, b, c \cdots$ ion pairs, respectively, per particle, is $D^2=a^2x+b^2y+c^2z+\cdots$, regardless of whether the separate effects are added or subtracted by the experimental arrangement. For tube-counters, point-counters, scintillation screens and particle counting chambers, $a=b=c=1$; for ionization chambers $a, b, c \cdots$ are unequal. II. From the standpoint of statistical fluctuations, the use of two identical instruments in a differential circuit is inferior to the use of a single instrument. III. The natural observational limit for the measurement of x particles against a background of y particles is $x=0.67(y)^{\frac{1}{2}}$. IV. The statistical fluctuations in the ionization produced by cosmic rays in a spherical ionization chamber are treated rigorously and the fluctuations due to heterogeneity of range and to showers are derived. V. Application to existing data shows that the showers observed in cloud-chamber photographs of the cosmic radiation are also present in the ionization chamber in about the same frequency and multiplicity as indicated by the cloud-chamber results. The tube-counter investigations of the cosmic-ray flux are also in agreement with the deductions from the statistical fluctuations in the ionization chamber. An upper limit of 70 ± 10 ion pairs per cm in air at 1 atmosphere is set for the *total* ionization along the path of an individual cosmic-ray secondary. The size and the relative frequency of occurrence of showers is appreciably greater at 14,700 feet elevation than at sea level. These showers are quite distinct from the ionization bursts or Stösse observed by Hoffmann, Steinke and others.

INTRODUCTION

MANY physical processes which appear to proceed at a continuous and uniform rate are shown to be discontinuous and spasmodic when examined with very sensitive apparatus. Thus the emission of α-particles from radioactive bodies has long been known to consist of the emission of individual particles randomly distributed in time. Ionization by x-rays, disintegration of matter by α-particles, protons, deutons or neutrons, and the flux of cosmic-ray secondaries are similar processes which exhibit an apparently constant rate when large effects are measured over long time intervals, but show measurable fluctuations from the average rate when feeble sources or short time intervals are employed.

The mathematical theory of these fluctuations for the simple case of α-particle emission has been given by H. Bateman[1] and others, and discontinuities in light emission and x-ray absorption have been considered by N. Campbell[2] and by Colm-Peters and Lange.[3] The theory of statistical fluctuations is here generalized, after which several modern physical problems are treated as special cases of the general theory.

THE GENERAL EQUATION

We shall assume that the physical process involved takes place at an average rate which is constant. This is true for the flux of cosmic-ray particles and for many other processes. If the emission of particles from radioactive bodies is considered, the decay of the parent substance must be negligible during the time of observation, otherwise the probability of emission and the average rate of emission would not remain constant. If λ is the average rate of appearance of particles in the measuring instrument and t is the length of the unit of time over which the individual observations are made, then λt is the average number of particles measured in a single

* National Research Fellow.

[1] H. Bateman, Phil. Mag. **20**, 704 (1910). E. v. Schweidler, Premier Congres intern. de Radiologie, Liege 1905. K. W. F. Kohlrausch, Ergebnisse der exakten Naturwissenschaften **5**, 192 (1926).

[2] N. Campbell, Proc. Camb. Phil. Soc. **15**, 301 (1909).

[3] Colm-Peters and Lange, Ann. d. Physik **4**, 453 (1930).

observation. Call this average value x. Then the probability, P_l, that l particles, instead of x particles, will appear in a single observation period is

$$P_l = x^l e^{-x}/l! \ , \tag{1}$$

as is proved in detail by Bateman.[1]

If each particle produces a specific effect, a, (e.g., a ion pairs per particle) then the variation, v_l, from the average value ax is $a(l-x)$ when l particles appear. Employing the definition of Bessel and Gauss, we speak of the mean deviation, D, which is the square root of the most probable value of the square of the deviation. The most probable value being the arithmetic average of a large number, n, of observations, we have

$$D^2 = \sum v_l^2/n. \tag{2}$$

In the general experimental case, there will be several processes acting simultaneously on the measuring apparatus. Thus, in ionization chamber measurements of α-particles, there will also be present a background ionization due to cosmic-ray secondaries and to α-particles emitted from radioactive contamination in the walls of the apparatus. The statistical fluctuations observed in the apparatus will therefore be due to the joint action of the fluctuations from several independent and individually random processes. Let these independent processes produce an average of $x, y, z, \cdots$, particles, respectively, in the unit of time chosen. Let each particle from the first process produce a specific effect a and each particle from the other processes specific effects $b, c, \cdots$, respectively, measured in the same units. In any single observation each process will produce $l, m, n, \cdots$, particles, instead of the average value $x, y, z, \cdots$, particles. Then the net variation due to the joint action of the separate processes will be $a(l-x)+b(m-y)+c(n-z)+\cdots$, if the effects from the separate processes are additive, as they are in the single ionization chamber experiment considered above. The probability that $l, m, n, \cdots$, particles will be produced by the several independent processes is $P_l P_m P_n \cdots = (x^l y^m z^n \cdots / l!m!n! \cdots) e^{-x-y-z-\cdots}$, hence the mean deviation is given by

$$D^2 = \sum_{l=0}^{\infty} \sum_{m=0}^{\infty} \sum_{n=0}^{\infty} \cdots \frac{x^l y^m z^n \cdots}{l!m!n! \cdots} e^{-x-y-z-\cdots} \times [a(l-x)+b(m-y)+c(n-z)+\cdots]^2. \tag{3}$$

Upon expansion, Eq. (3) reduces to

$$D^2 = a^2 x + b^2 y + c^2 z + \cdots, \tag{4}$$

which is the general equation for the statistical fluctuations due to the joint action of any number of independent processes.

If the apparatus arrangement involves the instrumental subtraction of one effect from another, as in differential ionization chamber measurements, the signs between the parentheses in the final bracket of Eq. (3) change but Eq. (4) remains unaltered. Eq. (4) is therefore general for any number of processes and for any arrangement of the apparatus.

In any finite series of observations we can never actually measure the exact average rate of appearance of particles. We can only find its most probable value, which is the arithmetic average obtained from a large number n of independent observations. The probable variation r of a single observation, i.e., that variation which is equally as likely to be exceeded by the observed variation v as not, is

$$r = 0.6745(\sum v^2/(n-1))^{\frac{1}{2}}. \tag{5}$$

Combining Eqs. (2) and (5) we find D reated to r by

$$r = 0.6745D(n/(n-1))^{\frac{1}{2}}. \tag{6}$$

The summation involved in Eq. (3) is equivalent to making an infinite number of observations, hence when applied to Eq. (4), Eq. (6) becomes

$$r = 0.6745D. \tag{7}$$

The Poisson law of Eq. (1) gives an asymmetric distribution about the average value x, favoring values of l which are less than x. The asymmetry is the order of 10 to 5 percent for $x = 10$ to 100 and vanishes as $x \to \infty$, when the distribution becomes essentially Gaussian. The asymmetry for $x \geq 10$ does not invalidate Eq. (7).

Differential Circuits

In the detection of minute quantities of radioactive substances with ionization chambers,[4] the detection of mitogenetic rays with tube-counters[5] and in many similar problems, observers have used two instruments in a differential hook-up, thus cancelling out the cosmic-ray background by means of a dummy chamber or counter. It has been claimed by some experimenters that a differential circuit also cancels out the statistical fluctuations in the background, the magnitude of which usually imposes the limit of precision on the measurements. Actually, when the background is received independently by two identical instruments, the resulting statistical variation is $2^{\frac{1}{2}}$ times the variation for a single instrument, regardless of whether the two instruments are connected to oppose or to assist each other. This can be seen from Eq. (4), where, for strictly differential circuits, $a=b$ and $x=y$ and these refer to the background in the two identical instruments, while c and z refer to the effect being studied.

Whether a single instrument or a differential circuit employing two such instruments is used, a control, or background test, must be made, independent of the actual run which consists of the background plus the effect being measured. In taking the difference between these two readings as a measure of the effect, the statistical fluctuation in the background enters both measurements. Since the statistical fluctuation of the background is $2^{\frac{1}{2}}$ times larger in the differential circuit than in the single circuit, the uncertainty of measurement, which arises from these fluctuations, is greater when the differential circuit is used. Thus if the average background in a single instrument is x particles during the time interval employed, the value of the background actually observed will be $x\pm0.67\ (x)^{\frac{1}{2}}$, by Eqs. (4) and (7). Similarly, the background in a differential circuit with two such instruments will be $0\pm0.67\ (2x)^{\frac{1}{2}}$. When an effect to be measured, consisting of y particles, is added, the reading on the single instrument will be $x+y\pm0.67\ (x+y)^{\frac{1}{2}}$, and on the differential instrument $y\pm0.67\ (2x+y)^{\frac{1}{2}}$. Now in subtracting the background from these readings, in order to obtain the value of the effect y, we have for the single instrument,

$$[x+y\pm0.67\ (x+y)^{\frac{1}{2}}]-[x\pm0.67\ (x)^{\frac{1}{2}}]$$
$$=y\pm0.67\ (2x+y)^{\frac{1}{2}},$$

and for the differential instrument

$$[y\pm0.67\ (2x+y)^{\frac{1}{2}}]-[0\pm0.67\ (2x)^{\frac{1}{2}}]$$
$$=y\pm0.67\ (4x+y)^{\frac{1}{2}},$$

by the principles of the propagation of errors. Thus the uncertainty is greater in the differential circuit by an amount which depends on the ratio of y to x. If $y\gg x$, the two apparatus arrangements have equal merits but if $y\ll x$, as is the case near the observational limit, then the fluctuations are $2^{\frac{1}{2}}$ times larger in the differential circuit. Differential circuits, though suffering from this defect, do possess advantages which at times outweigh this disadvantage. Their effectiveness in spreading a differential effect over a large scale, thus permitting more accurate readings, and in balancing out battery variations, transient local radiations and other systematic errors often justifies their use, even near the natural observational limit.

The Natural Observational Limit

Many physical measurements involve the detection of some effect over and above a background or "zero effect." When the effect to be measured becomes so small that it is just equal to the probable statistical variation in the background the observer cannot establish its presence and the natural observational limit is reached.[6] If the small effect being observed is the emission of x particles per unit time, and each particle produces a specific effect a (e.g., a ion pairs per particle) while the background is due to y particles of specific effect, b, z particles of specific effect, c, etc., then the observational limit is defined by

$$r=ax=0.67\ D=0.67\ (a^2x+b^2y+c^2z+\cdots)^{\frac{1}{2}} \quad (8)$$

and if* $a^2\ll4\ (b^2y+c^2z+\cdots)/(0.67)^2$, the observational limit is

[4] Halledauer, Akad. Wiss., Wien **134**, 39 (1925); Paneth and Koech, Zeits. f. physik. Chemie, Bodenstein-Festband, 145 (1931); Evans, Rev. Sci. Inst. **4**, 223 (1933).

[5] Siebert and Seffert, Naturwiss. **21**, 193 (1933).

[6] Evans, Rev. Sci. Inst. **4**, 229 (1933).

* This means also that $4x\gg1$.

$$ax = 0.67\ (b^2y + c^2z + \cdots)^{\frac{1}{2}}. \qquad (9)$$

Eq. (9) applies to all ionization and counting measurements. When tube-counters, point-counters, scintillation screens or particle-counting chambers are used, $a = b = c = 1$.

The common case of counting x particles per unit time against a background of y particles per unit time has the observational limit $x = 0.67\ (y)^{\frac{1}{2}}$. Substituting appropriate values for x, we find, for example, in α-ray emanation-measurements of minute quantities of radon, that if y is the number of α-particles emitted per hour from the walls of the ionization chamber, then the natural observational limit in grams of radium or curies of radon is $0.36 \times 10^{-14}\ (y)^{\frac{1}{2}}$ for a one hour reading. Since an ordinary brass cylindrical ionization chamber 15 cm high and 15 cm in diameter emits about 200 α-particles per hour into the chamber, such a typical chamber has a practical natural observational limit of 5.1×10^{-14} g Ra. If y is reduced to 50, one-fourth of its usual value, the limit is 2.5×10^{-14} g Ra for a one hour reading. The radon and decay products from 10^{-14} g Ra send 2.5 α-particles per hour into an ionization chamber. It is therefore difficult to substantiate the suggestion that 10^{-14} g Ra can be measured with certainty in a series of ten 7 minute readings, as has been asserted by Halledauer.[4]

Precision in measurements approaching the natural observational limit imposed by the statistical variations of the background can be improved only by lengthening the time of observation or by decreasing the absolute magnitude of the background. Methods for doing this in ionization chambers have been described elsewhere.[6] Lead shields may be used to absorb local γ-rays, electrometers may be evacuated, lampblack may be painted on the inside wall of the ionization chamber to absorb wall α-rays or a Hoffmann net may be used for the same purpose.

In the use of tube-counters there is another method available. This consists of protecting the counter on which the active agent acts, by surrounding it with other counters which will respond to coincidences between the central counter and these guard counters. In this way the background of long range cosmic-ray secondaries in the central counter may be cancelled exactly, particle by particle, and the observational limit for any feeble effect which is superposed on the background in the central counter may be greatly decreased. γ- or x-ray background should be eliminated by absorption in lead which is free from its isotope, Ra D. Either a pentode or triode vacuum tube amplifiers connected in a Y circuit may be used, the output being arranged to record only those events in the central counter which are not coincident with counts in the outside guard counters. Thus a cosmic-ray secondary entering one of the guard counters, or passing through both a guard counter and the central counter, will not be recorded. Since nearly all the cosmic-ray secondaries traversing the central counter will have originated outside it and will, therefore, have traversed a guard counter, nearly all the background due to cosmic rays in the central counter can be eliminated.

Cosmic Rays in Spherical Ionization Chambers

Cosmic-ray secondaries traversing an ionization chamber have various effective path lengths, depending upon what part of the chamber they traverse. This heterogeneity of effective range introduces a term in the equations describing the fluctuations. Since the ionization j, per cm of path, is nearly the same for all the secondaries, the fluctuations due to heterogeneity of range may be computed from Eq. (4) and the geometry of the ionization chamber. Eq. (4) also will describe the fluctuations due to the occurrence of showers of associated secondaries in the ionization chamber.

For purposes of geometrical analysis, we consider only particles moving in one direction. Where the total number of particles is large, this involves no loss in generality. If there are n_1 particles having a track length h_1 and hence a total ionization $A_1 (= h_1 j)$ and n_2 particles with ionization A_2, etc., then the total ionization Q, and the average value of the square of the mean deviation, $D^2 \equiv (\delta Q)^2$, are given by:

$$Q = A_1 n_1 + A_2 n_2 + \cdots \equiv A \sum n = A(N\pi R^2), \qquad (10)$$

$$(\delta Q)^2 = A_1^2 n_1 + A_2^2 n_2 + \cdots$$

$$\equiv \omega A^2 \sum n = \omega A^2 (N\pi R^2), \qquad (11)$$

where A is the average number of ion pairs per particle, N is the number of particles per cm² in the time interval t, R is the radius of the ionization chamber and ω is a numerical coefficient which we shall now evaluate for the case of the spherical ionization chamber. In Fig. 1 consider

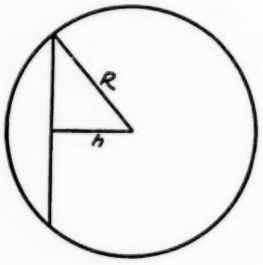

FIG. 1.

the particles which pass vertically through the spherical chamber; h is the perpendicular distance from the path of such a particle to the center of the chamber. The length of the path of such a patricle is $2(R^2-h^2)^{\frac{1}{2}}$, and its ionization is $2j(R^2-h^2)^{\frac{1}{2}}$, while there are $N2\pi hdh$ such particles between h and $h+dh$ from the center. Eqs. (10) and (11) then become:

$$Q=\int_0^R 2j(R^2-h^2)^{\frac{1}{2}}N2\pi hdh=4\pi jNR^3/3, \quad (12)$$

$$(\delta Q)^2=\int_0^R 4j^2(R^2-h^2)N2\pi hdh=2\pi j^2NR^4. \quad (13)$$

Combining these results with the final terms of Eqs. (10) and (11) we find, for spherical ionization chambers:

$$A=4jR/3, \quad (14)$$

$$\omega=9/8. \quad (15)$$

Cloud-chamber photographs and the new theories of electron pair production have disclosed the association of double, triple and higher multiple groups of cosmic-ray tracks in showers. If x_1 is the total number of single cosmic-ray secondaries traversing the chamber in the unit time interval t, and a_1 the average total ionization per track $(=4jR/3)$, x_2 the number of associated pairs of tracks, and a_2 the ionization produced by the average pair $(=2a_1)$, while $x_3, \cdots x_n$ and $a_3 \cdots a_n$ are the analogous quantities for higher multiple tracks up to showers of n tracks, then

$$\begin{aligned} Q&=a_1x_1+a_2x_2+a_3x_3+\cdots+a_nx_n \\ &=a_1x_1\left(1+\frac{a_2x_2}{a_1x_1}+\frac{a_3x_3}{a_1x_1}+\cdots+\frac{a_nx_n}{a_1x_1}\right) \\ &=a_1x_1(1+2r_2+3r_3+\cdots+nr_n) \\ &\equiv a_1x_1\sum nr_n, \end{aligned} \quad (16)$$

$$\begin{aligned} (\delta Q)^2&=\omega(a_1^2x_1+a_2^2x_2+a_3^2x_3+\cdots+a_n^2x_n) \\ &=(9/8)a_1^2x_1(1+4r_2+9r_3+\cdots+n^2r_n) \\ &\equiv(9/8)a_1^2x_1\sum n^2r_n, \end{aligned} \quad (17)$$

where $r_n \equiv x_n/x_1$, and is the relative frequency of occurrence of showers of n tracks with respect to single tracks. Combining Eqs. (14), (16) and (17), we obtain

$$j\cdot\sum n^2r_n/\sum nr_n=(2/3R)\cdot(\delta Q)^2/Q. \quad (18)$$

If N_1 is the number of single tracks per cm² per unit time t, an ideal tube counter, which would record each single particle and each shower of n particles as one count each, would register N counts per cm² per unit time, where

$$N=N_1\sum r_n=x_1\sum r_n/\pi R^2. \quad (19)$$

Combining Eqs. (14), (16) and (19), we obtain

$$j\cdot N\cdot\sum nr_n/\sum r_n=3Q/4\pi R^3. \quad (20)$$

The terms $\sum n^2r_n/\sum nr_n$ and $\sum nr_n/\sum r_n$ occurring in the final Eqs. (18) and (20) are directly determined by the frequency of occurrence r_n and the multiplicity n of the showers of associated cosmic-ray secondaries such as would be observed in a cloud chamber having the same geometry as the ionization chamber. The summations $\sum n^2r_n$, $\sum nr_n$ and $\sum r_n$ and their ratios in Eqs. (18) and (20) are each unity when no multiple tracks exist and each exceeds unity when showers are present, $\sum n^2r_n/\sum nr_n$ increasing more rapidly than $\sum nr_n/\sum r_n$.

COMPARISON WITH AVAILABLE COSMIC-RAY DATA

Eqs. (18) and (20) permit a direct test of the consistency of measurements made with the spherical ionization chamber, cloud chamber and tube-counter. The recent discovery by Anderson of the positive electron and of the production by cosmic radiation of positive and negative elec-

trons in pairs suggests that many, if not all, of the single cosmic-ray tracks observed in cloud-chamber photographs are in reality isolated branches of showers occurring near the apparatus. The recent observations of Rossi and others indicate that elements of high atomic number are more efficient in the production of large showers than those of low atomic number. Therefore, for the rigorous application of Eqs. (18) and (20) the geometry and shielding of the ionization chamber, cloud chamber and tube-counter should be identical. No such apparatus exist, but, bearing in mind these limitations, the application of Eqs. (18) and (20) to existing data does yield preliminary results of some interest.

The frequency r_n and multiplicity n of showers in cylindrical cloud chambers have been studied by several observers. Quantitative agreement is poor because the large showers are quite rare and enough photographs to give a good statistical average have not yet been taken. Where the cloud chamber is expanded by a tube-counter coincidence arrangement, as in Blackett and Occhialini's[7] apparatus and in a recent modification of the Anderson-Millikan arrangement for the measurement of particle energies up to 3×10^9 volts, the natural distribution of multiple showers is distorted, since even a small shower in the apparatus has a much greater chance of setting off the coincident counters than has an isolated single track. The number of photographs of tracks and the corresponding values of the summation ratios for Eqs. (18) and (20), computed from the occurrence of multiple tracks in randomly expanded cloud chambers, are given in Table I.

TABLE I. *Distribution of showers in cloud-chamber observations.*

	Number of Photographs							$\frac{\Sigma n^2 r_n}{\Sigma n r_n}$	$\frac{\Sigma n r_n}{\Sigma r_n}$
n	1	2	3	4	5	6–10	over 10		
Anderson[8]	708	82	7	7	3	7	1	1.92	1.23
Locher[9]	148	14	5	0	1	0	0	1.40	1.17
Skobelzyn[10]	23	3	1	0	0	0	0	1.51	1.15

[7] Blackett and Occhialini, Proc. Roy. Soc. **A139**, 699 (1933).

[8] Anderson, Phys. Rev. **44**, 406 (1933).

[9] Locher, Phys. Rev. **39**, 883 (1932).

[10] Skobelzyn, Zeits. f. Physik **54**, 686 (1929).

The number of counts per cm² per minute in a tube-counter near sea level is rather uncertain because of the difficulty of eliminating local γ-rays and radioactive contamination in the counter but it is near unity. Blackett and Occhialini[7] suggest 1.5 counts per cm² per minute, Bothe and Kölhorster[11] found about 1.0, Kölhorster and Tuwim[12] and Mott-Smith and Locher[13] found less than 1.0, Korff[14] finds approximately 1 in Pasadena. Values for the ionization j in ion pairs per cm of path in air at one atmosphere given by various observers are as follows: Skobelzyn,[10] 40 ion pairs per cm; Bothe and Kölhorster,[11] 90; Kölhorster and Tuwim,[12] 135; Messerschmidt,[15] 110; Locher,[16] 36; Blackett and Occhialini,[7] 80; Anderson,[8] 31 for primary ionization by drop-counts on diffuse tracks, and 120 to 140 from energy loss in lead. Theoretical considerations by Carlson and Oppenheimer[17] and by Heisenberg[18] suggest that the primary ionization by high energy electrons, such as cosmic-ray secondaries, should not exceed 50 to 60 ion pairs per cm in standard air unless the energy of the electron is far above 10^9 electron-volts.

The continuous photographic records of cosmic-ray intensity now being obtained by R. A. Millikan and H. V. Neher provide more suitable data for application to Eqs. (18) and (20) than the data of Messerschmidt[15] because of the higher charge sensitivity of their electroscopes. The records are conveniently divided into 15 minute intervals and these exhibit statistical variations of the order of 2 percent at sea level. Series of 66 quarter hours at Pasadena and of 55 quarter hours at 14,700 feet in the Peruvian Andes have been analyzed as typical examples of the present method. The electroscope is 15 cm in diameter, contains air at 30 atmospheres and is shielded from local radiation by 4 inches of lead. The observed ionization Q and the statistical variations $(\delta Q)^2$ about the mean value were corrected for lack of saturation of the ion-current, for ionization

[11] Bothe and Kölhorster, Zeits. f. Physik **56**, 751 (1929).

[12] Kölhorster and Tuwim, Zeits. f. Physik **73**, 130 (1931).

[13] Mott-Smith and Locher, Phys. Rev. **38**, 1399 (1931).

[14] Korff, personal communication, June 1933.

[15] Messerschmidt, Zeits. f. Physik **78**, 668 (1932).

[16] Locher, Phys. Rev. **39**, 883 (1932).

[17] Carlson and Oppenheimer, Phys. Rev. **41**, 763 (1932).

[18] Heisenberg, Ann. d. Physik **13**, 430 (1932).

bursts or Stösse, for the electroscope's "zero," due principally to α-particles from the walls, and for the observational uncertainty in reading the photographs. The uncertainty in each of these corrections is small compared with the statistical variations in cosmic-ray intensity. The usual barometer and temperature corrections were made; these exert no influence on the statistical variations. Comparison of several short series of observations shows that $(\delta Q)^2$ can be obtained to within ± 15 percent, which is better than the present agreement in the various values of j, N and $\sum n^2 r_n / \sum n r_n$, as shown above. Tables II and III contain the results of the analysis of the two sets of data mentioned. Q and $(\delta Q)^2/Q$ are in terms of total ion pairs formed in the electroscope per 15 minutes in air at 30 atmospheres; j is ion pairs per cm in air at 1 atmosphere; N is effective counts per cm^2 per minute, as defined by Eq. (19).

TABLE II. *The distribution of showers in the electroscope.*

	$\frac{(\delta Q)^2}{Q}$ at 30 atm.	$j \cdot \frac{\sum n^2 r_n}{\sum n r_n}$ at 1 atm.	$\frac{\sum n^2 r_n}{\sum n r_n}$ $j=50$	$j=80$	$j=100$	$j=150$
Pasadena	4.38×10^4	130.	2.60	1.63	1.30	0.87
14,700 ft. elev.	7.75×10^4	230.	4.60	2.88	2.30	1.53

TABLE III. *The flux of cosmic-ray secondaries.*

	Q at 30 atm.	N $j=50$	$j=80$	$j=100$	$j=150$
Pasadena	8.43×10^7	1.7	1.1	0.86	0.57
14,700 ft. elev.	20.8×10^7	4.2	2.6	2.1	1.4

Eq. (18) involves two unknowns, j and $\sum n^2 r_n / \sum n r_n$ and only their product can be evaluated from the electroscope data. Table II therefore shows the distribution of showers in the electroscope when j is given values ranging from 50 to 150 ion pairs per cm. These shower values may be compared with Anderson's Pasadena values shown in Table I, while remembering that his cylindrical cloud chamber is 16.5 cm in diameter and 4 cm deep and is shielded[8] principally by copper and iron, whereas Millikan and Neher's spherical electroscope is 15 cm in diameter and is shielded by 10 cm lead. Because of shielding and geometrical differences it is therefore to be expected that showers would be more abundant in the electroscope. The data therefore dictate an upper limit of 70 ion pairs for the *total* ionization per cm along a cosmic-ray secondary track in air at 1 atmosphere and suggest that the actual value is appreciably lower, a conclusion which agrees with Anderson's[8] latest observations and with theoretical considerations.[17, 18]

The large statistical fluctuations in the electroscope at 14,700 feet elevation demand about a twofold increase in the shower abundance expression, $\sum n^2 r_n / \sum n r_n$, assuming that j is not appreciably changed. The softer components of the cosmic radiation, present at high altitudes, therefore appear to produce considerably larger showers of associated tracks than do the harder, sea-level components.

Eq. (20) involves three unknowns, j, N, and $\sum n r_n / \sum r_n$, their product being given by the electroscope data. Table III shows the values for N, the number of counts per cm^2 per minute, which are obtained by assuming Anderson's value for $\sum n r_n / \sum r_n$ from Table I and assigning values from 50 to 150 ion pairs per cm to j. Here again, because of geometry and shielding, the cloud-chamber value of the shower distribution term, $\sum n r_n / \sum r_n$, is undoubtedly lower than the electroscope's value and hence the upper limit of the product $j \cdot N$ is given by Table III. Comparison of the Pasadena values with the published results on N for tube-counters, summarized above, shows an upper limit of about 80 ion pairs per cm for j and suggests a somewhat lower value.

At 14,700 feet elevation the increased abundance of large showers, shown by Table II, requires an increase of the shower distribution term, $\sum n r_n / \sum r_n$, of Eq. (20). Again assuming j to be independent of altitude, Eq. (20) shows that the counting rate N for tube-counters does not rise as rapidly with increasing altitude as does the ionization Q in the electroscope. This is because the tube-counter fails to distinguish between showers and single particles.

The high and low altitude showers here considered produce much less total ionization and are entirely distinct from the ionization bursts or Stösse reported by Hoffmann, Steinke and many other observers.

The theoretical work was done by the first of the authors, the experimental work on cosmic rays by the second. The authors record their thanks to Professors H. Bateman, R. T. Birge and J. R. Oppenheimer for reading the manuscript and to Professor R. A. Millikan for permitting us to use the facilities and the data developed and accumulated by himself and his associates, through the aid of a grant made by the Carnegie Corporation of New York, administered by the Carnegie Institution of Washington, for the support of his cosmic-ray researches.

A Note on the Photographic Measurement of the Transmission of Fluorite in the Extreme Ultraviolet

EDWIN G. SCHNEIDER, *Research Laboratories of Physics, Harvard University*

(Received December 18, 1933)

The measurement of the transmission of a piece of colorless fluorite was made by photographic methods and the results are compared with those obtained with a photoelectric cell for the same crystalline plate. The wave-length range covered was between 1240 and 1600A.

THE transmission of a piece of colorless fluorite (1.9 mm thick) from Zelle in Baden was measured by using a vacuum spectrograph of the type described by T. Lyman in his book, *Spectroscopy of the Extreme Ultraviolet*. The light from a hydrogen discharge tube passed through a 0.15 mm slit, fell on a 15,000 line to the inch glass grating of one meter radius, and was recorded by a Cramer Contrast plate sensitized with a ten percent solution of Cenco Pump Oil, 11,021-C, in petroleum ether. A windlass turned by a stopcock served to move a holder carrying the fluorite in and out of the path of light without disturbing the discharge. When in position the fluorite plate was about 1.5 cm in front of the slit and about twice that distance from the end of the capillary which served as the source.

Preliminary tests showed that moderately high pressures and current densities in the discharge gave the most constant intensity and that under these conditions the variations from this part of the apparatus were quite masked by the irregularities due to the inhomogeneities in the emulsion of the plate. These inhomogeneities gave rise to discrepancies of six or seven percent between individual readings in spite of such precautions as soaking the plate in distilled water before developing, brush development and slow drying.

It was also found that the amount of scattered light in the spectrograph was almost negligible. To test this point plates of fluorite, quartz and glass were used to cut out the waves below their limits of transmission and exposures of over ten times the longest used in the experiment failed to give more than a possible trace of darkening in the regions where the light was absorbed by these filters. This showed that there was practically no light of long wave-length scattered onto the short wave end of the plate. Since there is no simple way of cutting out the longer wavelengths while allowing the shorter ones to pass into the spectrograph, it was assumed that the short wave-length light was not scattered into the long wave regions in large amounts.

The formula for the transmission T of a substance at any given wave-length is

$$T = I_1/I_2 = (t_2/t_1)^p,$$

where I_1 and t_1 are the intensity and time of exposure through the substance, and I_2 and t_2 those with the material removed from the path of light, and where either or both values of I and t are adjusted to give the same blackening of the plate for the two exposures. It is customary to keep the intensity of the source constant and to vary the time of exposure to meet these conditions.

Since this method necessitates a knowledge of the value of the exponent, p, the relationship between the intensity and time to produce a given photographic density was studied at the fluorescent wave-length of the oil, 3400–4400A, as suggested in the report of Harrison and Leighton.[1] Pieces of exposed photographic plate which had been calibrated for λ4385 by the Bureau of Standards were used to cut down the intensity of light from a mercury arc by known amounts, and comparison of the density-log exposure curves obtained by holding the time constant in

[1] G. R. Harrison and P. A. Leighton, J. O. S. A. **20**, 313 (1930).

one case and the intensity in the other showed that the value of p was 0.96 ± 0.01. Although the wave-length used for this computation was about 500A longer than that of the maximum of the oil fluorescence, the correction seems valid since wire screens as described by G. R. Harrison[2] also gave this value for λλ4046, 3650, and for λ2537 if the plate was sensitized with the oil solution. The results obtained with the wire screens were not as accurate as the value given above, however, as their transmission was not as closely determined.

The final results are embodied in Fig. 1 where the accuracy is of the order of magnitude of three percent. For the purposes of comparison the transmission obtained by W. M. Powell with a photoelectric cell for the same piece of fluorite is given.

It appears that the photographic method gives slightly higher values, but this discrepancy is small enough to be accounted for by the fact that in the measurements with the photoelectric cell the crystal was placed approximately at the focus of the grating whereas in the photographic measurements it was between the source and the slit. Under the latter circumstances, since the source more than filled the grating, slight imperfections in the polish of the fluorite tended to scatter additional light into the cone subtended by the grating at the slit.

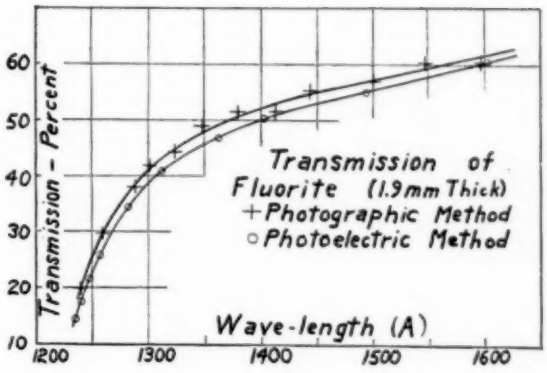

FIG. 1.

In conclusion the author wishes to express his gratitude to Professor T. Lyman for his kindness in suggesting the problem and his continued interest in its progress.

[2] G. R. Harrison, J. O. S. A. **18**, 492 (1929).

Photoelectric Measurements of the Transmission of Fluorite in the Schumann Region

W. M. POWELL, JR., *Research Laboratories of Physics, Harvard University*

(Received December 18, 1933)

The absorption of several pieces of clear, colorless fluorite from Zell in Baden was measured in the Schumann region at ten different wave-lengths between 1600 and 1235A. A grating vacuum spectrograph was used with a photoelectric cell taking the place of the photographic plate. The relationship between the intensity of the light entering the cell and the current from the cell was found to be of the form $I = \text{const.}\, i^z$. Z was found for all the wave-lengths used. All intensity ratios were determined with an inaccuracy not exceeding one percent. It has been possible to distinguish between the light absorbed by the body of the fluorite and that removed by the surfaces. Although every precaution was taken to produce a good polish, the loss of light at the surfaces was much greater than would be expected from Fresnel's law of reflection and the index of refraction of fluorite.

INTRODUCTION

IN 1901 Kreusler[1] used a hydrogen-filled photoelectric cell with a platinum cathode to measure the absorption of a number of substances including fluorite down to λ1850. Later Meyer[2] used the same apparatus to measure the absorption of ozone. In 1912 Kruger and Moeller[3] used a potassium cell filled with hydrogen or helium for the same purpose. No absorption measurements appear to have been made for wave-lengths shorter than λ1850 with a photoelectric cell.

APPARATUS

The vacuum spectrograph, Fig. 1, is used as a monochromator to throw light of different wave-lengths into the photoelectric cell L, which is stationary. The light from the large hydrogen discharge tube H enters the spectrograph through a small slit 0.025 mm wide and 2 mm long not shown in the diagram. The monochromator is focussed by moving the slit F, with a device working through the vacuum taper E, the photoelectric cell itself remaining fixed. By turning the grating C around a vertical axis with the vacuum taper A, light of any wave-length can be sent through the slit F into the photoelectric cell. The piece of fluorite under observation can be placed between slit F and the cell by turning the vacuum taper D. To prevent grease vapors from contaminating the surfaces of the piece J, the fluorite is situated inside a small cylindrical box closed at one end, except for the small slit F, 0.05 mm wide, and at the other by the large fluorite window K. The grating is made of speculum metal, has a 1-meter radius of curvature and 15,000 lines to the inch. The ruled surface measures approximately 7.8 by 3 cm.

The discharge tube H is made in two parts. The cathode is connected to a 3000 volt d.c. generator delivering one ampere through 1000 ohms resistance. The large Pyrex tube H, contains a cylindrical aluminum cathode 252 cm² in area in contact with the glass. The quartz capillary, internally coated with platinum, is waxed to the mouth of the cathode tube. The inside diameter measures 1.7 mm. Its other end is waxed to the housing of the slit through which the light enters the spectrograph. This housing also acts as the anode. All parts are cooled by a rapidly circulating stream of water.

The photoelectric cell L is made of Pyrex glass with a fluorite window waxed to one end. The cathode consists of a thin sheet of platinum. It is connected to one pair of quadrants of a Compton electrometer. The anode is connected to a battery delivering from 300 to 450 volts. The cell is filled with argon at a pressure of a few mm of mercury. A high resistance of 1.18×10^{11} ohms[4] connects the cathode with a po-

[1] H. Kreusler, Ann. d. Physik **6**, 412 (1901).
[2] Meyer, Ann. d. Physik **12**, 849 (1903).
[3] Kruger and Moeller, Phys. Zeits. **13**, 729 (1912).
[4] A. K. Brewer, Rev. Sci. Inst. **1**. 325 (1930).

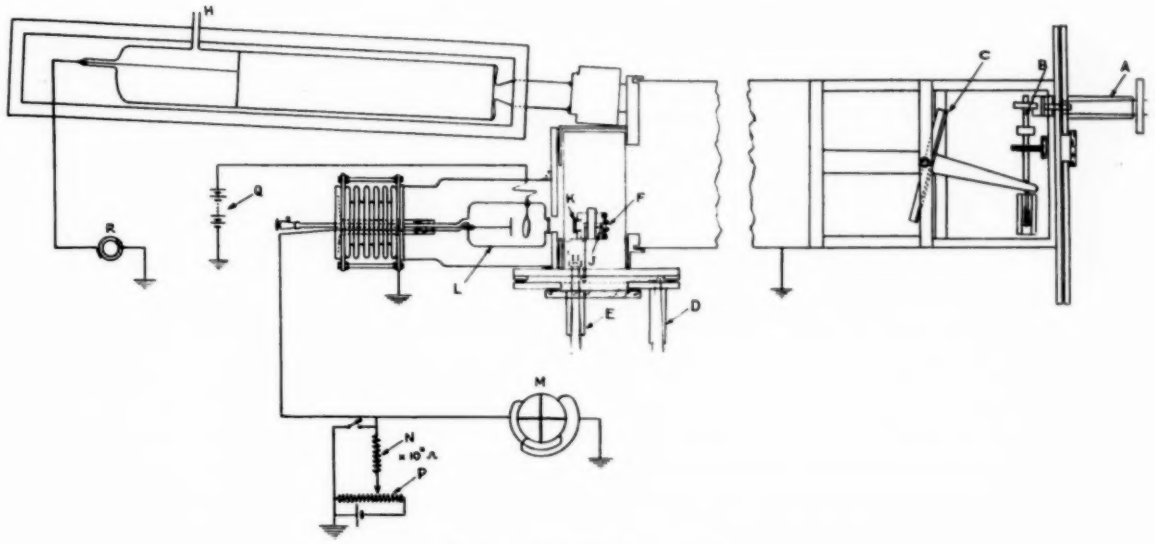

FIG. 1. Diagram of apparatus.

tentiometer P, which is adjusted so as to make the electrometer read zero potential. The difference between the potentiometer settings with and without the light entering the cell gives the change in the potential across the high resistance due to the light alone. This procedure automatically subtracts the potential due to the dark current of the cell. The voltage readings range from 0.7 to 0.08 volt. The sensitivity of the electrometer is 2480 mm/volt. The capacity of the electrical circuit is about 75 micro-microfarads.

The quantities measured are all ratios of the current i produced by the light passing through the fluorite of intensity I to the current i_0 resulting from the unobstructed beam of intensity I_0.

If we let $(1-r)$ be the fraction of the light removed by one surface, μ be the absorption coefficient and x the thickness of a piece of fluorite, then $I=I_0(1-r)^2e^{-\mu x}$. By finding the value of I/I_0 for two pieces of fluorite of different thicknesses, x_1 and x_2, it is possible to calculate the value of μ and $(1-r)$ or of r. This is true only if μ is a constant throughout the medium and if the polish on all surfaces is the same. If the polish were perfect then r should correspond to the coefficient of reflection.

It was necessary to use three abrasives consecutively to give a polish sufficiently reproducible. The first abrasive was a very fine alundum with no particles larger than 0.0025 mm in diameter.[5] A large lead lap was charged with the alundum, and very slightly dampened with kerosene. The second abrasive was a fine rouge used on a piece of silk backed by a square of plate glass. Sufficient rouge and kerosene were used to produce a shiny paste after a little polishing. Chemically precipitated fluorite powder mixed with water on silk on glass formed the third abrasive. The surface of the lap was of the consistency of ordinary flour paste.

CALIBRATION OF THE PHOTOELECTRIC CELL

The ratio i/i_0, where i is the current produced by the light traversing the fluorite of intensity I and i_0 that from the unobstructed beam of intensity I_0, was found not to be a function of the brightness of the source. Now, since I/I_0 is not a function of the brightness of the source, the current-intensity relationship must be of the form $I=\text{const.}\ i^z$. This form of relationship is a common one for gas-filled cells.[6, 7] The following experiment was performed to find the value of the exponent z.

A fluorite lens was placed between the exit slit F of the monochromator and the photoelectric

[5] J. W. Vanderwilt, *The Nature of Polished Surfaces, Abrasion instead of Amorphous Flow*, Doctor's Thesis, May, 1930. Roche Laboratory Library.

[6] G. Kortum, Phys. Zeits. **32**, 417 (1931).

[7] Steinke, Zeits. f. Physik **7**, 18 (1921).

cell L in such a position that an image of slit F was formed on the cathode of the cell. Two doors were placed between slit F and the lens, close to the lens. When both doors are open the brightness of the image on the cathode is I. With door 1 closed the brightness is I_2 and with door 2 closed I_1. With both closed, the light coming through the crack between them gives a brightness I_b. The optical arrangement makes $I=I_1+I_2-I_b$. The corresponding currents obey the law $i^z=i_1^z+i_2^z-i_b^z$. If z equals 1 then the currents will add. If they do not add they can be made to add by raising them to the correct power, z. Z was found at three wave-lengths with a probable error of 0.0003. A curve was drawn through the three points and used to interpolate to other wave-lengths. An added check was made by moving the doors perpendicular to the beam of light and testing the cell with the doors in several different positions. The values of z for any one wave-length remained the same. Then the transmission of a piece of fluorite was measured with the lens in focus and out of focus with the hope of finding some variation in z with the size of the spot of light on the cathode of the cell. No variation in the value of i/i_0 was found and therefore no variation in z.

Errors introduced through inaccuracy in the determination of the current-intensity relationship are around 0.1 percent. Those arising from fluctuations in the source, which did not change more than 10 percent during a set of readings, never amounted to more than 0.5 percent. This is due to the fact that each point is the average of 14 alternate readings with and without the fluorite in the beam.

Results

A large crystal of clear, colorless fluorite from Zell in Baden was cut up into six small pieces varying in thickness from 0.0767 to 0.4321 cm. These were measured at ten different wave-lengths. Then the thickest piece was cleft parallel to the polished surfaces and the two pieces polished and measured. The logarithm of the transmission for each wave-length was plotted against the thickness of the piece. If the transmission coefficient μ were constant throughout the body of the fluorite and the condition of all the surfaces the same, then this curve should be a straight line. However, the points did not lie on a straight line. Since the transmission of any one piece did not vary more than 1.5 percent when it was repolished and since the average of three polishings was taken in all cases the trouble must be laid to inhomogeneity in the fluorite or a variation in μ from one specimen to the other.

In the plot of the logarithm of the transmission against thickness the results for two specimens appeared to lie far off the best straight line. These results were discarded in the determination of μ and r. This proceeding was further justified by the fact that when the thickest piece was cut in half the two halves gave the same value for the transmission, for this implies that this particular specimen was comparatively free from inhomogeneity.

The best straight line through the points corresponding to the remaining specimens was determined by the method of least squares.

The high probable errors in μ and r are not due to experimental error, which is never more than 1 percent. They are an indication of the inhomogeneity to be found in a single crystal of the best Zell fluorite or fluorite chosen with the greatest possible care for homogeneity. The method of measurement of intensities is accurate to at least 0.5 percent and is much simpler to use than the photographic plate. The errors introduced by variations in polish are never more than 1.5 percent. Therefore, entire responsibility for the large probable errors rests with the variations in the absorption of the fluorite. The

Table I.

Wave-length	μ	% probable error in μ	r	% probable error in r	z
1603.3	0.488	8.4	5.91	8.70	1.0387*
1495.5	0.538	18.0	10.73	11.09	1.0360
1403.8	0.475	28.6	15.09	10.76	1.0321*
1363.4	0.509	27.0	15.91	10.31	1.0298
1312.9	0.791	16.6	16.63	9.46	1.0262
1283.4	1.127	9.7	18.15	7.17	1.0235*
1257.1	1.740	7.3	21.34	5.22	1.0211
1247.3	2.127	1.1	23.74	3.59	1.0201
1241.5	2.815	0.7	25.34	0.85	1.0195
1235.8	3.506	0.7	28.80	1.76	1.0189

* These values of z were experimentally determined. The others were found by interpolation.

fact that these high errors appear only between λ1495.5 and λ1312.9 shows that they are due to the presence of some impurity in the fluorite which absorbs strongly in that region. At shorter wave-lengths the effect is less because the absorption of the pure fluorite predominates, while at longer wave-lengths the impurity has a smaller absorption and therefore does not affect the accuracy of the results as much. (See Table I.)

The absorption coefficient μ is curve 1 in Fig. 2. The units are defined by the equation I/I_0

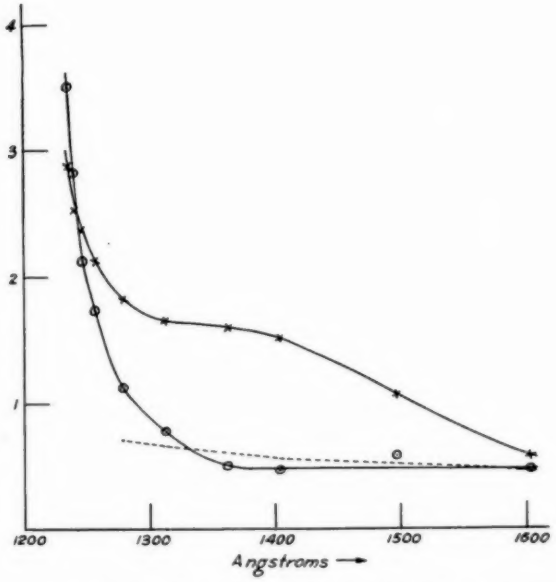

FIG. 2. Absorption and reflection coefficiency of fluorite. Curve 1 (with circle-dots) absorption coefficient. Curve 2 (with crosses) reflection coefficient $\times 10^{-1}$. Broken curve, theoretical reflection coefficient $\times 10^{-1}$.

$=(1-r)^2e^{-\mu x}$ where x is in centimeters. μ is almost constant at 0.48 from λ1600 to λ1400. Beyond this point it begins to increase until it becomes too great to measure, just after λ1235.8.

Curve 2 gives the value of r. The dotted curve is the reflection coefficient calculated from the index of refraction. In all cases r is larger than the theoretical reflection coefficient. The flat character of the curve around λ1400 is a real phenomenon and not due to experimental error. It is more pronounced when the polish is poor. Cleaved surfaces were not smooth enough to give any improvement over the polished ones.

There are three possible explanations for the high value of r. First, polish may be the cause. Second, there may be an adsorbed layer of water vapor. Third, the surface may be covered with a thin layer of abrasive. The first explanation is suggested by a number of properties of the surfaces. A poor polish would be expected to be worse at short wave-lengths first because of the decrease in wave-length and second because of the increase of the index of refraction. It is found that if a piece of fluorite is given a better polish the increase in transmission is greater at shorter wave-lengths than at longer.

The second explanation is not contradicted, for the absorption of water vapor though not accurately known is found to be quite high in this region.[8]

The third explanation seems unlikely because there is no marked change when a different abrasive is used. Also, the last abrasive is fluorite powder which should absorb only a very small amount of light.

In conclusion the author wishes to express his thanks to Professor T. Lyman for suggesting this problem and for his helpful guidance in completing it.

[8] Liefson, Astrophys. J. **63**, 73 (1926).

The Reflection Spectrum of Quartz in the Region of 9 mu

S. SILVERMAN, *Physical Laboratory, The Johns Hopkins University*

(Received November 22, 1933)

The reflection spectrum of quartz, cut perpendicularly to the optic axis, has been previously studied in the region of 9μ. It was felt advisable to repeat this work by using polarized light and a crystal section cut parallel to the optic axis. With the same high resolution spectrometer and a new type of resonance radiometer which employs a Nichols type radiometer, sufficient sensitivity was obtained to bring out a maze of fine structure. It is to be noted that much of this fine structure is produced at identical frequencies for both the ordinary and the extraordinary rays. This might indicate that these frequencies are produced by a lattice rather than by an ionic motion, or that such agreement is entirely fortuitous because of the extreme complexity and closeness of the lines.

INTRODUCTION

THE reflection spectrum of quartz has been studied many times. Recently, the author in conjunction with J. D. Hardy[1] studied the 9μ reststrahlen with a grating spectrometer of high resolution and the newly developed resonance radiometer. The results obtained at that time confirmed the general position of the bands and the reflecting power as obtained by previous investigators. In addition, an unsuspected degree of fine structure was obtained for both crystal and fused quartz. These indications of complexity were found for a section of crystal quartz which was cut and polished perpendicularly to the optic axis. The incident, and therefore, the reflected beams were unpolarized. It occurred to the present author that the problem should be attempted again with a polarized beam incident upon a section cut parallel to the optic axis. By this means one is easily able to separate the ordinary and the extraordinary rays by securing the proper orientation of electric vector and optic axis and to study each one individually.

EXPERIMENTAL

The spectrometer employed was the same as the one used in the earlier investigation in this laboratory.[1] A few minor changes were made. Among these was the substitution of a globar element for the usual Nernst glower; a special water-cooled mounting was devised, to be described elsewhere, which gave excellent service. The radiation from the heater was rendered parallel and allowed to fall upon a selenium plate at the Brewsterian angle. Following the directions for producing a selenium polarizer which were given by Pfund[2] many years ago several plates as large as 15×8 cm were prepared. The figure of the one finally selected was about equal to that of good window glass. In visible light it was possible with a crossed nicol completely to extinguish the light from a bright filament. The polarized radiation then fell upon the quartz plate at an angle of incidence of 20°, this being the smallest angle possible with the present set-up.

In place of the old resonance radiometer with two thermocouples and two under-damped galvanometers, a new instrument was built. The time of response of the old galvanometer system was somewhat long, and although electromagnetic disturbances were so slight as to be negligible, two difficulties were encountered. One was drift due to temperature fluctuations; this is only partially avoided at the high sensitivities by a compensated couple. The other was drift due to changes in the torsion of the suspensions and slight warping of the supports in the subbasement room in which the apparatus is situated. Because of previous encouraging results obtained in this laboratory it was felt that the

[1] Hardy and Silverman, Phys. Rev. **37**, 176 (1931).

[2] Pfund, Astrophys. J. **24**, 19 (1906).

compensated Nichols type radiometer offered possibilities. In general, to obtain large deflections with the radiometer, the system is built as lightly as possible. Such an instrument, in the ideal case, has a high, sharp sensitivity maximum at a pressure of about 0.02–0.06 mm mercury and is critically damped at this pressure. In our case, inasmuch as we were seeking resonance, we desired an underdamped system. This meant either a light system, working at a pressure so far below optimum conditions as to produce very small sensitivity; or a heavy system with relatively low sensitivity which would be underdamped at optimum pressure. The last alternative was accepted for several reasons. First, the loss in sensitivity is much smaller than was at first feared; our final radiometer was fully half as sensitive in "straight" deflection as the lighter ones. Secondly, it was much more rugged and more stable. Thirdly, the period could be managed so as to bring it up to a value where the resonance was of maximum benefit. Last, and perhaps most important, the dependence of sensitivity and damping upon pressure are very slight in the region of 0.01 mm, so that small leaks were of no importance, and it was possible to maintain uniform sensitivity for days, without recourse to pumping. The radiometer as finally built consisted of two vanes made of charred lens paper, as described by Pfund and Silverman,[3] dimensions 0.7×8 mm separated by 8 mm. The mirror was a piece of silvered glass 4×4 mm. The suspension was a quartz fibre, 12 cm in length, so chosen for thickness as to yield a period of 10 seconds. The entire mass was 0.020 gram, moment of inertia (calculated) 3×10^{-4} c.g.s. units. The amplifier consisted of two very coarse grids, 1 cm wide. This is necessary to allow for large angular displacement, as the radiometer has a considerably higher "deflection" sensitivity than does the thermocouple-galvanometer. As the Brownian motion limit is apparently very nearly the same for the radiometer as for the galvanometer-thermocouple circuit, the degree of useful amplification obtainable is correspondingly reduced. In place of the second thermocouple a Weston photronic cell and short-period, high resistance Leeds and Northrup galvanometer were used. The latter was critically damped and very closely followed the long, periodic impulse from the swinging radiometer. One difficulty was encountered. The light from the amplifier bulb was focussed upon the radiometer mirror and very severe disturbances were immediately set up, probably due to convection currents from the heated mirror or the radiometer-effect itself upon the mirror. Filters of copper chloride and green glass were introduced, until finally the focussed spot could be cut on and off without producing any disturbance. The radiation from the globar itself was interrupted by means of a magnetically operated shutter which was controlled by a carefully tuned electromagnetic pendulum.

The radiometer was so damped that it required 9 or 10 swings to return to rest and 5 complete periods to attain maximum deflection. An amplification of 50 was used, which by calculation showed our experimental accuracy to be quite near the theoretical limit set by the Brownian motion. The instrument was some 4 to 5 times more sensitive than the old one, due chiefly to the longer period, increased stability and the possibility of sharper resonance.

The instrument yielded, under these conditions, readings of 30 cm and above, which could be reproduced to within 2 mm. The random zero disturbance ranged from 5 to 12 mm, depending upon wind and building conditions. These deflections were as large as those obtained on the previous instrument with an energy source of similar power, in face of the handicap of the selenium polarizer which has a reflecting power of only some 35 percent.

The standard MgO filter was used. This consists of a mirror coated with a sufficiently heavy layer of the oxide to quench completely overlapping orders of shorter wave-lengths. Readings were taken with the electric vector parallel and then perpendicular to the optic axis; immediately following, the quartz plate was replaced by a gold mirror and the reading repeated. The curves (Fig. 1) were plotted by taking ratios. Readings were taken for wave-length settings separated by 0.005μ and are accurate to 0.0015μ.

[3] Pfund and Silverman, Phys. Rev. **39**, 64 (1932).

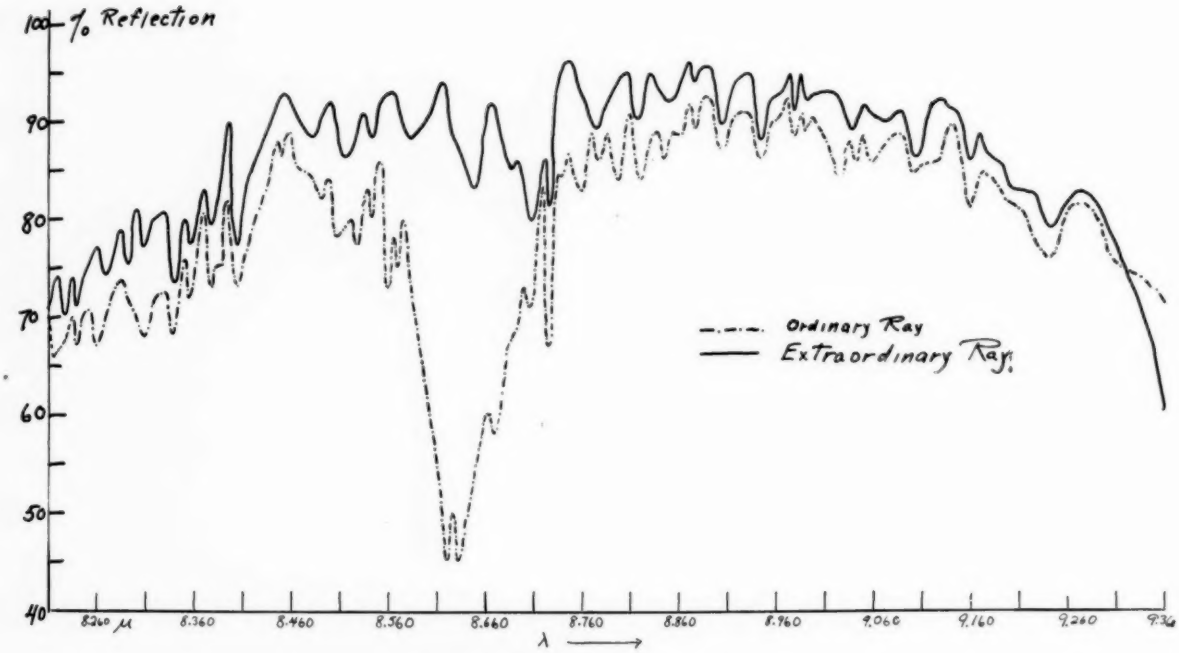

FIG. 1. Reflection spectrum of quartz.

RESULTS

As observed in the literature[4] the envelope of the extraordinary ray remains above that of the ordinary ray, and fails to show the deep triple minimum around 8.63μ. It is seen, however, that both bands possess a great amount of fine structure. The wave-lengths of the deep minima of the ordinary ray checked to within the experimental error those of the previous work.[1] Some new complexities were uncovered in this experiment due to the increased sensitivity. It is to be noted further that much of this structure is coincident for both bands. Inasmuch as the two rays are due to two vibrations at right angles to one another, it is amazing to find such a reproduction of frequencies in two such dissimilar vibrations. This might lead one to believe the fine structure to be caused by a superposition of a lattice frequency upon an ionic one. However, despite this coincidence and a similar observation concerning the resemblance of the reflection and absorption spectrum of calcite,[5] it must be born in mind that complete resolution in the case of solids is a matter of extreme doubt, and it is very possible that the structure is so complex that there exists a sufficient number of lines to make such agreement fortuitous and almost inevitable.

In conclusion, the author wishes to thank Professor R. W. Wood who has ruled the excellent echelette grating used in this spectrometer and Professor A. H. Pfund for many valuable suggestions. He also wishes to express his indebtedness to Dr. R. Canfield of the Naval Research Laboratory who has generously supplied the quartz plates.

[4] Lecomte, *Le Spectre Infrarouge*, page 145 ff.

[5] Silverman, Phys. Rev. **39**, 72 (1932).

The Refractive Index of H^2H^2O; The Refractive Index and Density of Solutions of H^2H^2O in H^1H^1O

DANIEL B. LUTEN, JR., *Department of Chemistry, University of California*

(Received December 5, 1933)

A determination has been made of the refractive index of nearly pure H_2^2O and of a 50 percent solution of H_2^2O in H_2^1O over a range of temperatures and wave-lengths. In both cases temperatures of maximum refractive index have been found. The differences between these temperatures and the temperature of maximum refractive index for ordinary water are in accord with the differences in those physical properties of the two kinds of water which have already been investigated. The dispersion of H_2^2O is lower than that of H_2^1O. The densities and refractive indices of solutions of different concentrations of H_2^2O in H_2^1O have been determined. It is found that these solutions do not obey the laws of the ideal solution to the extent that the partial molal volumes are functions of the concentration of the isotopic water. This deviation from ideality is not found in the refractive indices of these solutions.

WHEN the first water containing a high concentration of the hydrogen isotope was obtained in this laboratory, I found the refractive index to be appreciably smaller than that of ordinary water; this was mentioned by Professor Lewis[1] in his first communication on the hydrogen isotope. In these early experiments there was no way of determining the exact isotopic composition of the water and even after the specific gravity of pure H_2^2O had been ascertained with fair accuracy, it was still uncertain whether water containing varying amounts of the heavy isotope would obey the simple laws of mixing. Hence it seemed necessary to sacrifice a certain amount of nearly pure H_2^2O in order to find by actual dilution with ordinary water the exact relation between isotopic composition, specific gravity and refractive index.

Density and Concentration

The H_2^2O was prepared by Lewis and Macdonald according to the method described by them.[2] The experimental procedure was as follows: The specific gravity of a sample of water, which was about 98 percent H_2^2O, was determined with a pycnometer of about 0.35 cc capacity. Following this the refractive index was determined, after which the specific gravity was again ascertained. A weighed portion of the sample was then mixed with a known weight of ordinary water. Again specific gravity was ascertained before and after the determination of the refractive index; subsequent dilutions and specific gravity determinations were made in the same manner. The concentrations were thus obtained in terms of the concentration of the original sample independently (except as noted below) of any specific gravity determinations. All specific gravity determinations were made at 25.0°C. In the solutions where the concentration of H_2^2O was high, it was found that a certain amount of dilution (as evidenced by a change in density) had taken place in the course of the manipulations necessary for the determination of the refractive index. This was a consequence of the unavoidable exposure of the solution to the air. The dilution was small in amount and appeared to be consistent with obvious predictions: it was roughly dependent upon the time of exposure and upon the concentration of the solution. Accordingly, the concentrations obtained from the weight dilutions were corrected to take into account the dilution during handling. These corrections were small enough so that there should be no errors in concentrations greater than 0.2 percent. The probable error in the specific gravity determinations should be slightly less than 0.0001.

[1] G. N. Lewis, J. Am. Chem. Soc. **55**, 1297 (1933).
[2] Lewis and Macdonald, J. Chem. Phys. **1**, 341 (1933).

On the assumption that the equation,[3]

$$s = 1.0000 + 0.1056\, N_2 + \alpha\, N_1 N_2, \qquad (1)$$

is the best solution for the data, the best values for the mol fraction of the initial sample and for the constant α have been obtained. s is the specific gravity of the isotopic solution and N_1 and N_2 are the mol fractions of $H_2{}^1O$ and $H_2{}^2O$ (and also the atom fractions of H^1 and H^2), respectively. The agreement between the calculated and observed values is sufficient evidence of the satisfactoriness of this solution. In Table I the values observed and calculated for specific gravities and those observed for molecular volumes are given. In column 5 are given the differences between the observed molecular volumes and the molecular volumes calculated on the assumption that that quantity is a linear function of the mol fraction. The molecular volumes are based on specific gravities; the molecular weights used are 18.014 and 20.027.

TABLE I. *Specific gravities and molecular volumes of* $H_2{}^2O$ *solutions in* $H_2{}^1O$.

N_2	Spec. gr. (obs.)	Spec. gr. (calc.)	Mol. vol. (obs.)	Deviation from linearity
1.0000	(1.1056)	(1.1056)	(18.114)	0.000
0.970	1.1024	1.10241	18.112	.001
.817	1.0863	1.08613	18.097	.001
.617	1.0649	1.06489	18.083	.007
.460	1.0482	1.04827	18.069	.009
.340	1.0356	1.03561	18.055	.007
.164	1.0171	1.01718	18.036	.006
.000	(1.0000)	(1.0000)	18.014	.000

Now if this were a perfect solution, the specific volume would be a linear function of the weight fraction (1), the molecular volume (of the solution as a whole) a linear function of the mol fraction (2); the density would not be a linear function of the weight fraction (3), nor of the mol fraction (4) (i.e., the constant α in Eq. (1) would not be zero even for a perfect solution). But from the fact that the last two functions are not linear it may be deduced that the solution is not perfect.

Any of the four functions above may be approximated satisfactorily to a function of the form of Eq. (1). Eq. (1) itself becomes, on supplying the constant α,

$$s = 1.0000 + 0.1056 N_2 - 0.0012 N_1 N_2. \qquad (2)$$

Eq. (2) is of practical importance only in determining concentrations from densities.[4] Also of interest is the relation between molecular volume and mol fraction:

$$V_m = 18.014 + 0.100 N_2 + 0.031 N_1 N_2, \qquad (3)$$

where V_m is the molecular volume of the solution. From Eq. (3) the partial molal volumes may be obtained. At $N_2 = 0.5$ the partial molal volume of $H_2{}^2O$ is 0.05 percent higher and at $N_2 = 0$ it is 0.2 percent higher than at $N_2 = 1$.

Refractive Index and Concentration

The refractive index was determined for all solutions interferometrically. For the most concentrated solution, and also for the solution of mol fraction 0.459, it was also determined with a Pulfrich refractometer.

In all the determinations with the Pulfrich refractometer the zero setting of the micrometer screw was left unchanged. Under these conditions the refractive index of ordinary water was also determined at 20°C. To all values obtained, both for ordinary water and for the isotopic solutions, a correction was added (0.00007) such that the results for ordinary water should show least deviation from the values given by the *International Critical Tables*. All refractive indices are referred to air.

The interferometric determinations of the differences between the refractive index of ordinary water and of the isotopic solutions depend upon the well-known equation,

$$\Delta n = M\lambda/2L, \qquad (4)$$

where M is the displacement of the fringe system in terms of the number of fringes and L is the length of the chamber used (the light passes through it twice). The quantity M was obtained

[3] Lewis and Macdonald (J. Am. Chem. Soc. **55**, 3057 (1933)) have given the provisional value of 1.1056 for the specific gravity of pure $H_2{}^2O$ at 25°C. In the light of later determinations this value seems a little low but we shall retain it until we can be much more certain of the true value.

[4] Cf. Lewis and Luten, J. Am. Chem. Soc. **55**, 5061 (1933).

as the quotient of the shift in the fringe system in terms of micrometer readings and the fringe width in terms of micrometer readings,[5]

$$M=(r'-r_0)/w. \tag{5}$$

The initial determination with the Pulfrich refractometer eliminated any uncertainty in the location of the central fringe. For the Rayleigh-Zeiss interferometer used, the apparent shift for pure $H_2{}^2O$ with white light is 22.0 fringes when the actual shift is only 15.8 fringes. Finally, since the chamber used was only 1 mm long, there may have been a constant error as great as 1 percent in the direct determination of its length and, as a consequence, in all the results obtained from the interferometer. Since the results obtained with the Pulfrich refractometer are more reliable a small correction was made to bring the interferometric results into agreement with those obtained with the Pulfrich.

The refractive index shows no deviation from linearity with mol fraction. In Table II the differences between ordinary water and the solutions in question are given for three wave-lengths at 25.0°. The values calculated by the equation

$$n_1-n=N_2(n_1-n_2) \tag{6}$$

where n_1, n_2 and n are the refractive indices of $H_2{}^1O$, $H_2{}^2O$ and the solution, are given in columns 3, 5, and 7.

TABLE II. n_1-n at 25.0°C.

Mol fraction	5461 Hg	5461 calc.	5800 white light	5800 calc.	5893 Na_D	5893 calc.
1.000		.00461		.00449		.00445
0.977	.00451	.00451	.00439	.00438	.00436	.00435
.967	.00444	.00446	.00433	.00434	.00430	.00431
.816	.00378	.00376	.00367	.00366	.00365	.00364
.616	.00285	.00284	.00278	.00276	.00275	.00274
.459	.00212	.00212	.00205	.00206	.00203	.00204
.340	.00155	.00157	.00152	.00153	.00150	.00152
.164	.00076	.00076	.00073	.00074	.00074	.00073

[5] Cf. L. H. Adams, J. Am. Chem. Soc. **37**, 1181 (1915); J. Wash. Acad. Sci. **5**, 267 (1915) on the question of interferometer calibration.

REFRACTIVE INDEX AND TEMPERATURE

There is a temperature of maximum refractive index for ordinary water as has been shown by Pulfrich. The maximum lies between −1 and −2°C. I have found maxima also in the refractive indices of 97.7 and 45.9 mol percent solutions. For the former the maximum is close to +6°C and for the latter close to +3°C. For ordinary water the point of maximum refractive index lies between five and six degrees below the point of maximum density; the same is true of $H_2{}^2O$.[6] Aside from the displacement in both coordinates there is little difference in the curves of the three solutions of mol fractions 0.0 (light), 0.459 (medium) and 0.977 (heavy), shown in Fig. 1. (In Fig. 1 the scale is the same for each of the curves but is displaced vertically to bring the curves closer together.) The temperature coefficients are practically independent of wave-length over the range studied. The maxima for all five wave-lengths fall within a few tenths of a degree of the values given above. Table III gives the experimental results over the whole range of temperature and wave-length.

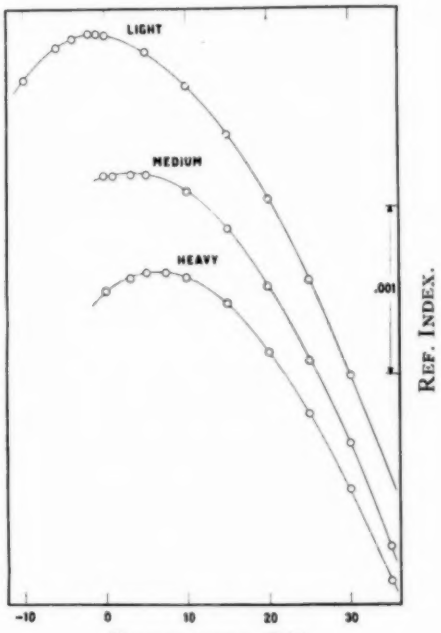

FIG. 1.

[6] Lewis and Macdonald (J. Am. Chem. Soc. **55**, 3057 (1933)) give + 11.6° as the point of maximum density for $H_2{}^2O$.

TABLE III. *Refractive indices.*

T(°C)	6563 Hα	5893 Na_D	5461 Hg	4861 Hβ	4358 Hg
		Ordinary water from I.C.T.			
20.0	1.33115	1.33300	1.33447	1.33714	1.34030
		Observed for ordinary water			
20.0	1.33118	1.33300	1.33449	1.33712	1.34025
		Mol fraction $H_2^2O=0.459$			
35.0	1.32764	1.32936	1.33075	1.33330	1.33630
30.0	1.32825	1.32998	1.33137	1.33391	1.33693
25.1	1.32875	1.33048	1.33186	1.33443	1.33743
20.0	1.32920	1.33092	1.33232	1.33490	1.33789
15.1	1.32953	1.33127	1.33265	1.33523	1.33824
10.1	1.32976	1.33150	1.33290	1.33546	1.33848
5.1	1.32987	1.33160	1.33301	1.33557	1.33858
3.2	1.32988	1.33160	1.33302	1.33558	1.33859
0.9	1.32987	1.33159	1.33301	1.33558	1.33858
−0.2	1.32986	1.33159	1.33301	1.33556	1.33857
		Mol fraction $H_2^2O=0.977$			
35.0	1.32552	1.32715	1.32844	1.33089	1.33376
30.05	1.32608	1.32770	1.32900	1.33144	1.33436
25.0	1.32654	1.32816	1.32947	1.33192	1.33482
20.1	1.32692	1.32853	1.32986	1.33231	1.33520
15.0	1.32720	1.32882	1.33013	1.33259	1.33550
10.0	1.32734	1.32897	1.33028	1.33274	1.33564
7.5	1.32737	1.32900	1.33030	1.33278	1.33567
5.2	1.32738	1.32900	1.33031	1.33277	1.33567
3.1	1.32736	1.32897	1.33028	1.33276	1.33565
0.1	1.32727	1.32889	1.33021	1.33265	1.33556

TABLE IV. *Refractive index of pure* H_2^2O.

T(°C) λ	6563	5893	5461	4861	4358
n_2 20.0	1.32683	1.32844	1.32976	1.33221	1.33509
n_1-n_2 20.0	0.00435	0.00456	0.00473	0.00491	0.00516
T(°C)	0	5	10	15	20
n_2D	1.32877	1.32888	1.32886	1.32871	1.32844
T(°C)	25	30	35		
n_2D	1.32806	1.32760	1.32705		

TABLE V. *Dispersion of* H_2^2O.

	$n_{4358}-n_{4861}$	$n_{4861}-n_{5461}$	$n_{5461}-n_{5893}$	$n_{5893}-n_{6563}$	$n_{4358}-n_{6563}$
H_2^1O	0.00313	0.00263	0.00149	0.00182	0.00907
H_2^2O	0.00288	0.00245	0.00132	0.00161	0.00826

The refractive index for pure H_2^2O is given in Table IV. The molecular refraction of ordinary water at 20° for the sodium D-line is 3.7121; for pure H_2^2O the corresponding value is 3.687.

DISPERSION

In Table V it is seen that the dispersion of pure H_2^2O is definitely less than that of ordinary water. Fig. 2 gives the dispersion for ordinary water, for 45.9 and 97.9 mol percent H_2^2O, at 20°.

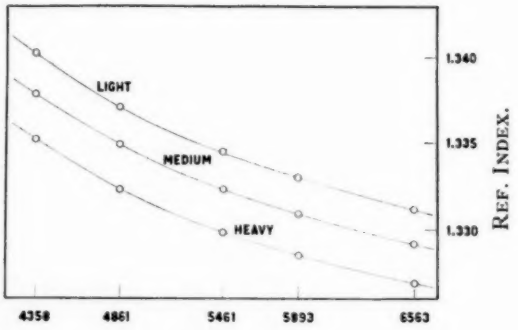

FIG. 2.

We have seen that the molecular refraction of H_2^2O is lower, which is to say that the refractive index is even lower than can be accounted for by the difference in molecular volumes. This abnormality and the lower dispersion, taken together, indicate that the effective position of the absorbing region in the ultraviolet, which is chiefly responsible for the refractive index of H_2^2O in the visible, is further removed from the visible than is the corresponding region for H_2^1O.

CONCLUSION

Within the last year two papers have appeared which deal, in part, with the refractive index of heavy water. In the first, Washburn, Smith and Frandsen[7] have given for the difference between the refractive indices of ordinary water and water of specific gravity 1.0014 for the sodium D-line at 25° the value $(60\pm2)\times10^{-6}$. If this be extrapolated to pure H_2^2O the difference is 0.00447 ±0.00015. The corresponding value given above is 0.00445. In the second paper Selwood and Frost[8] give results for the refractive index of pure H_2^2O which must be corrected slightly in the light of the relations, described herein, between concentration and density. The values obtained from their experimental data are given together with the corresponding results obtained in this investigation (see Table VI). There is the possibility that the difference may be due partially to the presence of O^{18} in the water used in this

[7] Washburn, Smith and Frandsen, J. Chem. Phys. **1**, 288 (1933).

[8] Selwood and Frost, J. Am. Chem. Soc. **55**, 4335 (1933).

TABLE VI.

	Selwood and Frost	This investigation
$(n_D20)_1-(n_D20)_2$	0.00473	0.00456
$(n_C20)_1-(n_C20)_2$	0.00429	0.00435

investigation, though there is no other reason to suspect its presence. O^{18}, if present in small amounts, can not affect the relations between density and concentration; it will, however, depress the values for n_1-n_2.

If it should be found that there are errors due to the facts that (1) the value 1.1056 for the specific gravity of H_2^2O at 25° is too small or (2) O^{18} is present, then the experimental results may easily be corrected in the light of such findings.

Finally, it is deserving to note, in view of recent misuse, that the value 1.1056 given by Lewis and Macdonald is for the *specific gravity* of H_2^2O at 25°C. Since the temperature coefficients of the two kinds of water are different they must be taken into account in work at other temperatures. The same caution applies even more pointedly to the use of the refractive indices, for there the difference in temperature coefficients is large.

It is a pleasure to acknowledge my indebtedness to Professor Lewis, who suggested and directed this work.

Isotope Displacement and Hyperfine Structure in the Arc Spectra of Chromium, Molybdenum and Tungsten

NORMAN S. GRACE AND KENNETH R. MORE, *Department of Physics, University of California*

(Received November 3, 1933)

Several of the stronger lines of Mo I and W I in the region 4000 to 6100A are found to possess structure. The W I lines are separated into three components which are roughly equally spaced with an overall separation of 0.1 cm^{-1}. This structure is attributed to an isotope displacement of the even isotopes. Some of the Mo I lines are resolved into two components, while others, though not resolved, are broad and nonsymmetrical. The two component lines, with separation of 0.05 cm^{-1}, are interpreted as being due to spin splitting of the odd isotopes. The broad lines with a width of about 0.06 cm^{-1} are interpreted as being due to a small isotope displacement. There is some evidence that $I=1/2$ for the odd isotopes of both Mo and W. There is also evidence that the magnetic moments of these odd isotopes are not large. The isotope displacements in the spectra of several elements are compared and the direction of displacement is discussed.

INTRODUCTION

THE spectroscopically homologous elements Cr, Mo and W have even atomic numbers and possess several isotopes of both even and odd mass numbers. Their isotopic constitutions are given in Table I. The spectra of Cr, Mo and W may show structure due to isotope displacement and also due to the nuclear moments of the odd isotopes.

TABLE I. *Mass numbers of isotopes and their abundance.*[1]

Element	Z	Mass-number percentage abundance						
Tungsten	74	182 22.6	183 17.2	184 30.1	186 30.0			
Molybdenum	42	92 14.2	94 10.2	95 15.5	96 17.8	97 9.6	98 23.0	100 9.8
Chromium	24	50 4.9	52 81.6	53 10.4	54 3.1			

In general the levels that show the widest splitting due to nuclear magnetic moments are those which arise from configurations containing at least one tightly bound penetrating electron, as for example a single s electron. Widest isotope displacements, on the other hand, are generally found in lines that result from transitions between levels, one of which has a configuration containing two tightly bound penetrating electrons as s^2 and the other a configuration in which both the s^2 electrons are in less penetrating states as p, d. The Hg II transitions $5d^96s^2\ ^2D - 5d^{10}6p\ ^2P$ furnish an example of this.[2]

The types of configuration mentioned above occur in the lower levels of Cr, Mo and W, being $d^4s^2\ ^5D_{01234}$ and $d^5s\ ^5S_2$ and $^7S_3$. The upper levels for the Cr and Mo lines examined are $d^5p\ ^5P_{123}$ and $^7P_{234}$, while the configurations are not known for the upper levels in W.

EXPERIMENTAL

The source in each case was a metal Schüler tube cooled in liquid air. The tube was operated at 2000 volts with currents from 0.07 to 0.4 amp. With argon present in the tube rich metal spectra were excited, the lines of the metal being much more intense than those of argon.

The spectra were photographed with a three-prism glass spectrograph crossed with silvered Fabry-Perot etalons. The etalons were placed in the parallel beam between the collimating lens and the prisms. Invar etalon separators up to 58 mm were employed and exposure times ranged from a few seconds to half an hour.

RESULTS

No wide patterns are observed in any of the lines examined. A number of tungsten lines show a narrow but definite isotope displacement but no resolved hyperfine structure due to nuclear

[1] Aston, Nature **126**, 200, 348 and 913 (1930).

[2] Schüler and Jones, Zeits. f. Physik **76**, 14 (1932).

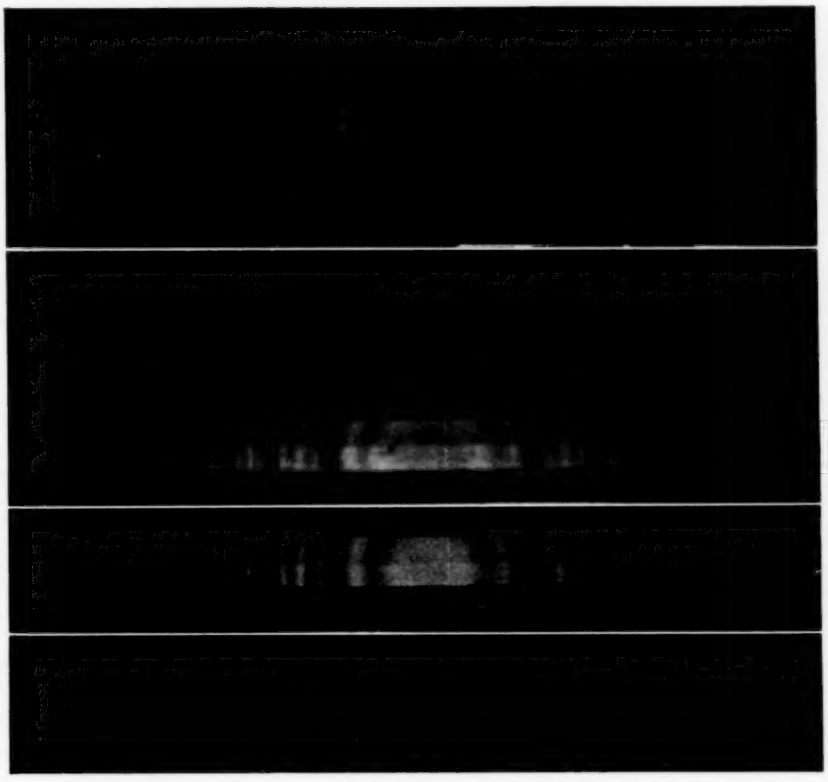

FIG. 1. Print of tungsten plate.

magnetic moments. Some of the molybdenum lines appear to show a very narrow hyperfine structure and others an unresolved isotope displacement. No structure is observed in the chromium lines examined. The lack of wide hyperfine patterns due to the odd isotopes in these spectra suggests that the nuclear magnetic moments of W^{183}, $Mo^{95 \text{ and } 97}$ and Cr^{53} are not large.

TUNGSTEN

Fig. 1 is a reproduction of a portion of a plate taken with a 29 mm interferometer separator. It shows a number of the lines resolved into three components which are roughly equally spaced and of the same order of intensity. Figs. 2 and 3 are microphotometer traces of λ4887 and 5515A respectively. The separations of the outside components from the center one are -0.050 cm^{-1} and $+0.061$ cm^{-1} for λ4887, -0.042 cm^{-1} and $+0.052$ cm^{-1} for λ5515, and values between these for many of the other lines. From the abundance ratios of the isotopes it seems almost certain that the three components are due to the three even isotopes. Moreover, the lines that show this structure arise from transitions to the levels $5d^46s^2\ ^5D_{01234}$ and thus might be expected to show an isotope displacement. There is no resolved structure of the odd isotope in any of the lines examined. However, the intensities of the three components vary somewhat from line to line. This suggests that the odd isotope is present and is showing hyperfine structure which is masked by the components of the three even isotopes. From λ5515 (Fig. 3) it appears quite certain that isotope 183 does not give rise to one sharp component lying half way between the components due to 182 and 184, because if it did the minimum between 182 and 184 would be much higher than it is. The interpretation regarding the odd isotope, though rather tentative, suggests that it possesses a nuclear spin of 1/2.

If the line due to isotope 183 is split into two components with separation a little less than the isotope displacement of 182 and 184, the ob-

served maxima would be separated by less than the true isotope displacement. The separation of the components due to 182 and 184, which is observed to be less than the separation of 184 and 186, may therefore in reality be nearly equal to it. This is in agreement with the results of Schüler and his associates[3] who found that the even isotopes of Zn, Cd and Hg show isotope displacements which are approximately equal for equal mass difference for constant Z (Table II).

TABLE II. *Isotope displacements.*

Spectrum	Z	Mass numbers	Displacement $cm^{-1}\times10^3$	Average displacement for $\Delta M=2$	Configurations of levels for lines showing structure
Cu I[4]	29	63			
		65	+72	+72	$3d^94s^2-3d^{10}4p$
Zn II	30	64			
		66	+95		
		68	+93	+94	$3d^94s^2-3d^{10}4p$
Mo I	42	92			
		94			
		96	<-60	<-15	$4d^45s^2-4d^55p$
		98			
		100			
Cd II	48	110			
		112	−54		
		114	−51	−52	$4d^95s^2-4d^{10}5p$
W I	74	182			
		184	+48		
		186	+56	+52	$5d^46s^2-$
Hg II	80	198			
		200	−500		
		202	−515		
		204	−520	−512	$5d^96s^2-5d^{10}6p$

Schüler attributes the wider isotope splitting to the s^2 electron configuration. If this be true for tungsten, then from the intensity of the components it appears almost certain that the energy level of the heaviest isotope lies deepest.

MOLYBDENUM

The lines λλ5571, 5533 and 5506A ($4d^55s\ ^5S_2-4d^55p\ ^5P_{123}$) are resolved into two components, one strong and to the red one very weak, with a separation of 0.05 cm^{-1} in each case, while the lines λλ6031, 5889, 5858, 5792, 5689 and 5650A ($4d^45s^2\ ^5D_{01234}-4d^55p\ ^5P_{123}$) are broad and non-symmetrical with a total width of about 0.06 cm^{-1}. Microphotometer traces of λ5571 and λ5889A are given in Figs. 4 and 5, respectively. These were obtained from a plate taken with 37 mm etalon separations. The curves show that the two structures are essentially different. Accurate measurement of the separations of the components is not possible because the structure is not completely resolved and the orders are very close together. This difficulty, along with the fact that the observed structure might be due to isotope shift or to hyperfine structure of the two odd isotopes, or to both, makes the interpretation of the results somewhat uncertain.

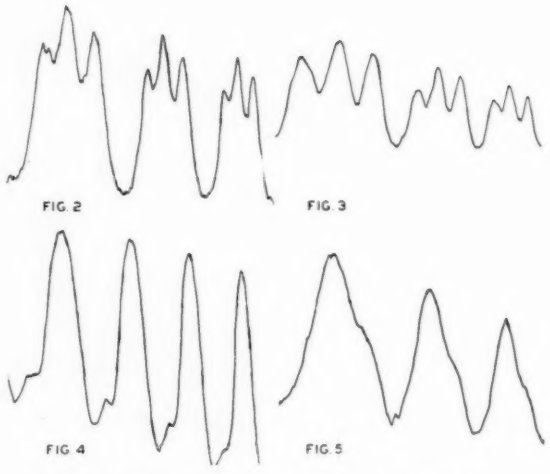

FIG. 2. Photometer curve of W I λ4887A.
FIG. 3. Photometer curve of W I λ5515A.
FIG. 4. Photometer curve of Mo I λ5571A.
FIG. 5. Photometer curve of Mo I λ5889A.

In the case of the lines showing two components it is probable that the structure observed is due to the splitting of the levels of the odd isotopes by virtue of their nuclear magnetic moments. The lower level, involving as it does a single penetrating s electron, might be expected to show splitting in the case of the odd isotopes. The intensity ratio, roughly 10 to 1, is in agreement with this interpretation. If the lower level ($4d^55s$) is split and the upper ($4d^55p$) is relatively sharp and if $I=1/2$ the odd isotopes would give rise to two components of intensity ratio three to two. Since the stronger component lies nearer to the center of gravity of the pattern than the weaker, it is more likely to be masked by the

[3] Schüler and Westmeyer, Zeits. f. Physik **81**, 565(1932); **82**, 685 (1933).
[4] Ritschl, Zeits. f. Physik **79**, 1 (1932).

strong line due to the even isotopes. If this is so the resulting pattern would show two components of intensity ratio about 10 to 1. The separations are so small and the structure so masked by the strong component due to the even isotopes that it has not been possible to determine the mechanical moments of the odd isotopes with certainty. It seems probable however that $I=1/2$ with higher values of I not definitely excluded.

The lack of symmetry of the lines arising from the transitions $4d^45s^2\ {}^5D_{01234}-4d^55p\ {}^5P_{123}$ appears to be due to a small unresolved isotope shift. Intensity curves which fit the general form of the photometer curves have been constructed by using the known relative abundances of the isotopes and assuming an isotope shift of 0.015 cm^{-1} for a mass difference of two units. If this interpretation is correct, molybdenum shows an isotope shift whch for equal mass differences is roughly one-fourth that of tungsten and appears to be in the opposite direction.

Chromium

In the Cr lines $3d^54s\ {}^7S_3-3d^54p\ {}^7P_{234}$ which might be expected to show structure due to splitting of the levels of the odd isotope, no structure was observed. These lines are however very easily self-reversed even with low current densities. This self-reversal might conceal any faint narrow structure due to the odd isotope which has a relative abundance of only ten percent. The critical examination of other Cr lines was not satisfactory because of overlapping of the lines when the slit was wide enough for the observation of the interference patterns, however no definite structure was observed.

Discussion

It is of interest to compare the isotope displacements of molybdenum and tungsten with those of other elements. A summary of some observed isotope displacements is given in Table II. These results show conclusively that the magnitude of observed isotope displacements differs materially from one element to another even when apparently similar electron configurations are involved. The interpretation of these differences in terms of energy levels is however much more uncertain, particularly regarding the direction of shift. In order to compare this direction from one element to another, we have tentatively adopted Schüler's convention and assumed that the wider splitting occurs in those levels with configurations involving the s^2 valence electrons. Adopting this assumption, and calling a shift in which the energy level of the heaviest isotope appears to lie deepest positive in direction, we get the signs in Table II. The fact that the sign of the shift, as interpreted above, changes several times as Z increases tends rather to cast doubt upon the assumption involved. In this connection the calculations of Breit[5] and also those of Bartlett and Gibbons[6] suggest strongly that isotope displacement may be quite complex in origin, there being several factors which may influence the direction and magnitude of shift observed. Until these factors have been more carefully examined in the light of additional experimental data one cannot say definitely whether the change of sign in Table II is real, or apparent only.

There is one significant feature illustrated in Table II which in view of Bartlett's[6] attempt to explain isotope displacement as purely a mass effect, might well be stressed: namely, that in any particular pattern showing isotope displacement, equal mass differences apparently produce roughly equal frequency differences. This may offer a useful criterion for distinguishing between patterns due to isotope displacement and those due to spin splitting, particularly in cases such as the rare earths where the isotopic constitutions are unknown.

We wish to thank Professor H. E. White for many helpful discussions in connection with this work.

[5] Breit, Phys. Rev. **42**, 348 (1932); **44**, 418 (1933).
[6] Bartlett and Gibbons, Phys. Rev. **44**, 538 (1933).

The Crystaldiamagnetism of Bismuth Crystals

ALEXANDER GOETZ AND ALFRED B. FOCKE, *California Institute of Technology*

(Received November 15, 1933)

A. Introduction. (A. Goetz and A. B. Focke)

The problem of crystaldiamagnetism (CDm) is a quality characteristic of the solid state. It depends on the coexistence of a *large* number of atoms in crystalline array (10^8 atoms in each direction), is "structure sensitive" and does not follow Curie's law. Previous work on polycrystalline material has shown large influences by metallic admixtures when within the solubility limits. Discrepancies were shown for polycrystalline material solidified *in vacuo*. The purpose of this investigation is to study these relations quantitatively on single crystals with special regard to the problem of solid solution.

B. Experimental Procedure and Results. (A. B. Focke)

The method of the magnetic measurement was the Gouy method, the field strengths used between 2500 and 22,500 gauss. The temperature control was cryostatic down to −185°C and thermostatic up to 271°C (melting point of Bi). For the *production of the crystals* spectroscopically analyzed material was used, for the growth the method of Goetz in a modified form. A special apparatus was built for growing the crystals *in vacuo* but no discrepancy with crystals grown in a neutral atmosphere was found. The results derived from several hundred crystals are partly given in tabulated form. The susceptibilities at 21°C for the purest Bi are $\chi_\perp = -(1.482 \pm 0.014) \times 10^{-6}$; $\chi_{||} = -1.053 \pm 0.010 \times 10^{-6}$. The values for alloyed crystals depend on the speed of growth for low speeds.

C. Description of Results and Discussion. (A. Goetz and A. B. Focke)

The effect of the type of insertion of admixtures upon CDm is found to be nonexisting in case of complete insolubility (Bi-Cu), to be random for macroscopic solubility (eutectic mixture) (Bi-Ag) and to be large and directional for atomic solubility, no matter whether the admixture enters the crystal as an atom (Sn, Pb and probably Ge) or as an intermetallic compound (BiSe, Bi_2Te_3). For atomic solubility the effect is smallest for an isomorphous admixture (Bi-Sb). The specific effect of the admixture is the larger the smaller the solubility limit. The effect of the nature of the dissolved atom upon the magnetic anisotropy is studied for the immediate neighbors of Bi in the periodic system; the electropositive admixtures Ge, Sn, Pb and the electronegative admixtures Se and Te. All of the former type increase the anisotropy $\chi_\perp/\chi_{||} = R$, all of the latter decrease it. The size of the influence among atoms of the same valency configuration is studied. The dependence of the anisotropy on the temperature is characterized by a decrease with increasing temperature irrespective of the sign and the magnitude of the effect of the admixture. The effect for high concentrations of electronegative admixtures can be so large for high concentrations that R becomes infinite: the crystal becomes paramagnetic in one and diamagnetic in the other direction. The relation $1/R = \rho = f(T)$ is linear for both types of admixtures. It is described by:

$$\chi_{||}/\chi_\perp = \rho = \rho_0 - (\gamma_0 + \gamma)(T_0 - T),$$

where ρ_0, T_0 are independent of the admixture. The discontinuity at the transformation point for Bi at 75°C changes only the value of ρ_0. The temperature coefficient γ is positive for electropositive and negative for electronegative admixtures, it increases with increasing concentrations (N). The dependence of the anisotropy on the concentration of the admixture is of exponential type at room temperature; at liquid air temperature a "critical" concentration is found at which the value of $d\rho/dN = \alpha'$ decreases suddenly. It lies for Pb at 0.08 percent, for Sn at 0.027 percent. It appears that the magnitude of the effect, admixtures of a certain valency configuration inflict upon χ for a certain low temperature, is definite; to produce this effect three times as many Pb (and probably Ge) atoms are necessary as Sn atoms. Electronegative admixtures show this effect much less distinctly. The dependence of $\chi_{||}$ and $\chi_\perp$ on the concentration and the type of admixture shows a critical concentration N_c for low temperatures normal to [111] for electropositive and parallel to [111] for electronegative admixtures. A number of other effects can be summarized: an electropositive admixture acts upon the CDm normal to [111] in the same way as an electronegative admixture parallel to it and *vice versa*. An isomorphous admixture has an electropositive effect normal to [111] and electronegative parallel to [111]. N_c has the following values: for Te $\leq$0.01 percent, for Sn 0.03 percent, for Pb and Se 0.09 percent. For high temperatures another critical concentration occurs around 0.01 percent, being the same for all admixtures studied. The temperature coefficient γ for pure Bi is: $\gamma_{||} = -1.1 \pm 0.05 \times 10^{-3}$ deg.$^{-1}$ and $\gamma_\perp = -1.5 \pm 0.08 \times 10^{-3}$ deg.$^{-1}$. The $\chi - T$ function does not show any fundamental difference between electropositive and electronegative admixtures. The transformation point at 75° is marked in the same way for all admixtures for small concentrations by a discontinuity which is positive for $\chi_{||}$ and negative for $\chi_\perp$. The discontinuity disappears for $N \gg N_c$. A hypothesis about the influence of the admixture upon the CDm encounters serious difficulties if one assumes a volume effect due to a superstructure in the usual sense.

Introducing a superstructure of planes according to previous suggestions of the authors with a parameter of 10^3-10^4A on which the admixture is adsorbed and accepting the Ehrenfest-Raman theory, the entire phenomenology can be accounted for satisfactorily in a qualitative way. The parameters for the plane structure thus obtained are in good agreement with the results of etch figures and the "critical" sizes of colloidal crystals. The interpretation of the pseudo-allotropic transformation at 75°C leads to the conclusion that this superstructure becomes instable at this point without however affecting the lattice.

A. Introduction. By A. Goetz and A. B. Focke

1. The problem of crystaldiamagnetism (CDm)

The following paper is to describe experiments covering CDm in Bi crystals as a function of the concentration and the type of admixtures of foreign atoms; it forms as such a part of a more general research program which was started a number of years ago and of which some results have been published already in a fragmentary manner.[1, 2, 3]

The problem under discussion divides itself naturally into two parts: to gain material for a better understanding of the nature of CDm as such, as well as a closer insight into the disturbing effect upon the electron configuration within the crystal lattice caused by the presence of small concentrations of admixed foreign atoms. The phenomenology of CDm so far known can be put as follows:

(1) The CDm is by definition a property of matter (chiefly of metals) in the crystalline state. Its magnitude and sign seem to be independent of the magnitude or sign of the susceptibility (scz) of the atoms or molecules in the gaseous or liquid state.

(2) The CDm is dependent on the crystallographic arrangements. Substances with different allotropic modifications show wide variations of scz. For example in α-Sn, $\chi=-0.35\times10^{-6}$, in β-Sn, $\chi=+0.025\times10^{-6}$. For C in diamond, $\chi=-0.46\times10^{-6}$, C in graphite $\chi=-3.5\times10^{-6}$.[4, 5]

(3) The scz in general increases very rapidly with decreasing temperature and does not follow Curie's law.

(4) The fundamental mechanism which produces CDm must involve a large number of atoms or molecules in an undisturbed crystalline array. This conclusion is to be drawn from the following two types of observations:

(4.1) The CDm is "structure-sensitive" since it can be changed considerably even for polycrystalline material by plastic deformation.[6, 7] In addition it has been proved recently that it is very sensitive to different states in superstructural (*Ueberstruktur*) configurations as, for instance, in Cu-Au alloys.[8]

(4.2) Observations on the magnitude of the scz in dependence on the size of the crystal have proved that below a certain magnitude of the latter the CDm becomes size-dependent.[9, 10, 11, 12]

The theoretical treatment of the problem of CDm is not very satisfactory. The theories of Langevin and Pauli do not apply. Any theory which describes it as an atomic property cannot succeed. Such theories do not explain the increase of negative scz at the transition into the solid state. The critical size below which the scz becomes dependent upon the dimensions of the crystal is of the order of 10^4A which suggests that cooperation of many thousand atoms is necessary to produce the diamagnetism typical of the crystal. The analogy to ferromagnetism is obvious.

Theories of the scz of a free electron gas are unsatisfactory since it appears that even for the alkali metals the assumption of completely free valency electrons is inconsistent so far as the calculation of the scz is concerned.[13]

To account for the behavior of metals having large CDm, P. Ehrenfest[14, 15] first proposed that electron orbits surrounding two or more nuclei are responsible for CDm.*

* The idea seems to be especially suggestive since the atoms in the Bi lattice are grouped along the axis [111] definitely in pairs which would mean that the probability of the electronic sharing among two close neighbors in the direction of the shortest distance is much larger than in any other direction. Thus the area of the electron orbits must be characterized by a larger projection into a plane perpendicular to the principal axis of the lattice than parallel to it. The result would be accordingly a maximum diamagnetic scz parallel to [111]. This, however, is just the opposite to the facts since the maximum diamagnetism occurs in a plane normal to this axis.

Raman[16] extended this hypothesis even farther by assuming electron orbits over large regions of the crystal, suggesting herewith the mentioned experiments on the size-dependence of the susceptibility due to artificial limitation of these orbits.

Because of the fundamental importance of CDm for an understanding of the electronic structure of solids, it seemed to us interesting to attack the problem by a method other than by measuring critical sizes of crystals. The production of very fine crystalline powders involves methods which do not exclude possible disturbances of the lattice, and also the lattice structure of small particles is not well known, especially with regard to the question whether or not and to what extent the surface forces affect the lattice structure of the crystal.

The following method was developed for determining the "effective cross section" of a foreign atom inserted into the lattice of a pure metal. If the type and size of the disturbance caused by foreign atoms be known as a function of their concentration, one is able to determine either the volume which is disturbed by one foreigner (effective cross section) or the volume within the lattice which has to remain undisturbed in order to have an intact mechanism of the CDm typical for the crystal lattice under investigation. If a crystal lattice of anisotropic character is used one should thus expect that the anisotropy as such should be changed by an insertion; and by this one expects to throw more light on the causes of the general inconsistency between the crystallographic anisotropies and the anisotropy of different physical properties in metallic crystals.

2. Discussion of previous work

Previous work by Johannson and Linde,[17] Endo,[18] Spencer and John,[19] on polycrystalline metals has shown the importance of admixtures. We find that their results on binary metallic systems may be summarized as follows:

(1) For a binary mixture of metals in the *liquid* state the scz follows the additive law

$$\chi_N = \chi_A + N(\chi_B - \chi_A)/100 \qquad (1)$$

and $\alpha^* = d\chi_N/dN = \text{constant}$, in which χ_N, χ_A and χ_B are the scz's of the mixture (N) and the components A and B, respectively, and N the percentage atomic concentration of B in A.

(2) The above law is fulfilled approximately* for binary systems with continuous solubilities in the solid state if χ_A and χ_B are taken for the solid metal. Such a case is shown in Fig. 1 for

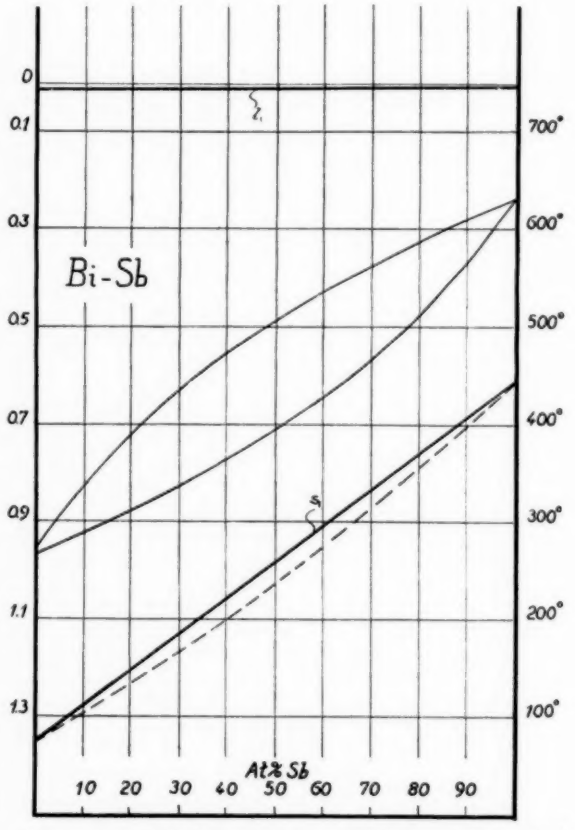

FIG. 1. Equilibrium diagram Bi-Sb (Otani).[21] Left ordinate indicates the scz's for the system in a liquid state (600°) (l) and the solid state (22°) (s). The dashed scz-curve gives the values of Shimizu, the full drawn lines those of Endo.[18, 20]

Bi-Sb. The equilibrium curves refer to the right ordinate, the left ordinate indicates the scz. The upper straight line (1) gives the scz for the liquid mixtures, the dashed curve (s) gives the values for the solid state obtained by Shimizu[20] and the full-drawn curve those by Endo. Both refer to the polycrystalline solid state (cf. below).

* Since there are many ways in which the components of a binary solid solution can arrange themselves (*Ueberstrukturen*), the function α^* (N) can be influenced largely by heat treatment (*Vergütung*, etc.)[8, 17], hence the constancy of α^* is a correct statement only in view of the distinctly different behavior in the following cases.

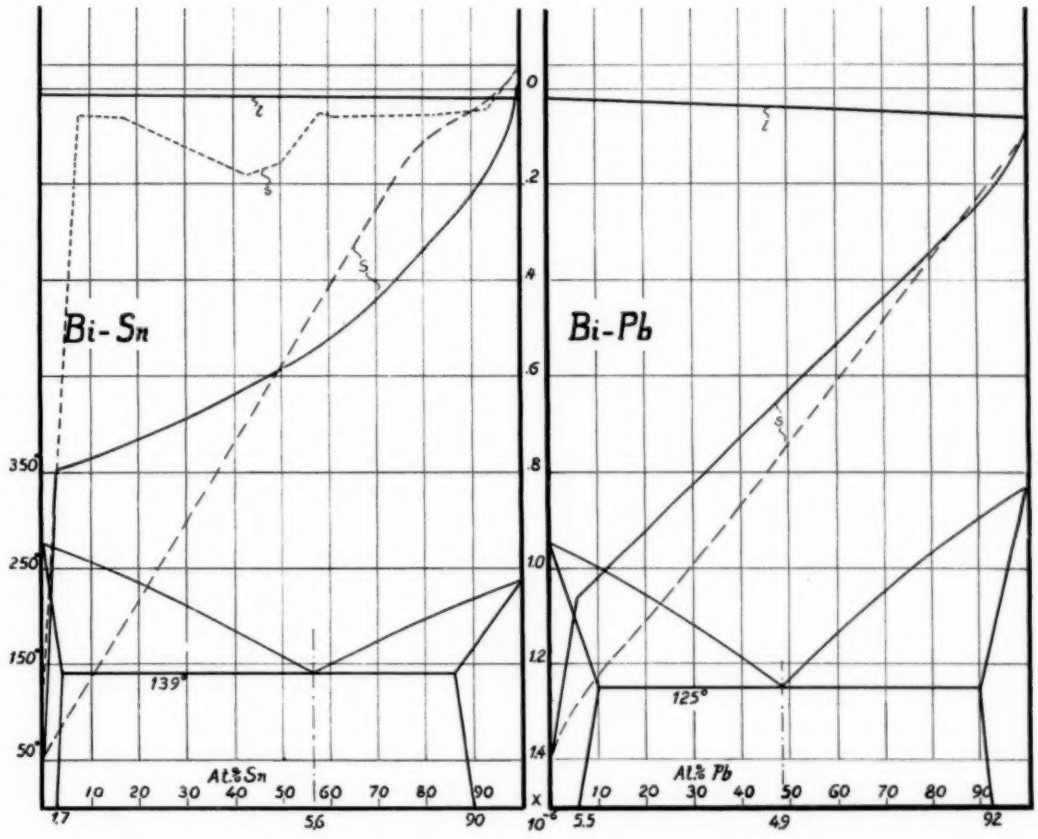

FIG. 2. Equilibrium diagram Bi-Sn (Endo).[18] The central ordinates indicate the scz's for the liquid (*l*) and the solid (*s*) states. The full drawn curve represents the results of Endo, the dashed curve those of Shimizu,[20] the dotted curve those of Spencer and John.[10]

FIG. 3. Equilibrium diagram Bi-Pb (Barlow).[22] The central ordinate indicates the scz's for the liquid (*l*) and the solid (*s*) states. The full drawn curve represents the results of Endo, the dashed curve those of Shimizu.[20]

(3) If the system has a limited solubility the above additive law does not hold, since the region of solubility is characterized in such cases by a large dependence of the CDm on the concentration of the admixture (large α^*); as soon, however, as the solubility limit is transgressed α^* decreases considerably. Such cases are the systems Bi-Sn (Fig. 2) and Bi-Pb (Fig. 3).† It is interesting to note that in contradistinction to the solubility region the eutectic point in both systems is not at all reflected in α^*.

(4) If the system is, in addition to (3), characterized by the existence of one or more intermetallic compounds, α^* is greatly affected, as should be expected since one has to deal in this case with interatomic valency shifts suggesting influential changes in the electron configuration. The diagram of the system Bi-Te (Fig. 4) shows this clearly.†

The observations described by Endo[18] have been made questionable by recent investigations of Shimizu[20] who repeated the measurements of previous authors, preparing however his alloys *in vacuo*. The results thus obtained are at great variance with the previous ones since his values of α^* (though the values of χ_A and χ_B, i.e., for the pure substances, are in precise agreement with the values for metals crystallized in the open) do not indicate at all in what form B is admixed to A. His obvious conclusion is that the effects previously observed are due only to

† The solubility region at the Bi side of the Bi-Sn system has not yet been confirmed metallographically but is thought to be correct in our opinion. As will be discussed later, it seems to be that very small solubilities can escape the usual metallographic analysis since, for instance, Bucher's results[23] do not show such a solubility. The same is true apparently for the systems Bi-Se and Bi-Te (cf. below).

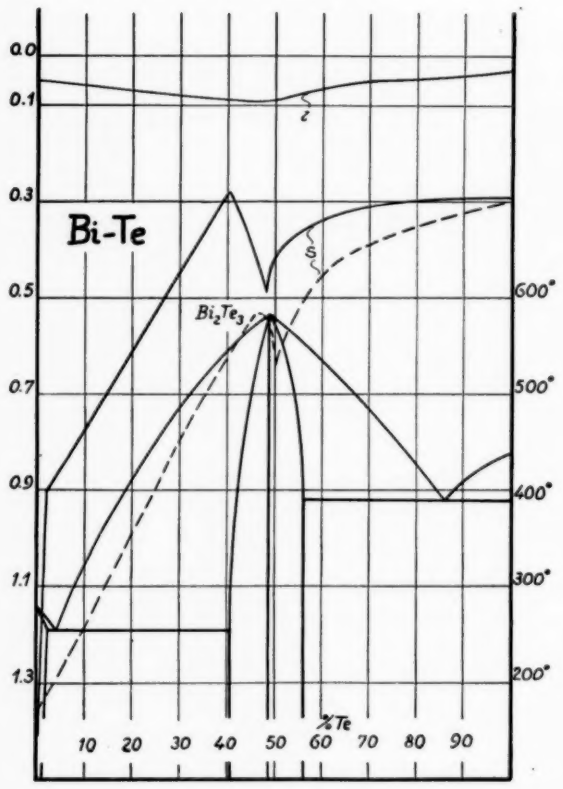

FIG. 4. Equilibrium diagram Bi-Te (Mönkemeyer[24] and K. Honda and T. Soné).[25] The left ordinate shows the scz for the liquid (*l*) and the solid (*s*) states. The full drawn curve represents the results of Endo,[18] the dashed curve those of Shimizu.[20]

absorbed gases. If this should be the case it seems very unexpected that the admixtures in a metal reflect the equilibrium-diagram in detail and perfectly only in the presence of uncontrolled amounts of gases and do not show the slightest effect in that respect in their absence. It may be anticipated at this point that our results for alloyed single crystals prepared *in vacuo* show that Shimizu's results cannot be transferred from the polycrystalline state for single crystals.

3. The purpose of this investigation

The purpose of the present investigation was chiefly to study the effect on single crystalline materials of atoms dissolved in the metallic crystal lattice. Concentrations from the smallest measurable up to the limit of solubility were used to determine the functional dependence of α on the concentration. Single crystals were used to avoid the deposition of unknown amounts of foreign materials within the boundaries of crystallites.

Because of its large CDm and anisotropic qualities Bi was used. It also possesses limited solubilities with a number of other metals and has been studied from various points of view in this laboratory.[3, 26, 27, 28, 29, 30, 31]

The effect of admixtures upon the CDm in different directions of the crystal, the influence of elements with respect to their relative position to *A* in the periodic system, and the dependence of the scz on the temperature were studied. Such studies should yield information concerning which of the differences between *A* and *B* (atomic volume, valency configuration, etc.) is effective. They should also give more definite conclusions about the equilibrium conditions of dissolved admixtures.

Finally one could expect more information about the causes of the discrepancies between the results obtained from crystals grown in a gas atmosphere (Endo) and those grown in vacuo (Shimizu). It has to be realized at the same time that the results to be expected even from an extended investigation of this kind will give only very limited information, since the problem of the limited solubility, especially between heteromorphous components in a microscopic single crystal is very complex and very little knowledge about such processes in general has so far been obtained.

B. Experimental Procedure and Results. By A. B. Focke[32]

1. Method and apparatus

(1.1) *Method of magnetic measurements.* Because of its distinct advantages for large single crystals the Gouy method was used. The twinning lamellae which always occur when a Bi crystal is cut or cleaved were located in the uniform region of the field and the perfect regions of the crystal extended over the inhomogeneous part of the field. Measurements showed that the scz did not change for field strengths varying from 2500 to 22,500 gauss so that the variable field used in the Gouy method introduced no errors and there were no ferromagnetic impurities.

The principal factors limiting the accuracy of

the measurements were: (1) the determination of the area of the cross section of the crystals, (2) the sensitivity of the balance and (3) the measurement of the strength of the magnetic field. The cross section was not measured directly but was calculated from the weight, length and density of each crystal for the part over which the field gradient occurred. All forces were measured with an accuracy of one-tenth of a milligram, which was in general less than one-half of one percent of the total forces produced by the magnetic field. The field strength was measured with a Grassot fluxmeter, with an accuracy of one percent. The theory and mechanical arrangement are described elsewhere.[1]

(1.2) *The temperature control.* The furnace is sketched in Fig. 5. It is wound non-inductively so that no correction to the field had to be made. The spacings of the winding, thickness of insulation and sheet aluminum lining were arranged to give a uniform temperature over the length of the crystal.

For measurements at liquid air temperature, a small flask (Fig. 6) was designed so that the crystal could be brought to this temperature without coming in actual contact with the liquid air. The crystal hangs in the inner tube which is open at the top only and is completely surrounded by liquid air. The liquid air chamber is further surrounded by an evacuated compartment. The upper part of the flask is provided with storage space for liquid air to insure the complete surrounding of the crystal chamber. This flask is found to be satisfactory, the only trouble encountered being the formation of liquid oxygen in the crystal tube when the liquid air was fresh.

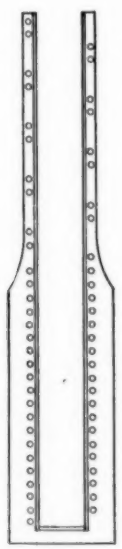

Fig. 5

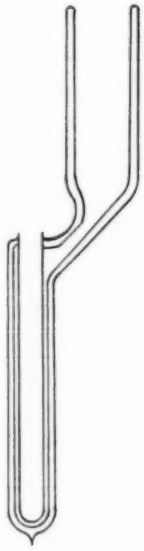

Fig. 6

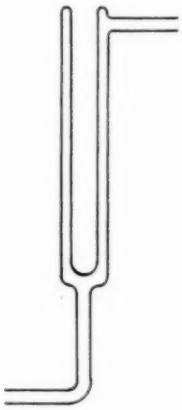

Fig. 7

FIG. 5. Furnace for heating the crystal during the determination of scz.

FIG. 6. Dewar flask for keeping the crystal at liquid air temperature during the determination of scz.

FIG. 7. Cryostatic arrangement for cooling the crystal during the determination of scz.

For some measurements at temperatures between −185°C and 22°C a cooling jacket similar to that used by Kapitza[34] was employed (Fig. 7). Cold gas from boiling liquid air passed through the jacket. The temperature was controlled by varying the rate of boiling of the liquid air. This control was very good but the cooler was very inefficient with this apparatus and was not used to any great extent.

2.1. The material

The Bi was the commercial grade sold by the Merck Chemical Company. Spectroscopic analysis performed by Mr. Hasler proved this grade to be freer from impurities than the so-called CP grades from various sources. Table I gives the atomic percentages of the impurities found and also the ratio of the principal scz's, (R).

TABLE I. *Atomic percentages of impurities in various bismuth samples. A*, Baker Corporation CP; *B*, Hartmann & Braun CP; *C*, Hartmann & Braun electrolytic; *D*, Kahlbaum-Berlin CP; *E*, *F*, *G*, *H*, Merck commercial.

Impurity	*A*	*B*	*C*	*D*	*E*	*F*	*G*	*H*
Copper	0.002	0.011	0.006	0.003	0.007	0.001		
Silver	.017	.028	.012	.046	.013	.006		
Tellurium	.000	.001	.000	.004	.000	.000		
Thallium	.000	.002	.000	.005	.000	.000		
Lead	.025	.061	.019	.020	.014	.002		
Total	.044	.103	.037	.075	.034	.009		
$R=$	1.499	1.597	1.440	1.460	1.430	1.410	1.430	1.435
			(Distilled)		1.423			

Lots *G* and *H* from Merck were not analyzed but their magnetic properties agree with bismuth *E*. The other metals used in making up the alloy samples were of commercial reagent quality. No special precautions were taken to insure their great purity, as all the alloys were limited to small percentages of the added metal.

The alloys were compounded by direct weighing. An attempt to use a base solution containing ten percent of the impurity (Pb and Ag) and to dilute further this solution was abandoned as some Pb was lost at each melting.

2.2. Production of crystals in an atmosphere

The procedure used in growing the crystals followed closely that developed by Goetz.[27] There were several variations which will be described. The desired amount of Bi was melted in a Pyrex crucible in an atmosphere of purified hydrogen and raised to about 500°C to reduce any oxide present. Then the Bi was cooled to 350°C and the impurity added. This procedure reduced the amount of chemical combination of the impurity with either the hydrogen or the glass. For alloys containing Pb and Sn it was necessary to use quartz crucibles as the metals reacted with the Pyrex.

After thoroughly stirring the melted alloy, it was drawn into Pyrex tubes (2–3 mm diam.) and quickly cooled. The rapid cooling prevented loss of impurities even of Pb and Sn. The alloys sometimes stuck to the glass tube. To prevent this, Bridgman's method[47] of heating the tube with a trace of oil in it until a light deposit of carbon was formed, was found to be satisfactory except for Te and Se. For these a clean tube was used and broken while wet with water. The capillary action of the water in the cracks formed in breaking the glass seemed to admit a film of water between glass and metal, so that the glass came off with ease.

The "second generation" of crystals as described by Goetz[27] was omitted. The lighter impurity metals tended to separate from Bi at each melting and Te, Se and Sb seemed to form gaseous hydrides, hence the single crystals were grown with as few operations as possible.

The "third generation" was carried out in the usual manner, the crystals being grown as rapidly as possible to obtain uniform distribution of the impurity.

2.3. Production of crystals *in vacuo*

Shimizu's paper[20] intimating that previous work on polycrystalline material was largely influenced by absorbed gases appeared when most of the measurements had been taken. To test the influence of gases on single crystals, some were grown *in vacuo*.

A "first generation" of rod was melted in an evacuated glass tube (*a*, Fig. 8) and degassed. The molten metal then was passed into a tube (*c*, Fig. 8) having the same size as those used in

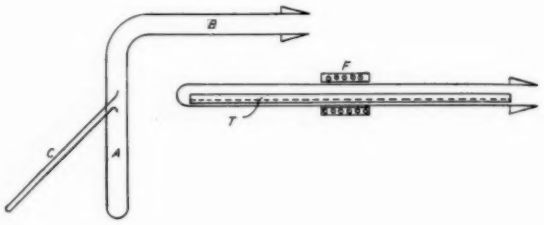

FIGURE 8. VACUUM CRYSTAL APPARATUS

FIG. 8. Arrangement for growing single crystals in vacuo.

the ordinary "first generation" and the tube sealed. When the final single crystal was made, the glass was cracked off and the rod placed in a soapstone trough *T* and enclosed in an evacuated tube. Soapstone was used in preference to graphite because of its lower heat conductivity. A short light furnace *F* was then moved without mechanical vibration along the glass tube. The seed crystal was attached to the rod by melting a part of it with a tiny hydrogen flame.

Crystals grown in vacuo were found to have magnetic properties identical with those grown in the presence of hydrogen or carbon dioxide, showing that for *single* crystals dissolved gases play little if any rôle. Those grown *in vacuo* did, however, show much brighter reflections after being etched than did any other crystals.

3. Results

(3.1) *The magnetic properties of pure bismuth.* It was first shown that the scz of Bi is independent of the field strength within wide limits and that the scz is invariant within any direction normal to the principal axis [111].

The measurement of the scz of five crystals at room temperature from $\theta^* = 0°$ to $\theta = 90°$ proved an excellent validity of the Voigt-Thomson law ($\cos^2$) and gave the following values:[1]

* All angles θ in this paper are taken with reference to the principal axis [111].

$$\chi_\perp = -(1.482 \pm 0.014) \times 10^{-6},$$

$$\chi_{\parallel} = -(1.035 \pm 0.010) \times 10^{-6}, R = \chi_\perp / \chi_{\parallel} = (1.408).$$

From these the value of the susceptibility to be expected of a polycrystalline aggregate is given by

$$(2\chi_\perp + \chi_{\parallel})/3 = -(1.340 \pm 0.013) \times 10^{-6},$$

which is in very good agreement with the values found by previous authors.[35]

The ratio of the principal scz's of the various kinds of Bi are given in Table I. These values do not involve errors of measurements of field strength or cross section.*

(3.2) *Dependence of the distribution of impurity on the speed of growth of crystals.* Materials are usually purified by crystallization. This effect is always amplified by slow crystallization and has been used to obtain pure Bi.[36] To determine the separation of Bi from the alloys and the effect on the magnetic properties, several samples of Bi containing Pb were made into similar rods and grown into crystals. One was grown at the rate of 6 mm/min. and the other at the rate of 1 mm/min. The magnetic anisotropy R was then measured at each end. Those grown at the fast or normal rate n showed uniform magnetic properties, and those grown at the slow rate s show large variations. Table II gives data on

TABLE II. *Ratio of principal susceptibilities for various kinds of Bi.*

		Pb content	R_1	R_2
188/11n	G	3.00%	2.619	2.625
188/21s	G	3.00%	2.130	2.764
166/12n	G	0.15%	1.630	1.627
166/22s	G	0.15%	1.605	1.751
192/11n	G		1.430	1.428
192/21s	G		1.438	1.429

such crystals. The first two columns show the type of crystal and source of supply. The last two columns present the anisotropy at the beginning (R_1) and at the end (R_2) of the crystal.

The choice of the proper speed of growth is important for if the speed is too great no uniform single crystals were obtained, and if too slow the properties vary along the crystal length. For example: A rod originally containing 2 percent of lead when grown at one-sixth the normal speed (1 mm/min.) was found to have magnetic properties of a normal one percent crystal at the end which crystallized first and of a normal three percent crystal at the other.

(3.3) *Tabulation of results.* An abbreviated account of the numerical results is given in Tables III and IV. The data in Table IV are so arranged that the first column gives the number of the individual crystal; the second column ("kind") indicates the chemical composition of the crystal; i.e., G 0.025 percent Cu shows that the sample is composed of G bismuth (see Table I) to which 0.025 atomic percent of copper has been added; this is followed by the force exerted by the field upon the crystal, in tenths of milligrams, the orientation of the crystal being indicated by the subscript of the letter χ; column R gives the magnetic anisotropy; and the other columns of data are self-explanatory. In all cases the scz used is the specific or mass scz (χ), i.e., the ratio of the magnetic moment per unit mass, to the magnetizing field.

Since the determination of the absolute value of the scz requires crystals of very uniform

TABLE III. *Data for crystals of uniformity sufficient to make determination of χ possible.*

Temp. °C	H	$F_\perp$	$F_{\parallel}$	R	$1/R$	$-\chi_\perp \times 10^6$	$-\chi_{\parallel} \times 10^6$
Crystal 123/41F							
−185	7	920	566	362	1.565	0.639	1.944	1.226
− 84	9	900	770	502	1.534	0.652	1.691	1.104
22	9	900	675	482	1.406	0.711	1.482	1.063
126	9	900	561	419	1.340	0.746	1.237	0.921
268	9	900	419	346	1.210	0.826	0.922	0.760
Crystal 224/21G 5.00% Sn								
−185	7	650	119	−76	− 1.56	−0.639	0.433	−0.283
−135	9	900	162	−81	− 3.18	−0.314	0.698	−0.219
−115	—	—	144	−36	− 4.08	−0.250	—	—
− 84	9	900	F=385		− 4.48	−0.224	0.850	−0.190
− 56	—	—	162	−18	−10.1	−0.099	—	—
+ 32	—	—	213	14	15.2	0.066	—	—
62	—	—	224	27	8.30	0.121	—	—
72	—	—	225	33	6.82	0.147	—	—
75	10	560	F=567		6.78	0.148	1.102	0.161
126	10	560	219	50	4.38	0.228	1.129	0.257
185	10	360	195	66	2.85	0.351	1.054	0.369
232	10	560	155	62	2.50	0.400	0.895	0.358

* These variations support the view of Goetz and Hasler[25] concerning the great differences observed in their work on crystals in a magnetic field. From the Table I it would be expected that bismuth B would be most affected by growth in a magnetic field, because of the larger torque acting on it. This is exactly the result found.

TABLE IV. *Summary of data.*

Crystal	Kind	R	$1/R$	$-\chi_\perp \times 10^6$	$-\chi_\parallel \times 10^6$
Temperature: −185°C; H =6850 gauss.					
249/11	*H* 0.01% Ag	1.564	0.639	1.920	1.228
251/11	*H* 0.09% Ag	1.595	0.626	1.920	1.200
253/11	*H* 0.81% Ag	1.618	0.618	1.950	1.203
254/11	*H* 2.43% Ag	1.575	0.634	1.900	1.203
256/11	*H* 0.01% Sn	1.850	0.541	2.232	1.207
257/12	*H* 0.03% Sn	2.325	0.429	2.568	1.104
258/11	*H* 0.09% Sn	2.460	0.406	2.275	0.925
260/11	*H* 0.81% Sn	3.740	0.267	1.070	0.286
261/11	*H* 2.43% Sn	−10.850	−0.092	0.704	−0.065
263/11	*H* 0.01% Pb	1.698	0.589	2.017	1.189
264/11	*H* 0.03% Pb	1.878	0.533	2.197	1.169
265/11	*H* 0.09% Pb	2.283	0.438	2.530	1.108
266/11	*H* 0.27% Pb	2.620	0.382	2.431	0.927
267/11	*H* 0.81% Pb	2.425	0.412	1.827	0.752
268/11	*H* 2.43% Pb	2.740	0.365	1.365	0.498
270/11	*H* 0.01% Te	1.080	0.925	1.682	1.478
271/12	*H* 0.03% Te	0.974	1.028	1.427	1.465
272/11	*H* 0.09% Te	0.830	1.205	1.224	1.474
273/11	*H* 0.27% Te	0.617	1.620	0.919	1.490
275/11	*H* 0.01% Se	1.306	0.765	1.800	1.376
276/11	*H* 0.03% Se	1.091	0.915	1.663	1.511
277/11	*H* 0.09% Se	0.995	1.005	1.530	1.535
278/11	*H* 0.27% Se	0.856	1.168	1.269	1.483
279/11	*H* 0.81% Se	0.772	1.295	1.004	1.333
280/11	*H* 0.01% Sb	1.552	0.644	2.025	1.303
281/11	*H* 0.03% Sb	1.514	0.660	1.920	1.270
282/11	*H* 0.09% Sb	1.462	0.684	1.875	1.330*
283/11	*H* 0.27% Sb	1.545	0.647	1.978	1.279
Temperature: 22°C; H =20,800 gauss.					
249/11	*H* 0.01% Ag	1.430	0.699	1.489	1.041
251/11	*H* 0.09% Ag	1.428	0.700	1.488	1.043
253/11	*H* 0.81% Ag	1.430	0.699	1.492	1.043
254/11	*H* 2.43% Ag	1.420	0.705	1.490	1.051
256/11	*H* 0.01% Sn	1.470	0.680	1.539	1.046
257/11	*H* 0.03% Sn	1.570	0.637	1.562	0.994
258/11	*H* 0.09% Sn	1.803	0.555	1.658	0.916
260/11	*H* 0.81% Sn	2.965	0.337	1.573	0.531
261/11	*H* 2.43% Sn	4.655	0.213	1.289	0.265
263/11	*H* 0.01% Pb	1.443	0.692	1.478	1.023
264/11	*H* 0.03% Pb	1.478	0.677	1.533	1.040
265/11	*H* 0.09% Pb	1.542	0.648	1.520	0.990
266/11	*H* 0.27% Pb	1.737	0.576	1.636	0.941
267/11	*H* 0.81% Pb	2.021	0.494	1.655	0.816
268/11	*H* 2.43% Pb	2.459	0.407	1.604	0.652
270/11	*H* 0.01% Te	1.329	0.753	1.442	1.073
271/11	*H* 0.03% Te	1.197	0.836	1.325	1.108
272/11	*H* 0.09% Te	0.903	1.108	1.122	1.244
273/11	*H* 0.27% Te	0.697	1.435	0.897	1.288
275/11	*H* 0.01% Se	1.381	0.724	1.483	1.073
276/11	*H* 0.03% Se	1.280	0.781	1.424	1.111
277/11	*H* 0.09% Se	1.203	0.830	1.396	1.161
278/11	*H* 0.27% Se	1.020	0.980	1.244	1.220
279/11	*H* 0.81% Se	0.966	1.034	1.176	1.216
280/11	*H* 0.01% Sb	1.423	0.702	1.490	1.046
281/11	*H* 0.03% Sb	1.421	0.703	1.480	1.040
282/11	*H* 0.09% Sb	1.420	0.704	1.468	1.032
283/11	*H* 0.27% Sb	1.427	0.700	1.468	1.023

Crystal	Kind	R	$1/R$	$-\chi_\perp \times 10^6$	$-\chi_\parallel \times 10^6$
Temperature: 65°C; H =8500 gauss.					
249/11	*H* 0.01% Ag	1.387	0.729	1.387	0.998
251/11	*H* 0.09% Ag	1.360	0.733	1.394	1.027
253/11	*H* 0.81% Ag	1.352	0.735	1.370	1.012
254/11	*H* 2.43% Ag	1.360	0.730	1.381	1.016
256/11	*H* 0.01% Sn	1.385	0.730	1.436	1.038
257/12	*H* 0.03% Sn	1.436	0.695	1.465	1.022
258/11	*H* 0.09% Sn	1.683	0.590	1.563	0.915
260/11	*H* 0.81% Sn	2.650	0.370	1.540	0.581
261/11	*H* 2.43% Sn	3.722	0.260	1.406	0.376
263/11	*H* 0.01% Pb	1.370	0.727	1.380	1.007
264/11	*H* 0.03% Pb	1.419	0.702	1.444	1.018
266/11	*H* 0.27% Pb	1.603	0.590	1.502	0.936
267/11	*H* 0.81% Pb	1.800	0.549	1.508	0.835
268/11	*H* 2.43% Pb	2.216	0.446	1.573	0.713
270/11	*H* 0.01% Te	1.287	0.775	1.330	1.050
271/12	*H* 0.03% Te	1.220	0.820	1.332	1.084
272/11	*H* 0.09% Te	0.958	1.041	1.132	1.182
273/11	*H* 0.27% Te	0.733	1.372	0.917	1.252
275/11	*H* 0.01% Se	1.340	0.743	1.418	1.058
276/11	*H* 0.03% Se	1.315	0.760	1.405	1.067
277/11	*H* 0.09% Se	1.197	0.833	1.358	1.133
278/11	*H* 0.27% Se	1.040	0.961	1.236	1.189
279/11	*H* 0.81% Se	1.022	0.979	1.194	1.167
280/11	*H* 0.01% Sb	1.351	0.736	1.384	1.023
281/11	*H* 0.03% Sb	1.340	0.742	1.328	0.990
282/11	*H* 0.09% Sb	1.351	0.736	1.440	1.064
283/11	*H* 0.27% Sb	1.351	0.736	1.400	1.040
Temperature: 75°C; H =8500 gauss.					
249/11	*H* 0.01% Ag	1.379	0.725	1.381	1.001
251/11	*H* 0.09% Ag	1.342	0.745	1.381	1.030
253/11	*H* 0.81% Ag	1.378	0.726	1.375	0.995
254/11	*H* 2.43% Ag	1.364	0.733	1.358	0.995
256/11	*H* 0.01% Sn	1.394	0.717	1.441	1.034
257/12	*H* 0.03% Sn	1.398	0.715	1.438	1.029
258/11	*H* 0.09% Sn	1.670	0.598	1.488	0.890
260/11	*H* 0.81% Sn	2.245	0.445	1.437	0.639
261/11	*H* 2.43% Sn	3.534	0.283	1.402	0.397
263/11	*H* 0.01% Pb	1.372	0.728	1.383	1.007
264/11	*H* 0.03% Pb	1.339	0.747	1.412	1.053
266/11	*H* 0.27% Pb	1.581	0.629	1.484	0.940
267/11	*H* 0.81% Pb	1.813	0.551	1.500	0.826
268/11	*H* 2.43% Pb	2.120	0.466	1.520	0.717
270/11	*H* 0.01% Te	1.205	0.829	1.330	1.103
271/12	*H* 0.03% Te	1.149	0.870	1.268	1.102
272/11	*H* 0.09% Te	0.974	1.026	1.184	1.233
273/11	*H* 0.27% Te	0.778	1.290	0.954	1.225
275/11	*H* 0.01% Se	1.242	0.801	1.372	1.102
276/11	*H* 0.03% Se	1.230	0.810	1.371	1.112
277/11	*H* 0.09% Se	1.163	0.258	1.298	1.114
278/11	*H* 0.27% Se	1.048	0.953	1.214	1.160
279/11	*H* 0.81% Se	1.040	0.960	1.219	1.170
280/11	*H* 0.01% Sb	1.572	0.725	1.392	1.013
281/11	*H* 0.03% Sb	1.319	0.755	1.332	1.011
282/11	*H* 0.09% Sb	1.336	0.746	1.404	1.050
283/11	*H* 0.27% Sb	1.332	0.748	1.356	1.020

* Large stranger may cause this deviation.

cross section, it was possible to use only the best crystals for this purpose. This cross-section requirement was not of importance for anisotropy measurements, so the less uniform crystals were used for this purpose only, and are included in Table IV; the series in Table III are taken from crystals which were uniform enough to permit the evaluation of χ.

C. DESCRIPTION OF RESULTS AND DISCUSSION. BY A. GOETZ AND A. B. FOCKE

1. The effect of the type of insertion of foreign atoms into the crystal

First of all it is important to state which of the different manners in which a foreign atom can be held within a macroscopic single crystal

TABLE IV. (*Continued.*)

Crystal	Kind	R	$1/R$	$-\chi_\perp \times 10^6$	$-\chi_\parallel \times 10^6$
Temperature: 101°C; H =8500 gauss.					
249/11	*H* 0.01% Ag	1.301	0.790	1.300	0.997
251/11	*H* 0.09% Ag	1.285	0.778	1.299	1.010
253/11	*H* 0.81% Ag	1.320	0.757	1.288	0.974
254/11	*H* 2.43% Ag	1.343	0.744	1.305	0.970
256/11	*H* 0.01% Sn	1.332	0.750	1.351	1.015
257/12	*H* 0.03% Sn	1.354	0.736	1.341	0.990
258/11	*H* 0.09% Sn	1.536	0.651	1.392	0.905
260/11	*H* 0.81% Sn	1.890	0.532	1.348	0.716
261/11	*H* 2.43% Sn	3.195	0.313	1.364	0.426
263/11	*H* 0.01% Pb	1.310	0.764	1.293	0.986
264/11	*H* 0.03% Pb	1.294	0.773	1.397	1.079
266/11	*H* 0.27% Pb	1.440	0.690	1.435	0.996
267/11	*H* 0.81% Pb	1.656	0.604	1.413	0.845
268/11	*H* 2.43% Pb	1.920	0.515	1.445	0.758
270/11	*H* 0.01% Te	1.196	0.835	1.259	1.052
271/12	*H* 0.03% Te	1.109	0.902	1.221	1.102
272/11	*H* 0.09% Te	1.000	1.000	1.168	1.169
273/11	*H* 0.27% Te	0.776	1.285	0.958	1.225
275/11	*H* 0.01% Se	1.228	0.813	1.304	1.063
276/11	*H* 0.03% Se	1.197	0.833	1.273	1.063
277/11	*H* 0.09% Se	1.171	0.852	1.264	1.080
278/11	*H* 0.27% Se	1.050	0.952	1.178	1.123
279/11	*H* 0.81% Se	1.060	0.941	1.210	1.142
280/11	*H* 0.01% Sb	1.311	0.760	1.304	0.993
281/11	*H* 0.03% Sb	1.287	0.774	1.269	0.986
282/11	*H* 0.09% Sb	1.280	0.777	1.332	1.040
283/11	*H* 0.27% Sb	1.309	0.760	1.279	0.978
Temperature: 150°C; H =8500 gauss.					
249/11	*H* 0.01% Ag	1.267	0.790	1.228	0.968
251/11	*H* 0.09% Ag	1.212	0.825	1.211	1.000
253/11	*H* 0.81% Ag	1.256	0.796	1.198	0.953
254/11	*H* 2.43% Ag	1.241	0.805	1.156	0.930
256/11	*H* 0.01% Sn	1.300	0.769	1.268	0.975
257/12	*H* 0.03% Sn	1.281	0.780	1.230	0.958
258/11	*H* 0.09% Sn	1.416	0.706	1.338	0.944
260/11	*H* 0.81% Sn	1.650	0.606	1.251	0.757
261/11	*H* 2.43% Sn	2.619	0.382	1.270	0.484
263/11	*H* 0.01% Pb	1.296	1.296	1.229	0.947
264/11	*H* 0.03% Pb	1.268	0.789	1.254	0.989
266/11	*H* 0.27% Pb	1.287	0.774	1.248	0.972
267/11	*H* 0.81% Pb	1.442	0.693	1.217	0.842
268/11	*H* 2.43% Pb	1.629	0.608	1.239	0.760
270/11	*H* 0.01% Te	1.151	0.868	1.160	1.008
271/12	*H* 0.03% Te	1.133	0.882	1.161	1.048
272/11	*H* 0.09% Te	1.020	0.980	1.139	1.116
273/11	*H* 0.27% Te	0.843	1.190	0.961	1.141
275/11	*H* 0.01% Se	1.211	0.823	1.234	1.019
276/11	*H* 0.03% Se	1.170	0.852	1.188	1.014
277/11	*H* 0.09% Se	1.182	0.843	1.201	1.015
278/11	*H* 0.27% Se	1.093	0.913	1.163	1.064
279/11	*H* 0.81% Se	1.078	0.928	1.222	1.134
280/11	*H* 0.01% Sb	1.228	0.810	1.179	0.958
281/11	*H* 0.03% Sb	1.242	0.801	1.197	0.964
282/11	*H* 0.09% Sb	1.252	0.796	1.240	0.990
283/11	*H* 0.27% Sb	1.242	0.801	1.201	0.965

Crystal	Kind	R	$1/R$	$-\chi_\perp \times 10^6$	$-\chi_\parallel \times 10^6$
Temperature: 201°C; H =8500 gauss.					
249/11	*H* 0.01% Ag	1.238	0.808	1.084	0.876
251/11	*H* 0.09% Ag	1.251	0.798	1.145	0.930
253/11	*H* 0.81% Ag	1.235	0.810	1.119	0.905
254/11	*H* 2.43% Ag	1.214	0.823	1.050	0.865
256/11	*H* 0.01% Sn	1.220	0.820	1.164	0.954
257/12	*H* 0.03% Sn	1.178	0.848	1.116	0.930
258/11	*H* 0.09% Sn	1.364	0.733	1.210	0.887
260/11	*H* 0.81% Sn	1.566	0.638	1.160	0.740
261/11	*H* 2.43% Sn	2.290	0.436	1.201	0.523
263/11	*H* 0.01% Pb	1.273	0.785	1.143	0.896
264/11	*H* 0.03% Pb	1.225	0.816	1.186	0.968
266/11	*H* 0.27% Pb	1.288	0.774	1.163	0.905
267/11	*H* 0.81% Pb	1.360	0.735	1.128	0.829
268/11	*H* 2.43% Pb	1.508	0.658	1.103	0.732
270/11	*H* 0.01% Te	1.172	0.853	1.107	0.945
271/11	*H* 0.03% Te	1.131	0.854	1.098	0.970
272/11	*H* 0.09% Te	1.088	0.919	1.098	1.008
273/11	*H* 0.27% Te	0.895	1.120	0.957	1.070
275/11	*H* 0.01% Se	1.200	0.830	1.177	0.979
276/11	*H* 0.03% Se	1.153	0.865	1.107	0.958
277/11	*H* 0.09% Se	1.171	0.852	1.137	0.970
278/11	*H* 0.27% Se	1.075	0.930	1.097	1.020
279/11	*H* 0.81% Se	1.084	0.919	1.115	1.028
280/11	*H* 0.01% Sb	1.223	0.815	1.089	0.889
281/11	*H* 0.03% Sb	1.223	0.814	1.109	0.906
282/11	*H* 0.09% Sb	1.240	0.805	1.148	0.925
283/11	*H* 0.27% Sb	1.189	0.839	1.062	0.894
Temperature: 245°C; H =8500 gauss.					
249/11	*H* 0.01% Ag	1.169	0.855	0.958	0.820
251/11	*H* 0.09% Ag	1.213	0.824	1.058	0.872
253/11	*H* 0.81% Ag	1.153	0.866	0.981	0.850
254/11	*H* 2.43% Ag	1.142	0.875	0.968	0.845
256/11	*H* 0.01% Sn	1.170	0.855	1.044	0.892
257/12	*H* 0.03% Sn	1.135	0.880	0.979	0.863
258/11	*H* 0.09% Sn	1.304	0.766	1.105	0.847
260/11	*H* 0.81% Sn	1.473	0.679	1.030	0.700
261/11	*H* 2.43% Sn	1.893	0.528	0.985	0.520
263/11	*H* 0.01% Pb	1.215	0.823	1.044	0.859
264/11	*H* 0.03% Pb	1.188	0.841	1.022	0.860
266/11	*H* 0.27% Pb	1.223	0.813	1.057	0.863
267/11	*H* 0.81% Pb	1.310	0.763	1.005	0.766
268/11	*H* 2.43% Pb	1.397	0.710	0.906	0.650
270/11	*H* 0.01% Te	1.145	0.873	1.014	0.836
271/12	*H* 0.03% Te	1.220	0.819	0.992	0.814
272/11	*H* 0.09% Te	1.104	0.903	1.038	0.940
273/11	*H* 0.27% Te	1.003	0.995	0.929	0.925
275/11	*H* 0.01% Se	1.153	0.865	1.087	0.940
276/11	*H* 0.03% Se	1.148	0.870	1.018	0.886
277/11	*H* 0.09% Se	1.096	0.910	0.992	0.905
278/11	*H* 0.27% Se	1.041	0.961	0.940	0.902
279/11	*H* 0.81% Se	1.106	0.900	0.987	0.892
280/11	*H* 0.01% Sb	1.208	0.825	0.998	0.828
281/11	*H* 0.03% Sb	1.277	0.279	0.972	0.761
282/11	*H* 0.09% Sb	1.180	0.845	1.076	0.911
283/11	*H* 0.27% Sb	1.159	0.861	0.951	0.820

affects the CDm. The types of insertion can be enumerated as follows:

(a) *Complete separation of both components*, i.e., neither atomic nor microscopic solubility. Example, the system: Bi-Cu.[37] It has been found that the anisotropy of Bi crystals grown from a melt to which Cu was admixed in different proportions (from 0.025 to 1.00 percent in 20 different crystals) is *not* affected within the limits of experimental error.

(b) *Existence of a eutectic mixture*, i.e., microscopic but no atomic solubility. Example, the system: Bi-Ag.[38] The phase-diagram (Fig. 9) shows no atomic solubility on the Bi-side, however a eutectic mixture at 2.5 percent Ag-concentration. From Fig. 10 it is realized that the influence upon CDm of Ag-admixtures is very remarkable though entirely irreproducible. The fact that it is possible to affect the anisotropy R by the insertion of foreign atoms with no solubility seems very interesting, since such insertion does not influence the lattice con-

FIG. 9. Equilibrium diagram Bi-Ag (Petrenko).[38] The system is characteristized by the absence of atomic solubility on the Bi-side.

figuration at all. The fact that it is not difficult to grow good single crystals from such mixtures shows that also the macroscopic structure of the crystal is not very much distorted. (For further discussion see Section 7.)

(c) *Complete atomic solubility.* Example, the system: Bi-Sb (Fig. 1) (Table V).[21, 39, *] In this case the effect upon CDm is a simple volume effect and the additive law (Eq. (1)) is valid, also very little discrepancy exists between Endo's and Shimizu's results. Our results show no influence of Sb as far as the anisotropy is concerned, because of the small value of α and the comparatively small concentrations used (Fig. 15). ($\alpha = (\alpha R/dN)$.)

TABLE V. $T = -185°C$.

Bi +	N %	$-\chi_\perp \times 10^6$	$-\chi_{\perp r}$ %	$-\chi_{\parallel} \times 10^6$	$-\chi_{\parallel r}$ %	$lg\alpha_{\perp r}$	$lg\alpha_{\parallel\alpha}$
−	0.0?	1.945	100	1.230	100		
						+2.24	−1.26
Sn	0.01	2.282	117.3	1.207	98.2	+1.86	−1.62
	0.03	2.568	132.0	1.104	89.8	−1.40	−1.39
	0.09	2.275	117.0	0.925	75.0	−0.93	−0.86
	0.81	1.070	55.0	0.286	23.2	−0.68	−0.15
	2.43	0.704	36.2	0.065	0.5		
						+1.56	−1.51
Pb	0.01	2.017	103.7	1.189	96.8	+1.67	−0.95
	0.03	2.197	113.0	1.169	95.0	+1.45	−0.93
	0.09	2.530	130.1	1.108	90.1	−0.45	−0.92
	0.27	2.431	125.0	0.927	75.2	−0.76	−0.92
	0.81	1.827	94.0	0.752	61.0	−0.16	−0.42
	2.43	1.365	70.3	0.498	40.5		
Sb	0.01	2.025	104.1	1.303	105.9		
	0.03	1.920	98.8	1.270	103.2		
	0.09	1.875	96.5	1.330?	108.1		
	0.27	1.978	101.7	1.279	104.0		
						−1.88	+2.08
Se	0.01	1.800	92.5	1.376	112.0	−1.54	+1.73
	0.03	1.663	85.5	1.511	122.8	−1.06	+0.82
	0.09	1.530	78.7	1.535	124.8	−0.87	−0.38
	0.27	1.268	65.3	1.482	120.5	−0.40	−0.35
	0.81	1.004	51.6	1.333	108.4		
						−2.13	+2.31
Te	0.01	1.682	86.5	1.478	120.2	−1.81	−0.60
	0.03	1.427	73.5	1.468	119.4	−1.29	+0.78
	0.09	1.224	62.9	1.474	119.8	−0.94	−0.85
	0.27	0.919	47.2	1.490	121.1		

(d) *Limited atomic solubility.* In this case several variations are possible:

α. Limited solubility of pure A in pure B, i.e., limited solubility only on the Bi-side. No example.

β. Limited solubility of B-A-Solution in A, i.e., limited solubility on both sides. Example, the systems: Bi-Sn (Fig. 2) and Bi-Pb (Fig. 3) and according to our results also Bi-Ge.

γ. Limited solubility of $A_mB_n + A$ in A, i.e., existence of an intermetallic compound and limited solubility on both sides. Example, the systems: Bi-Se,[40, 48] (Fig. 11) and Bi-Te,[24, 25] (Fig. 4).

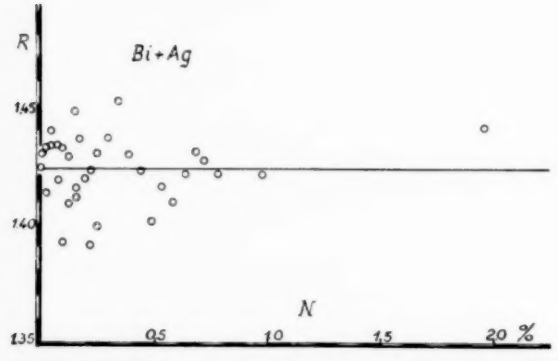

FIG. 10. R-N diagram for Bi+Ag for T = 22°C. The full drawn line indicates R for pure Bi crystals. Evidence of the random, i.e., undirectional, influence of an atomically insoluble admixture.

* There is some discrepancy among different authors about the shape of the solidus curve; Fig. 1 was copied from the most recent investigation.

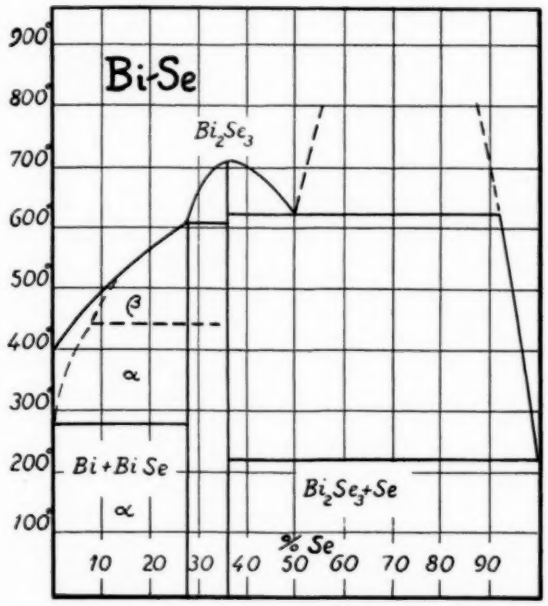

FIG. 11. Equilibrium diagram Bi-Se (Parravano[40] and Tomashige).[41] The full drawn liquidus curve represents the results of Parravano, the dashed curve those of Tomashige indicating the existence of two allotropic modifications for BiSe (α and β). According to our results the diagram should show a region of limited solubility of α-BiSe in Bi<2 percent.

As has been mentioned already (Part A, Section 2) the specific effect of atomically dissolved foreign atoms upon CDm is very large even for polycrystalline material and this investigation of single crystals has supported this fact very largely. According to our results it can be said generally that the specific influence of atomically dissolved atoms (i.e., the effect per inserted atom) is many times larger than that of any other type of admixture and furthermore that among atomically dissolvable admixtures *the specific effect is the larger the smaller the solubility limit*. Thus the atomic effect of Sn and Te upon the CDm is larger than of Pb and Se, corresponding to the solubility of Se and Pb which is larger than of Sn and Te.

Another observation may be mentioned in this connection: It is to be expected that an alloyed metal can only be grown in single crystalline form as long as the concentration does not exceed the solubility limit, because in case the component *B* exists in too large concentration the system disintegrates in two phases which upset the macrocrystalline arrangement. It is however surprising to see that the solubility of Bi in single crystalline form is much larger than for the polycrystalline material if one measures the solubility limit by the concentration beyond which it is impossible to grow single crystals without inclosures of crystal elements of different orientation or observable heterogeneous deposits. The solubility of a dissolvable admixture seems therefore to depend upon the size of the crystal complexes in such a manner that the solubility is larger for large than for small complexes. This dependence is analogous to the observations of previous authors[42, 43, 44] for the solubility of Ag in Cu. (The phase-relations of Ag-Cu are similar to Bi-Pb (Fig. 3).) In the case of the system Bi-Sn this difference is of particular importance since the solubility of Sn in Bi was not known before the magnetic researches of Endo and was made again doubtful by the observations of Shimizu.[20] We have made therefore a precision determination[29, 30] of the lattice spacing in Bi along [111] as function of the Sn-concentration and found an increase of the atomic distance up to the highest concentrations for which a single crystal still could be obtained, i.e., approximately 5 percent atmos., whereas the solubility limit for polycrystalline material is given as 1.7 percent.[18] We consider this as a proof that Sn is partially soluble in Bi and hence the phenomena observed by the insertion of Sn in Bi crystals must be due to atomically dissolved Sn.

2. The effect of the nature of the dissolved atom upon the magnetic anisotropy

If a section of the periodic system is chosen with the Bi-metals in the center it is to be considered most fortunate (and certainly not accidental) that all neighbors of the Bi metals form limited solutions with the latter. Accordingly all such combinations with Bi with its immediate neighbors have been investigated with the exception of Po, in order to study the variation of the effect upon the CDm with the electron configuration of the dissolved admixture. The arrangement is seen from Table VI and the valency configuration from Table VII.

The present investigation has shown that *all dissolved neighboring atoms which possess one valency electron less than Bi* (left (electropositive) neighbors) *increase the anisotropy* $\chi_\perp/\chi_{||}=R$,

TABLE VI.

32	33	34
Ge	As	Se
50	51	52
Sn	Sb	Te
82	83	84
Pb	Bi	Po

TABLE VII.

		N	*O*	*P*
Ge	*K*–*M* complete	2 2		
Sn		2 6 10	2 2	
Pb		2 6 10 14	2 6 10	2 2
As		2 3		
Sb		2 6 10	2 3	
Bi		2 6 10 14	2 6 10	2 3
Se		2 4		
Te		2 6 10	2 4	
Po		2 6 10 14	2 6 10	2 4

whereas a decrease of the anisotropy takes place for dissolved right (electronegative) *neighbors*. This behavior is definitely different from Ag (see Section 1.b, Part C) where R was decreased or increased at random. Among the great number of crystals with atomically dissolved mixtures such irregularities as to sign or magnitude of the effect upon R were not observed once.

The valency structure of the foreign atom decides upon the sign of the change of R whereas the magnitude of the effect seems to depend upon the same cause as the solubility which is not obvious. (See 1, Part C.) It is certain however that the crystal structure of B has nothing to do with this effect since nearly all neighbors of Bi crystallize differently.* In spite of this fact Ge (of which however only 2 crystals were grown) has the same effect as Pb which again is comparable in magnitude to Se. One should accordingly expect for Po the same magnitude as for Se and Pb. The effect of Sn and Te is however 3–4 times larger. It is thus evident that the atomic radius of the foreign atom with a given valency configuration has no simple relation to the size of the influence caused by it (Section 5.4).

3. The dependence of the anisotropy on temperature

The above relation has to be correlated with the temperature since its influence adds an important factor to the whole phenomenology. Our investigation included the range from liquid oxygen (90°abs.) to the melting point of Bi (543°abs.). The variation of R with the temperature T can generally be stated as follows: *The effect of any dissolved admixture on R irrespective of its sign and magnitude increases with lower temperatures and decreases approaching the melting point.*

(3.1) *Electropositive admixtures.* The dependence of the anisotropy on the temperature can be described more easily if one plots $1/R = \chi_{\parallel}/\chi_{\perp} = \rho$ against T as is done for pure Bi (F) and different concentrations of electropositive admixtures in Fig. 12, illustrating that:

α. The temperature coefficient γ of the anisotropy ρ is positive and increases with the concentration of the dissolved admixture.

β. The effect for high concentrations can be so large at sufficiently low temperatures that R can become ∞ and even negative, i.e., *the crystal can be paramagnetic in one* ($\parallel$) *and diamagnetic in the other direction* ($\perp$).[3]

γ. The anisotropy ρ is seemingly a linear function of T such that the extrapolation of all $\rho-T$ lines beyond the melting point results in an accurate intersection at a temperature T_0. This relation is not obeyed for the highest concentration of Sn at low temperatures which is apparently due to an instability of the solid solution at low temperatures.* Another deviation which seems to be of more fundamental character occurs in the region below and above the temperature of the pseudo-allotropic transformation of Bi for medium concentrations of Sn and Pb. To what extent a linear inter- and extrapolation of the $\rho-T$ function of small concentrations is

* Ge—Diamond; Sn—tetragonal; Pb—cubic; Se—hexagonal, special; Te—hexagonal special; Sb—rhombohederal.

* This is already indicated by the fact that the solubility limit for polycrystalline material is given by Endo at 1.7 at percent at room temperature.

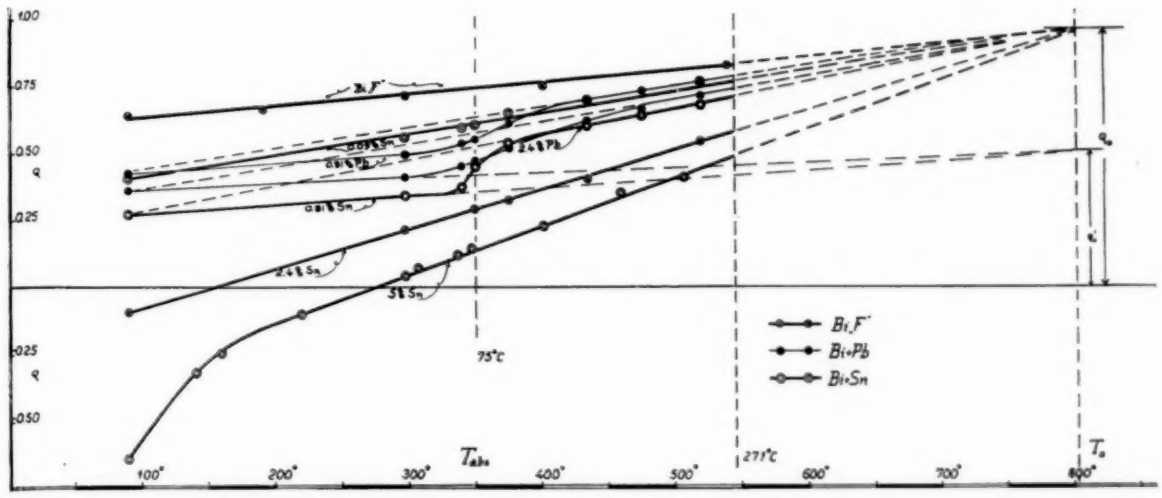

FIG. 12. $\rho - T$ diagram for electropositive admixtures (Tables IV and V). The dashed lines represent linear interpolations across the region of possible anomaly and the extrapolations to T_0, ρ_0 and ρ_0'. Only the large concentrations are shown.

justified cannot be stated since the measurements in the region between 90° and 300°abs. are still missing for these concentrations. However, a considerable number of crystals especially of the larger concentrations (not shown in Fig. 12) justify the linear extrapolation.

The temperature T_0 is characterized by the fact that an (imaginary) crystal at T_0 would have a magnetic anisotropy ρ_0 common to pure crystals as well as to alloyed crystals; in other words: the effect of any of the studied admixtures would have disappeared and their ρ would be identical with that of the pure metal. The analytical relation is accordingly:

$$\chi_{\parallel}/\chi_{\perp} = \rho = \rho_0 - \gamma'(T_0 - T) \qquad (2)$$

where ρ_0 and T_0 are constants independent of the concentration and the kind of dissolved admixture. The temperature coefficient γ' varies with concentration and type of the admixture and is best expressed by its two components, the coefficient of pure Bi (γ_0) and the additional coefficient (γ) which latter is always positive for electropositive admixtures. Accordingly:

$$\chi_{\parallel}/\chi_{\perp} = \rho = \rho_0 - (\gamma_0 + \gamma)(T_0 - T). \qquad (2a)$$

The temperature T' at which the change of sign of the scz in one direction within the crystal occurs is thus given by:

$$T' = T_0 - \rho_0/\gamma'. \qquad (2b)$$

The values of the constants are:

$$\rho_0 = 0.95, \qquad R_0 = 1/\rho_0 = 1.05,$$

$$T_0 = 803°\text{abs.}, \qquad \gamma_0 = 4.9 \times 10^{-4}\ \text{deg.}^{-1}.$$

(3.2) *Electronegative admixtures.* The variation of ρ with the temperature T for electronegative admixtures is in many ways similar to the above relation. Fig. 13 illustrates this in the same scale as Fig. 12 for a different section of the ordinate, the line for pure Bi (F) being used as reference. It is seen that:

α. *The temperature coefficient γ of the anisotropy increases with the concentration of the dissolved admixture* (same as Section 3.1α).

β. *In contradistinction to the electropositive admixtures the temperature coefficient γ is negative.*

γ. Below the pseudo-allotropic transformation point (75°C) the $\rho - T$ functions are linear and the extrapolation for the large concentrations of Te intersect with good accuracy at the values for ρ_0 and T_0 given above. The transformation point, however, is characterized by a discontinuity in the ρ values being negative for large and positive for small concentrations of Te and Se.

δ. Above the transformation point the linearity of the $\rho - T$ function holds still true, at least for larger concentrations whereas the accuracy of the measurements for the smaller concentrations makes the validity of this statement less certain. The extrapolations of the $\rho - T$ line

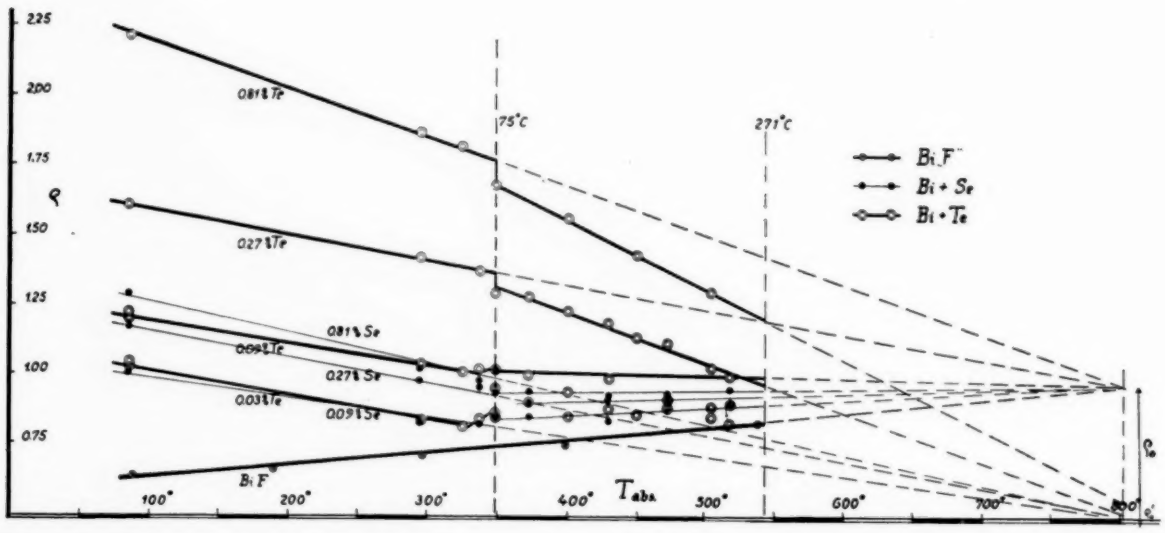

FIG. 13. $\rho - T$ diagram for electronegative admixtures. The dashed lines represent the linear extrapolations beyond the transformation point and the melting point to T_0, ρ_0 and ρ_0'. Only large concentrations of Te and Se are shown.

above 75°C intersect very well at T_0, though, for a different value of $\rho_0 = \rho_0' = 0.5$. The same is apparently true for Se and the small concentrations of Te, in such a manner that only two cases are possible: *If the $\rho - T$ line of an electronegative admixture has an extrapolated intersection at ρ_0 for $T < 75°$, the discontinuity at the transformation point is negative and the extrapolated intersection for $T > 75°$ occurs at ρ_0'. The other case is the exact opposite: If ρ_0' holds for $T < 75°$, ρ_0 holds for $T > 75°$ and the discontinuity is positive.* (A discussion of the possible nature of the transformation point is to be found in Section 7.)

The first case is only true for large concentrations of Te, whereas the second holds for all concentrations of Se and the small concentrations of Te which is in perfect agreement with the later (Section 4) discussed fact that a much larger amount of Se produces the same effect as a small quantity of Te, the effect produced, however, being almost exactly the same. The alikeness of the influence of Se and Te is so close, especially at higher temperatures, that the measured points cover each other and hence the lines for Te admixtures are not shown in the diagram.

The existence of two values for ρ_0 is probably not restricted only to electronegative admixtures, since it is possible to describe the deviation from the straight line relation for electropositive admixtures (Fig. 12) in terms of ρ_0', though the much smaller accuracy of the measurements in the region of higher temperature for those admixtures did not seem to justify such a procedure. For comparison it has to be realized that these are not strictly commensurable since Bi forms with its right neighbors only solutions with the compounds BiSe and Bi_2Te_3 (Fig. 11 and Fig. 4) whereas the left neighbors go into atomic solution.

4. The dependence of the anisotropy on the concentration of the admixture

For a closer understanding of the mechanism of the insertion of the foreign atom within the crystal it is necessary to study the dependence of ρ on the concentration of the admixture (N). The observations of Spencer and John[10] as well as of Endo[18] (Figs. 1–4) indicate in their concentration diagrams a linear dependence of the total susceptibility on N. Since the number of different concentrations studied within the region of solubility by these authors is much too small for the accurate determination of this function we have prepared a great number of single crystals with different concentrations of the elements under consideration. Some of the results are shown in Fig. 14 representing the run of ρ with N for the electropositive elements Pb and Sn for room temperature. It is immediately

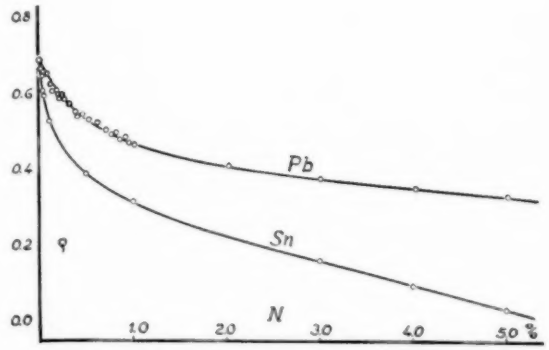

FIG. 14. $\rho - N$ diagram for electropositive admixtures for room temperature.

realized that the *dependence is not linear and approaches more a parabola*. Both curves are of the same character with the difference that the absolute influence of the Sn atom is larger than of the Pb atom. The relative effects of different impurities for different temperatures is seen more easily in Fig. 15. Here ρ is plotted in the same manner against the concentration N, the values for room temperature being represented by dashed curves, the corresponding values for liquid air temperature by full drawn lines. ρ_p—the anisotropies of the pure metal for the two temperatures—is taken as axis of reference and is seen to coincide with the admixtures Cu (see Part C, 1a), Sb (see Part C, 1c) and the average of the Ag crystals (see Part C, 1b). In order to show the dependence for small concentrations, the left side of the diagram is repeated in a large scale in the right upper corner. One realizes that the curves for room temperature for electro-

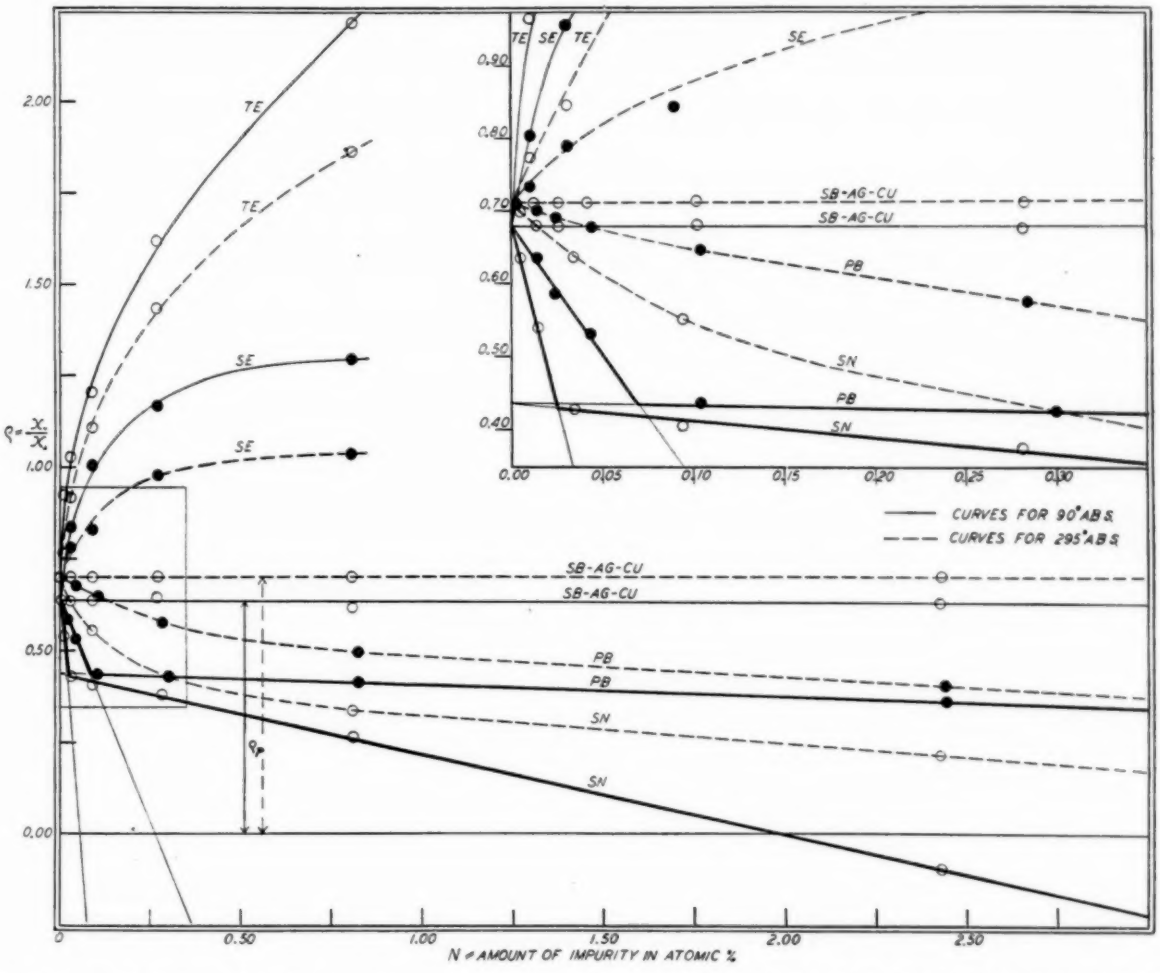

FIG. 15. $\rho - N$ diagram for electropositive and electronegative admixtures at liquid air and room temperature. The diagram in the right upper corner represents only small concentrations on a magnified scale.

positive admixtures lie almost perfectly symmetrical to the curves for electronegative atoms if taken with reference to the pure metal. Pb and Ge correspond to Se and Te to Sn as indicated by their position in the periodic system (see Section 2).

This symmetry as well as the general parabolic shape of the curve disappears at liquid air temperature where the electropositive curves are changed into two linear dependences which change their direction abruptly at a certain "critical" concentration which occurs for both elements at very small values: approximately 0.027 percent for Sn and 0.08–0.09 percent for Pb. This relation is illustrated by the derivative curves of Fig. 15 in Fig. 16 for both temperatures. This sudden change of $d\rho/dN$ indicates already the fact that the mechanism of the insertion of foreign atoms in a very small concentration is different from larger concentrations, suggesting evidently the existence of two different types of solid solution. It is also important to note that this "critical" concentration, being three times larger for Pb than for Sn, occurs for almost exactly the same value of ρ. In other words: the *magnitude of the effect, admixtures of a certain valency configuration are able to inflict upon ρ for a certain (low) temperature, is definite; to produce this effect three times as many Pb (and probably also Ge atoms) atoms are necessary as Sn atoms.*

The dissimilarity of the curves in Fig. 15 on the electronegative side is only apparent and is caused by the much less distinct discontinuity of $d\chi_{\parallel}/dN$ (see Section 5.2). These relations are discussed more thoroughly after the treatment of the directional scz's (Section 7).

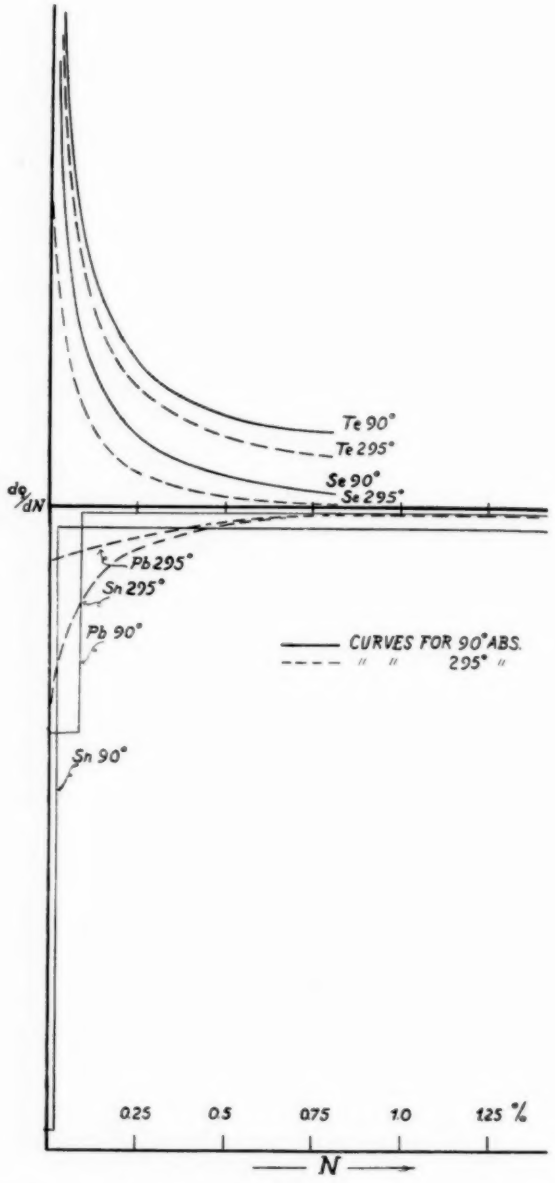

FIG. 16. $d\rho/dN=f(N)$ diagram for electropositive and electronegative admixtures. The values for room temperature are indicated by dashed, for liquid air temperature by full drawn lines.

5. The dependence of the susceptibilities $\chi_{\parallel}$ and $\chi_{\perp}$ on the concentration and the type of admixture

The described peculiar dependence of the anisotropy on the temperature and the concentration of the admixture proves beyond doubt that the insertion of an atomically soluble foreign atom follows very definite laws, in other words, there must be a definite equilibrium condition for the insertion in the two principal directions within the crystal. It was therefore very desirable to measure in addition to the ratio of the susceptibilities the absolute value of the susceptibility in at least one direction. The absolute determination of χ involves, however, the destruction of each single crystal in order to determine its exact cross section. Since this cross section, however, was of a shape not easily to be determined, the mass of the section of the crystal which was exposed to the field gradient had to be measured. Only one susceptibility

was determined and the other calculated from the known values of the anisotropy.

(5.1) *Electropositive admixtures*

The variation of the absolute values of the scz's in different directions within the crystal for electropositive admixtures is shown in Figs. 17–20. In each diagram a family of curves describes the variation at a series of temperatures from liquid-air temperature to 25° before the point of fusion. The curves for $T<75°$ are full drawn and are dashed for $T\geqq 75°$C.

(5.11) *Electropositive admixtures and scz parallel to* [111]. The almost perfect analogy of the influence of Sn and Pb is realized from comparison of Figs. 17 and 18. Since the only

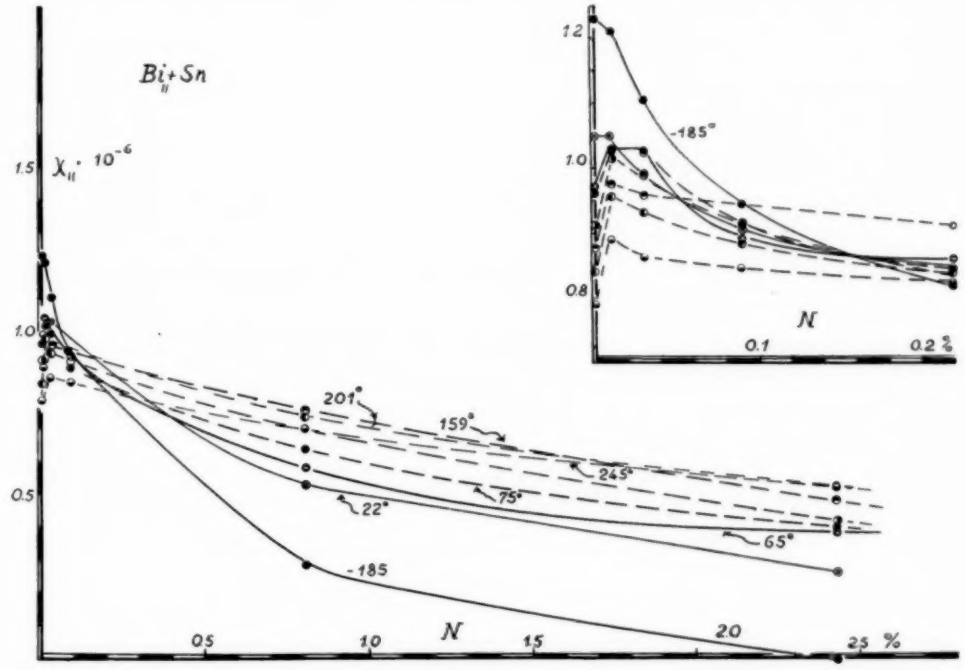

FIG. 17.

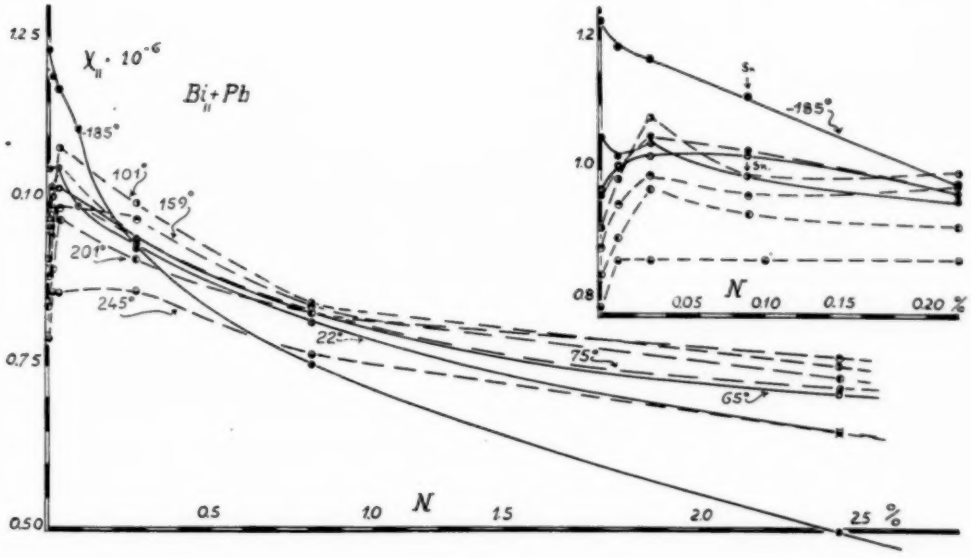

FIG. 18.

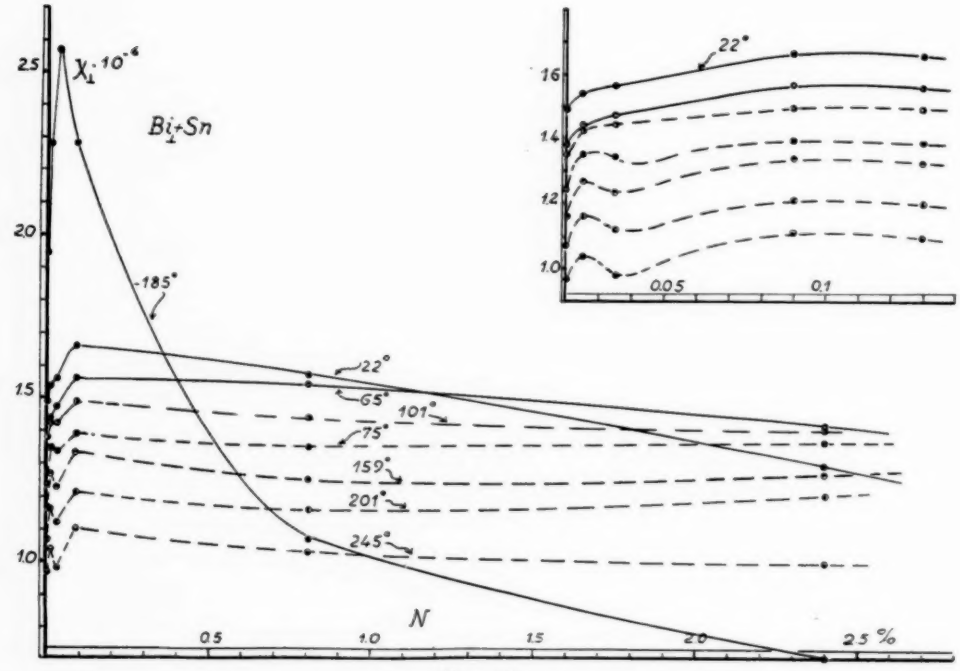

FIG. 19.

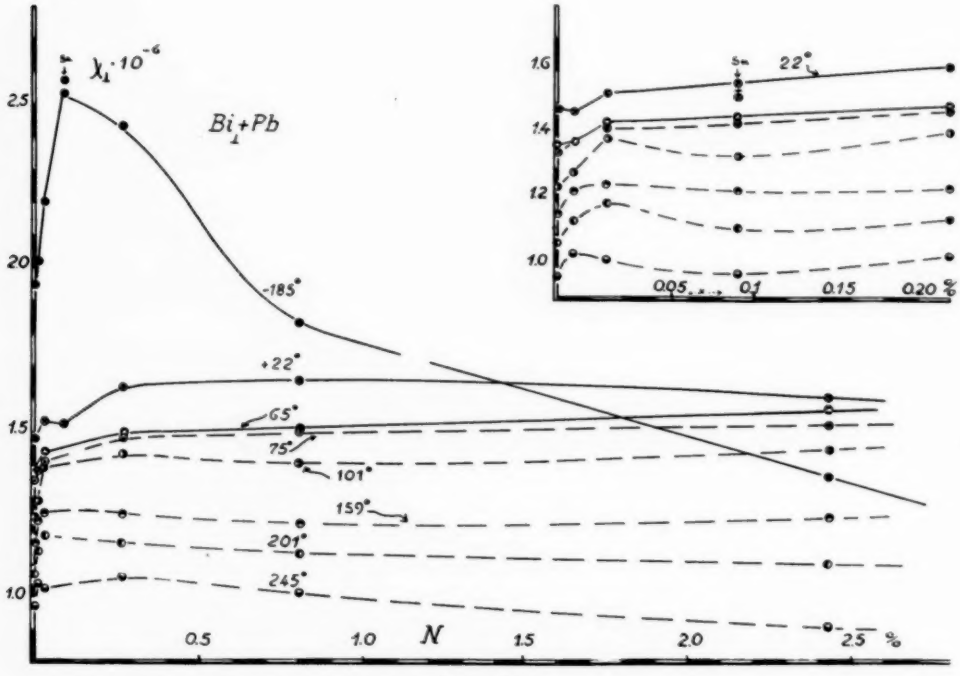

FIG. 20.

FIGS. 17–20. $\chi - N$ diagrams for electropositive admixtures (Table IV). The scale of the abscissae in all main diagrams is the same, whereas the zero point of the ordinates is different and also the scale for Fig. 18. The diagrams in the right upper corner are enlarged representations for small N; in Fig. 20 a specially large scale was chosen for the small values of the abscissa. Observations for different temperatures are indicated by points of different pattern, this being the same throughout all $\chi - N$ diagrams. The curves for $T < 75°C$ are indicated by full drawn lines, for $T \geqq 75°C$ by dashed lines. In Figs. 18 and 20 certain observations missing in Table IV are replaced by observations for Sn according to $\alpha_{Sn}/\alpha_{Pb} = 3$.

difference between these two admixtures is the value of $\alpha_{||}=d\chi_{||}/dN$, it was even possible to replace several missing Pb-observations (Table V) for 0.09 percent with Sn observations for 0.03 percent since $\alpha_{||Sn}/\alpha_{||Pb}=3$. In case both observations are present, the Sn point is marked as such.

The rather complicated relations between the different types of crystals shall be described in the following by an analogous enumeration of the four most prominent characteristics ($\alpha-\delta$) in the $\chi-N$ relation for different orientations and admixtures:

α. For *large* concentrations $\chi_{||}$ decreases with increasing concentration, i.e., $\alpha_{||}=d\chi_{||}/dN$ is negative. This holds for all temperatures.*

β. For *small* concentrations $\chi_{||}$ increases with N for temperatures larger than 75°C, i.e., $\alpha_{||}$ is positive.

γ. For *low* temperatures the sign of $\alpha_{||}$ does not show a difference between large and small concentrations.

δ. For *high* temperatures the transition from small to large concentrations is characterized by a critical concentration N_c' at which $\alpha_{||}=0$. For $N<N_c'\alpha_{||}$ is always positive, for $N>N_c'\alpha_{||}$ changes generally to negative values. The observations available at present make an independence of N_c' of the temperature probable for $T>75$°C. The most probable value of N_c' for Sn is around 0.01 percent and for Pb 0.03 percent, although it has to be realized that the uncertainty of the exact amount of the residual impurity in the Bi metal used as well as the lack of observations on very small concentrations renders this statement quantitatively uncertain.

(5.12) *Electropositive admixtures and scz normal to [111]*. Figs. 19 and 20 represent the $\chi_\perp-N$ relations analogous to Figs. 17 and 18. The relation can be described as follows:

α. Except for the lowest temperature where $\alpha_\perp$ is negative $\chi_\perp$ is practically independent on N for *large* concentrations, $\alpha_\perp\sim 0$. (Different from 5.11α.)

β. For small concentrations $\chi_\perp$ increases for all temperatures and is especially large for low temperatures. (Different from 5.11β.)

γ. For low temperatures the values for $\alpha_\perp$ are positive for concentrations smaller than a critical concentration N_c, the existence of which proves to be independent of N_c' (5.11δ). Whether or not N_c exists only for low temperatures cannot be decided yet: it is obviously much less prominent for high temperatures. The value for N_c is for Sn around 0.03 percent and for Pb 0.09 percent; these values coincide obviously with the critical concentration for the anisotropy.[4] (Different from 5.11γ.)

δ. The critical concentration N_c' for high temperatures exists with the same values in analogy to 5.11δ.

(5.2) *Electronegative admixtures*

Figs. 21 and 22 represent the variation of $\chi_{||}$ and $\chi_\perp$ with the concentration N of the electropositive admixtures Se and Te. Since the atomic solubility of Bi_2Te_3 and BiSe (see Figs. 4 and 11) are very different, abscissae of different scales were chosen.

(5.21) *Electropositive admixtures and scz parallel to [111]*. The comparison of Figs. 21 and 22 shows the very perfect analogy between the effect of Se and Te, the only difference being that the value of $\alpha_{||Se}$ is smaller than the value of $\alpha_{||Te}$. Since the production of an homogeneous crystal containing this type of admixture is very difficult, the observation especially for the high concentrations seems to be less trustworthy than the previous ones. The pattern of the points and lines follows the same system as in the previous diagrams. The results can be described as follows:

α. Except for the lowest temperature where $\alpha_{||}$ is apparently negative* it is nearly independent of N for *large* concentrations. (Same as 5.12α, different from 5.11α.)

β. For small concentrations $\alpha_{||}$ has a large positive value for all temperatures. (Same as 5.21β, different from 5.11β.)

γ. For *low* temperatures $\alpha_{||}$ is positive and the existence of N_c is definite, but it is doubtful if it holds for all temperatures. The value for N_c for Se lies at 0.09 percent, for Te around 0.01 percent. (Same as 5.12γ, different from 5.11γ.) Since the transition of $d\alpha/dN$ is much less marked, a discontinuity of $d\rho/dN$ (Figs. 15 and 16) could not be found.

* The details of the temperature dependence (χ, $\alpha=f(T)$) for this and all other types of crystals are treated separately in 6.

* The largest Te-concentration at −185° gives probably too large a value for $\chi_{||}$.

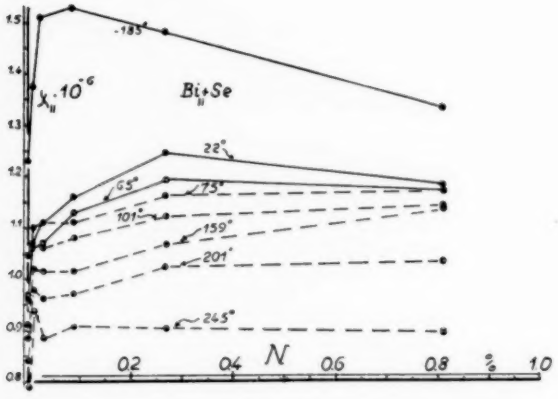

FIG. 21.

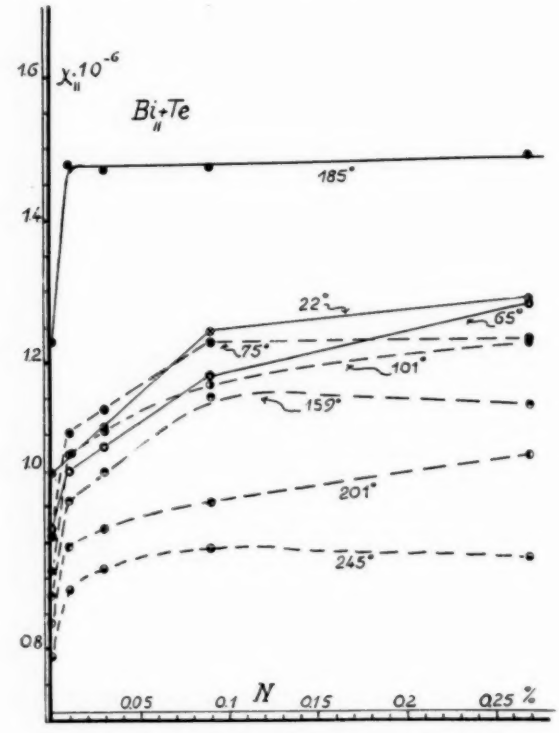

FIG. 22.

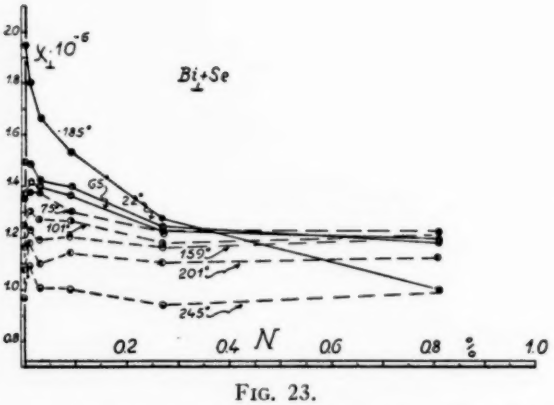

FIG. 23.

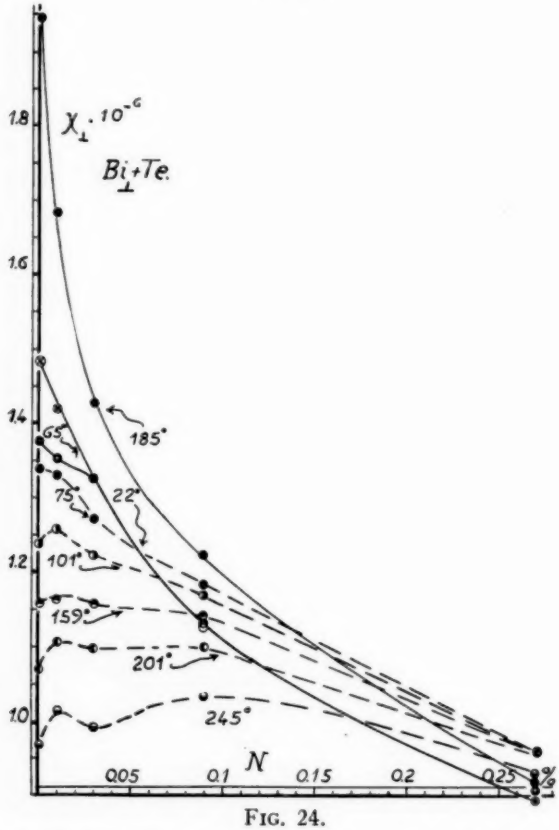

FIG. 24.

FIGS. 21–24. $\chi - N$ diagrams for electronegative admixtures (Table IV). The scale of the abscissae differs for Se and Te; the scale of the ordinate is the same for Te, but different for Figs. 21 and 23. The same pattern of observation points as in Figs. 17–20 is used and the same distinction between dashed and full drawn lines.

δ. For *high* temperatures the existence of N_c' is obvious for Se and is indicated at least for Te. (Apparently same as 5.11δ and 5.12δ.)

(5.22) *Electronegative admixtures and scz normal to* [111]. Figs. 23 and 24 represent the variations of $\chi_\perp$ with N analogous to previous diagrams; the results are:

α. $\chi_\perp$ decreases for *large* concentrations for *all* temperatures for Te and probably also for Se. (Same as 5.11α at least for Te, different from 5.12α and 5.21α.)

β. For *small* concentrations $\alpha_\perp$ is positive for $T>75$°C. (Same as 5.11β, different from 5.12β and 5.21β.)

γ. For *low* temperatures $\alpha_\perp$ has the same sign for large *and* small concentrations, i.e., N_c does not exist within the measured range of concentrations. (Same as 5.11γ, different from 5.12γ and 5.21γ.)

δ. N_c' exists for high temperatures for Se and Te. The value of N_c' is apparently the same for both admixtures at 0.01 percent. (Same as all previous δ-statements.)

(5.3) *Isomorphous admixture*

Of the two existing admixtures isomorphous to Bi—As and Sb—only Sb was measured. Fig. 25 represents the $\chi-N$ relation in the same scale (0/00) for both abscissae of which a section (from 0.04 percent to 0.25 percent) has been cut out. The scale of the ordinate varies in the usual manner.

(5.31) *Isomorphous admixtures and scz parallel to* [111]

α. For *large* concentrations $\alpha_{||}$ is very little depending upon N, being possibly positive only for high temperatures. (Almost perfect analogy to Te in 5.21α and similar to 5.12α, different from 5.11α and 5.22α.)

β. For *small* concentrations $\alpha_{||}$ has positive values for low and high temperatures. (Similar to 5.12β and 5.21β, different from 5.11β and 5.22β.)

γ. The existence of N_c is marked for the lowest temperature, although the value of $\chi_{||}$ for $N\leqq N_c$ is much smaller than in previous cases. The value of N_c is around 0.01 percent. (Analogous to 5.12γ and 5.21γ, different from 5.11γ and 5.22γ.)

δ. The critical concentration N_c' exists for high temperatures at 0.01 percent, being identical with N_c. (Same as all previous δ-statements.)

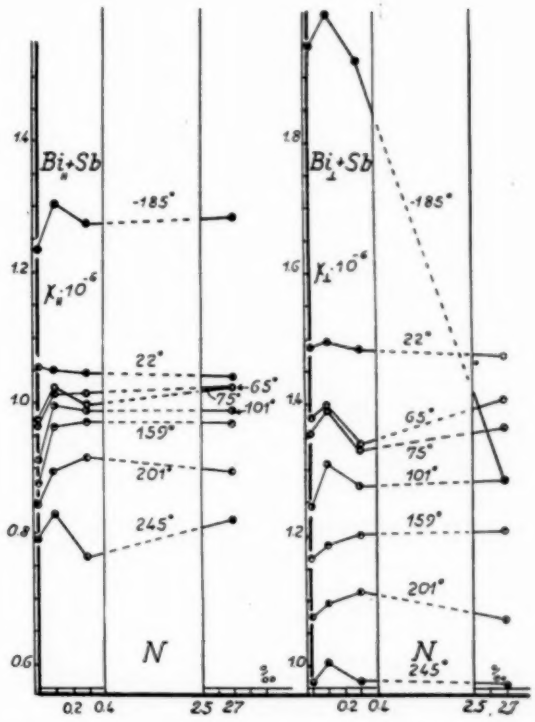

FIG. 25. $\chi-N$ diagram for the isomorphous admixture Sb (Table IV). The scales for the abscissae and the ordinates are identical, though the zero for the latter is different. The concentration between 0.04 percent and 0.25 percent is omitted, the N scale is marked in per mil. The pattern of the points is the same as previously, no distinction between lines is made.

(5.32) *Isomorphous admixtures and scz normal to* [111]

α. For *large* concentrations $\alpha_\perp$ is negative for low temperatures and very small (perhaps 0) for higher temperatures. (Same as 5.12α and 5.22α, different from 5.11α, 5.21α (?) and 5.31α.)

β. For *small* concentrations $\alpha_\perp$ is positive for high and low temperatures. (Similar to 5.12β, 5.21β and 5.31β, different from 5.11β and 5.22β.)

γ. The existence of N_c is marked, although the value of $\chi_\perp$ for $N\leqq N_c$ is much smaller than in previous cases. N_c lies around 0.01 percent. (Analogous to 5.12γ, 5.21γ and 5.31γ.)

δ. N_c' exists for high temperatures at 0.01 percent. (Same as all previous δ-statements.)

(5.4) *Summary concerning the* $\chi-N$ *relations*

It appears from the above statements that the effects of different types of admixtures in different directions within the crystal show a number of characteristic similarities and differences. These relations are seen easily from Table VIII.

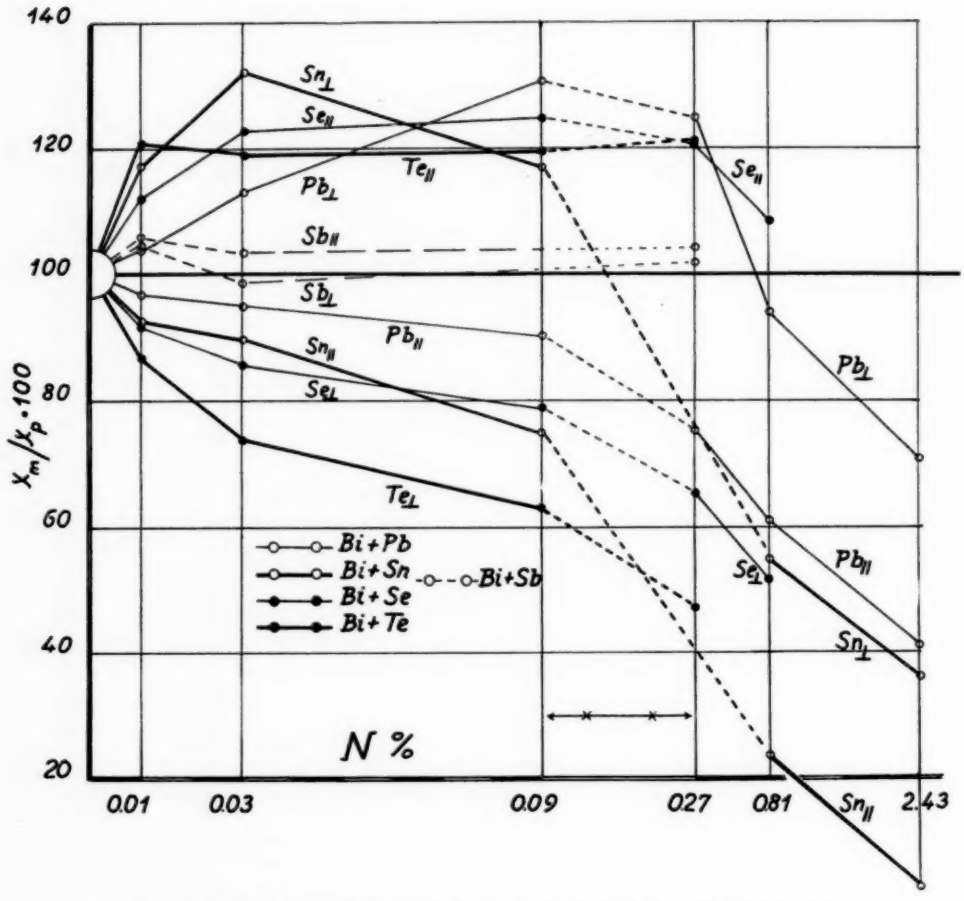

FIG. 26. The values of the relative scz's $\chi_r = \chi/\chi_p$ is plotted against N for all types of admixtures and all orientations. The abscissa consists of two different scales for $N<0.09$ percent and $N>0.27$ percent. The values refer to $T=-185°C$. (Table V.)

TABLE VIII. $\chi - N$ *relations.*

No.	large N	small N	N_c	N_c'	0, to [111]	Admixture	
5.11	$\leqq 0$	<0	none	{0.01% Sn, 0.03% Pb}	$\parallel$	electropositive	
5.12	$\leqq 0$	>0	{0.03% Sn, 0.09% Pb}	{0.01% Sn, 0.03% Pb}	$\perp$	electropositive	
5.21	$=0$	>0	{0.09% Se, 0.01% Te}	0.01%	$\parallel$	electronegative	
5.22	$=0$	<0	none	0.01%	$\perp$	electronegative	
5.31	$=0$	>0	0.01%	0.01%	$\parallel$	isomorphous	
5.32	$\leqq 0$	>0	0.01%	0.01%	$\perp$	isomorphous	

Certain similarities of the effects of different admixtures at *high* temperatures are apparent; here α is either slightly negative or zero for *large* N: the CDm is very little affected by a large concentration, the scz is generally slightly larger than of pure Bi.

All *small* concentrations increase the CDm up to a critical concentration N_c' which is apparently for all admixtures the same (0.01 percent) except for Pb (0.03 percent) which observation may be uncertain due to the fact that the most prominent residual impurity in Bi (*F*) and (*G*) is Pb (Table I).*

* The existence of N_c' depends of course on the correctness of the measurement of pure Bi at different temperatures and since the purity was not absolute the α-values for small concentrations are not quite correct, i.e., it could be that N_c' did not exist at all if the observed temperature coefficients $\gamma_{||}$ and $\gamma_\perp$ were too large. It is however seen easily that the values of χ at N_c' for different admixtures vary to a much larger extent as γ_p (γ for pure Bi) could vary, which fact would then result in the existence of a minimum for χ at N_c' in some cases and in a maximum in others.

The main similarity at *low* temperatures is best illustrated by plotting the relative scz's χ_r (in percent) against N for all types of admixtures, (Table V, Fig. 26). It is seen that here the CDm is very much affected by all types of admixtures (except by the isomorphous type), the effect being the *same* for *large* concentrations for both directions within the crystal, such that the scz *decreases* considerably.*

The most striking difference between electropositive and electronegative types of admixtures for *small* concentrations is their effect in different directions within the crystal, apparent from the varying occurrence of the critical concentration N_c. The relation can be summarized: *An electropositive admixture acts upon the CDm in the same way normal to the axis as an electronegative admixture parallel to it and vice versa.* A small concentration of an *electropositive* admixture *increases* the CDm *normal* to [111] to almost the same extent as an electro*negative* does *parallel* to [111], whereas the CDm is *decreased* by an electro*negative* admixture *normal* to [111] to approximately the same values as is done parallel to [111] by an electro*positive* admixture. Accordingly N_c exists in the cases 5.12 and 5.21 and is missing in 5.11 and 5.22. The magnitude of the effect produced on χ_r at N_c (Fig. 26) is almost the same (30–32 percent) for electropositive admixtures and seems to be slightly smaller for electronegatives (20–25 percent). Whether this difference is true or only apparent due to lack of a sufficient number of concentrations neighboring N_c cannot yet be decided. The values of N_c range as follows: Te, Sn, Se= Pb.

This commensurability does not hold for the *isomorphous* admixture Sb. First, the absolute magnitude of the influence is much smaller (only 1/8 to 1/10 of the previous effects), second, it stands in the middle between the two previous types because of the existence of N_c normal *and* parallel to [111]. Also for *large* concentrations the resemblance to electropositive admixtures is indicated *normal* to [111] and to electronegatives parallel to [111] (5.32=5.12, 5.31=5.21). Though the effects are close to the range of experimental error it seems thus probable that *normal to [111] the isomorphous admixture behaves electropositive and parallel to [111] electronegative.*

In order to illustrate the variation of α for large and small concentrations for the different types of admixtures and different orientations, the dependence of $d\chi_r/dN-\alpha_r$ on N obtained by differentiation of the curves in Fig. 26 is shown in Fig. 27 for electropositive and in Fig. 28 for electronegative admixtures for liquid air temperature. The value of this representation is only on the qualitative side since the number of observations is not by far sufficient for a quantitative evaluation. Accordingly the presentation is chosen such that the logarithms of α_r for $\alpha_r>1$ and $\alpha_r<(-1)$ are plotted in opposite directions against $\log N$, thus neglecting the small values of α_r. The analogy of $\alpha_r(N)$ in Fig. 27 for Sn and Pb is obvious: $\alpha_{r\perp}$ has large positive values for $N<N_c$ and changes its sign for $N>N_c$, *at a certain concentration (approximately 0.09 percent for Sn, 0.81 percent for Pb) the difference between* $\alpha_{r\parallel}$ *and* $\alpha_{r\perp}$ *disappears*, i.e., the directional influence of the admixture ceases to exist. This fact can be realized already from the parallelity of the α_r-N curves for large N in Fig. 26. The function $\alpha_r(N)$ for electropositive admixtures in Fig. 28 shows a similarity to the above as far as the change of sign of α_r at N_c is concerned, the difference consists in the values of $\alpha_{r\perp}$ for small N which indicate a straight line relation. Since the larger concentrations for Te were not reliable it is uncertain whether or not Te behaves similar to Se as far as the disappearance of the difference between $\alpha_{r\parallel}$ and $\alpha_{r\perp}$ is concerned. Se shows in any case the same analogy to Pb as was seen before in Table V. From the fair parallelity of the Pb and Se lines in Fig. 26 for large N results also that the absolute values of α_r in this region for both admixtures are the same.

The differences between the α_r-values become much smaller for high temperatures for the directional effect as well as for different elements.

Considering the different influences of admixtures of the same valency configuration the following can be said: The fact that the specific influence is largest (N_c smallest) for Te and Sn indicates that the disturbance within the crystal is largest by atoms of a structure $\nu-1$ where ν

* It does not seem probable that Te is an exception (see 5.21) mainly since Te could not be admixed in sufficiently large concentrations.

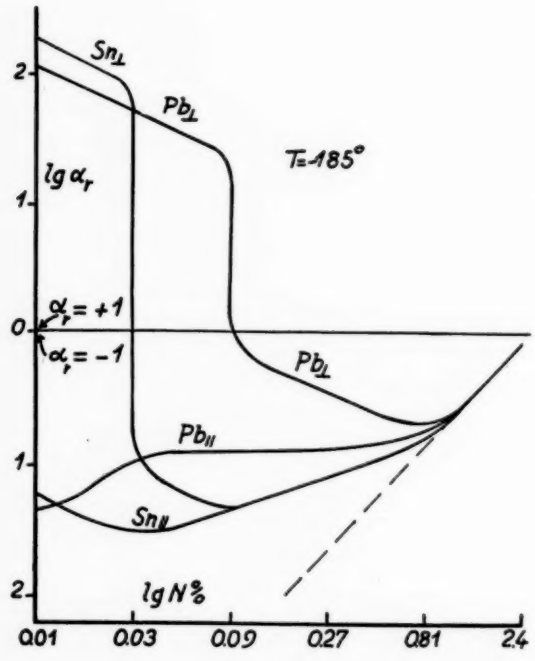

FIG. 27.

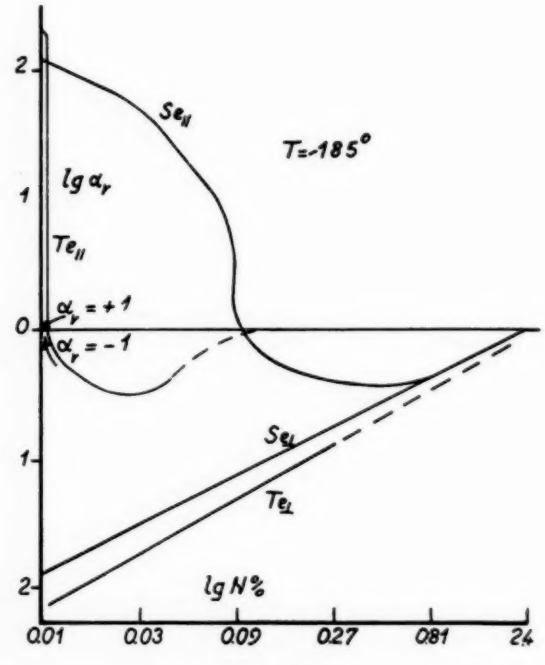

FIG. 28.

FIGS. 27–28. $\alpha_r - N$ diagram for electropositive[27] and electronegative[28] admixtures (Table V). The ordinates are arranged in such a manner that the logs of $\alpha > 1$ are plotted above the zero line and for $\alpha < (-1)$ are plotted below; the abscissa represents log N. The diagram is only a schematic representation of the most probable values of $\alpha_r = f(N)$ at $T = -185°C$.

is the level of the outermost completed shell of the crystal atom, i.e., the 0-shell for Bi. (See Table VII.) If the structure is the same as the structure of the crystal atom $(=\nu)$ the inserted foreign atom is apparently too similar to cause a disturbance as large as in the previous case. This is indicated already by the fact that the solubility of Pb in Bi is larger than of Sn in Bi. (See Figs. 2 and 3.) One should thus expect that the specific influence of Po would be smaller than of Te. If, on the other hand, the structure is of the type $\nu - 2$, the actual size of the atom seems to be too small to affect the crystal as is the case for Se and Ge where the last completed shell is on the M-level. Here the effect is smaller in comparison with the $\nu - 1$ type and commensurable with the ν-type. One should accordingly also expect that in case of a Sb-crystal the maximum influence should be found for Ge and Se instead of Sn and Te for a Bi crystal.

6. The dependence of the susceptibilities $\chi_{\parallel}$ and $\chi_{\perp}$ on the temperature

The dependence of the scz of pure Bi on the temperature is *linear* within the limits of experimental error, such that in both directions the CDm *increases* with *decreasing* temperature.*

If γ (see Eq. (2)) is the temperature coefficient in the usual definition:

$$\gamma = (1/\chi_0)(\chi_T - \chi_0)/(T - T_0) \qquad (3)$$

and if χ_0 is taken for $22°C = T_0$

$$\gamma_{\parallel} = -1.1 \pm 0.05 \times 10^{-4} \text{ deg.}^{-1},$$

$$\gamma_{\perp} = -1.5 \pm 0.08 \times 10^{-3} \text{ deg.}^{-1}.$$

Hence the dependence of CDm on the temperature is 40 percent larger normal to [111] i.e., in the direction of the densest packing then parallel to [111], the direction of the least dense packing.

This simplicity of the temperature dependence is changed very much by an admixture as is seen easily from the $\chi - N$ diagrams. The data of Table V were used for plotting the scz against the temperature for a number of characteristic

* The fact that ρ is also a linear function of the temperature (see Part C, Section 3) is caused by the small magnitude of the temperature coefficient which renders a deviation from linearity unobservable.

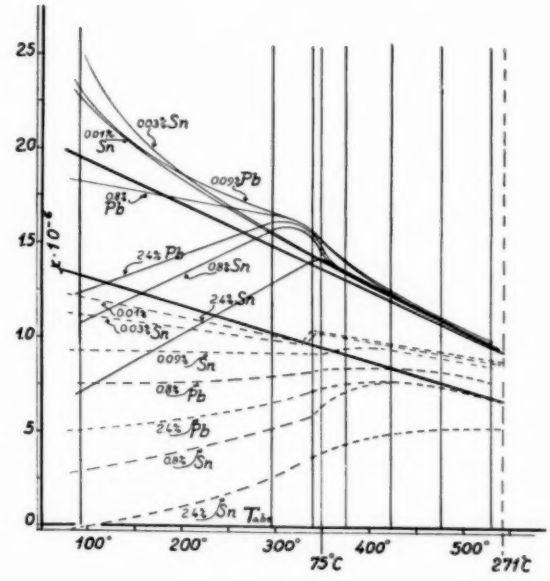

FIG. 29.

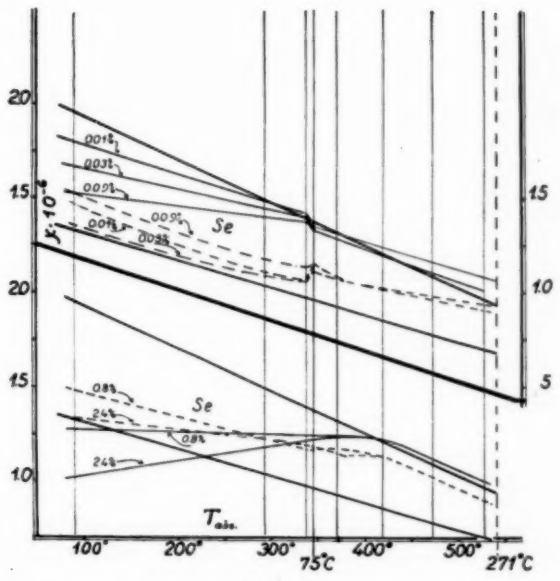

FIG. 30.

FIGS. 29–30. $\chi-T$ diagrams for electropositive[29] and electronegative[30] admixtures (Table IV). The scales of the coordinates are the same in both figures. The heavy drawn lines indicate χ_p (Bi "F") for both directions. The observed points are indicated by the intersection of the curves with the lines of equal temperature. The diagram Fig. 30 is divided into two: the upper (right and upper left scale) for $N \leqq N_c$, the lower (lower left scale) for $N > N_c$. In both figures the direction normal to [111] is indicated by full drawn, parallel to [111] by dashed lines.

concentrations for electropositive and electronegative admixtures in Figs. 29 and 30. The isomorphous admixtures were omitted on account of their very small temperature dependence.

(6.1) *Electropositive admixtures*

Fig. 29 represents the $\chi-T$ relations for electropositive admixtures from $-185°$ to $+245°$C for both principal directions in the crystal, the *normal* direction being drawn in *full* lines.

(6.11) *Electropositive admixtures parallel to [111]*

α. For *small* concentrations (N_c does not exist according to 5.11γ) and $T<75°$ the temperature coefficient γ of $\chi_{||}$ is smaller than for χ_p (χ_p of pure Bi) but still negative. Around 75° a positive discontinuity takes place, the exact temperature of which cannot be determined due to lacking observations. For $T>75°$C $\chi_{||}$ becomes larger than $\chi_{p||}$ whereas γ does not change appreciably. Below 75°C the admixture decreases the CDm, above it the opposite is true.

β. The behavior for *large* concentrations does not show typical differences. With increasing N γ decreases still further for $T<75°$ and becomes for very large concentrations positive. Here the discontinuity at 75° is marked much *less* and disappears finally in a point of inflection. At high temperatures $\chi_{||}$ is larger than $\chi_{p||}$ for the smaller concentrations and considerably smaller than $\chi_{p||}$ for the highest concentration; γ is slightly smaller than γ_p.

(6.12) *Electropositive admixtures normal to [111]*

α. For $N<N_c$ and $T<75°$ the scz is larger than χ_p, the same being true for γ. Hence the effect of the admixture decreases fast with the temperature towards χ_p as an asymptote. The transformation point at 75° is *not* marked.

β. For $N>N_c$ the temperature coefficient grows smaller with increasing N and reaches positive values for the highest concentrations analogous to 6.11 β, although the magnitude of γ is much larger. The difference with 5.11 β consists mainly in the occurrence of a maximum between 20 and 100°C. The transformation point is *marked* by a negative discontinuity beyond which all χ-values approach closely the values of the pure metal.

(6.2) *Electronegative admixtures*

The $\chi-T$ relations of the electronegative admixtures are represented in Fig. 30 in the same

scales. Since the effects of these admixtures go in the opposite direction, the diagram was divided in two: one for $N \leqq N_c$ and one for $N > N_c$, the abscissa being the same for both.

(6.21) *Electronegative admixtures parallel to [111]*

α. For $N < N_c$ and $T < 75°$ γ stays practically unchanged similar to 6.11 α. At $T = 75°$C the discontinuity is *positive*. Above 75°C χ becomes considerably larger than χ_p and γ slightly smaller than γ_p.

β. For $N > N_c$ and $T < 75°$C γ approaches zero with increasing N and is positive for the large concentrations. The transformation point is less distinct. For high temperatures the analogy with 6.11 β holds also with the only difference that $\chi_{||}$ is apparently only for the largest Te concentrations smaller than χ_p.

(6.22) *Electronegative admixtures normal to [111]*

α. For $T < 75°$ χ decreases with decreasing γ. The transformation point is marked by a negative discontinuity and the approximate equality of $\chi_\perp$ and χ_p. For higher temperatures γ is smaller than γ_p and $\chi_\perp$ is but slightly larger.

β. For *large* concentrations γ becomes more positive with increasing N. Though the discontinuity at 75°C is doubtful, it is of interest to see that in the neighborhood of this point the reversal of $\chi_\perp$ and $\chi_{||}$ takes place, such that above 75° $\chi_\perp$ is always larger than $\chi_{||}$, i.e., above 75° a dissimilarity of the anisotropy of the crystal does not exist regardless to the effect of the admixture. For $T > 75°$ $\chi_\perp$ approaches χ_p and $\gamma = \gamma_p$ in close analogy to 6.12 β.

(6.3) *Summary concerning the $\chi - T$ relation*

In realization of the fact that the number of observations as well as the accuracy of the measurements is not sufficient to ascribe a reality to the smaller variations the results are much simpler than for the $\chi - N$ relation; they can be summarized as follows:

α. In contradistinction to the $\chi - N$ relation *the $\chi - T$ function does not show any fundamental difference between electropositive and electronegative admixtures.*

β. *The effect of admixtures is different above and below 75°C. Above 75°C the influence is much smaller, though different for the two directions:* it is smallest (if existing at all) normal to [111] and comparatively large parallel to [111]. In the latter case the CDm is always increased except for the largest concentrations of electropositive admixtures (see 6.12 β). Otherwise there is no difference between different types.

γ. *The transformation point at 75°C is marked in the same way for all admixtures for small concentrations* by a discontinuity which is *positive for $\chi_{||}$ and negative for $\chi_\perp$*. No discontinuity was found for pure Bi in either direction, neither is it present (or at least so distinct) for $N \gg N_c$. The existence of a discontinuity for large concentrations seems improbable.

δ. For temperatures *below* 75°C the differences between different types of admixtures become increasingly larger with decreasing temperature: with it increases the influence of the temperature. *The effect of temperature in this range works always toward a greater similarity with the pure crystal regardless of the sign of the influence of the admixture, i.e., the absolute value of α is always decreasing with increasing temperature.*

7. Hypothesis regarding the influence of admixtures upon the CDm

The interpretation of the influence of admixtures upon the CDm is only possible along two lines: the assumption of a *volume*—or a *surface* effect. For the volume effect one has to assume a superstructure caused by the admixture similar to the many other systems of intermetallic solutions already studied. The existence of a critical concentration (N_c) indicating a certain saturation of the crystal with B atoms, means the completion of such a superstructure. If one considers however the values of N_c one obtains for the "effective radii" of the B atoms $= (1/N_c)^{\frac{1}{3}}$ expressed in A atoms the values: Te = 21.5; Sn = 14.9; Se = Pb = 10.3 and one arrives at elementary units in a crystal which contain 10^3–10^4 atoms which is highly improbable. Furthermore if such B atoms should cause a gradual distortion of the A lattice, one should have a periodicity equivalent to those radii, i.e., of the order of the depth of penetration of normal x-rays (e.g., in Bi for Mo $K\alpha$), which however should affect the intensity of the directed scattered radiation considerably. Such effect has not been observed.

A much more probable interpretation seems to be the following one which has the advantage of

accounting for almost the entire phenomenology of the effect. Following the hypothesis of Ehrenfest-Raman (see Part A, Section 1) concerning the CDm we assume large orbits of "free" electrons within the crystal. Since the scz is proportional to the areas circumscribed by these orbits, it must be proportional to $\lambda^2(\lambda = \text{m.f. path})$: only the largest paths contribute to the CDm. There is furthermore sufficient evidence that in a crystal certain directions are preferred for the propagation of the electrons, such that in an anisotropic crystal the components of the paths in different directions are different. Hence $\chi_{\parallel}$ equals the sum of components of all electron orbits normal to [111] etc.

If for *low* temperatures and *small* concentrations the assumption is made that the *B* atoms are not scattered at random throughout the crystal but are adsorbed in certain crystallographic planes which reoccur periodically over the whole volume of the crystal the smallness of N_c is easily understood. Such a superstructure of planes will cause potential barriers to the "free" electron owing to the different nature of the *B* atom; consequently the paths larger than the parameter of such a structure will be shortened and the electron will be scattered in different directions. The number of such scattered electrons will depend on the "opacity" of the wall, which in turn depends on the type and the density of the adsorbed *B* atoms. It is reasonable to assume that the capacity of the planes is filled if a mono- or bimolecular layer of *B* atoms is present, this being identical with the critical concentration N_c. It is obvious that such a mechanism can only shorten the path, i.e., *decrease* the CDm.

In case of an anisotropic crystal there are no planes of the same order parallel and normal to the principal axis, hence the stability of an atom adsorbed in a plane normal to [111] is different from its stability in any other plane. From this follows that the growing opacity of one type of planes will not necessarily affect the opacity of other types. Such a process results in the shortening of only *one* path-component, the other path-component is not affected: the number of electrons with the latter component will however increase: the CDm will *decrease* in one and *increase* in the other direction for approximately the same amount, which actually occurs. Furthermore: this latter component cannot be increased indefinitely as a complete opacity of the plane will only scatter a limited number of electrons. This means that for N_c the increase and the decrease must be independent from the type of *B* atoms, which is the case for Pb and Sn. (Figs. 15 and 26.) The fact that, e.g., 3 times as many Pb as Sn atoms are used for reaching N_c can be interpreted by the geometrical arrangement of the atoms in the plane, of which a suggestion is made in Fig. 31. The same result could be reached by assuming

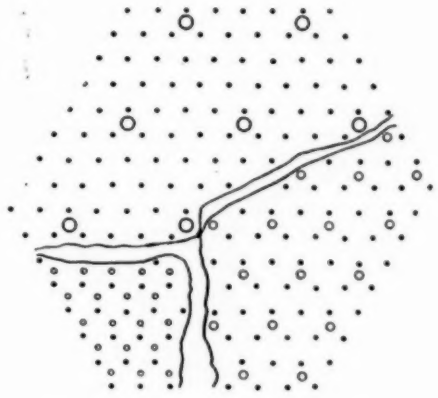

FIG. 31. Scheme of three different types of adsorption of B atoms on a (111) plane. The black dots represent Bi atoms, the smallest circles are B atoms adsorbed at the rate 1 : 1, the medium circle B atoms 1 : 3, the large circles for B atoms 1 : 9.

a different periodicity of the planes, but it is obvious that in this case the previous condition of equal increases or decreases for N_c would not be fulfilled.

An anisotropic crystal has a polarity asymmetric with respect to the principal axis, hence it can be understood that electropositive *B* atoms are more stabile in planes of a certain direction than in another. Accordingly α is quantitatively the same in opposite directions for admixtures of opposite type. With regard to the actual situation of these planes the following conclusion has to be drawn:

Since for $N = N_c$ *the scz increases* $\frac{\text{normal}}{\text{parallel}}$ *to* [111] *for electro* $\frac{\text{positive}}{\text{negative}}$ *B-atoms, the number of electrons with path-components* $\frac{\text{parallel}}{\text{normal}}$ *has increased by scattering on a wall* $\frac{\text{parallel}}{\text{normal}}$ *to* [111].

Since there is no prominent plane on Bi which is parallel one has to assume three with a large component in this direction which is either $(11\bar{1})$ or perhaps (110), both planes being predominant in the formation of the etch figures.[26] It may be added that sufficient evidence for such a difference between crystals containing electropositive and electronegative admixtures has been found in etch figures by one of us (G) and the existence of Te in (111) planes seems to be proved.

If one assumes the pseudo-octahedral planes to be equal to each other and also that N_c characterizes a concentration where each Bi atom on the wall is covered by a B atom one obtains for the distance between the (111) plane 0.4–0.5 micron which is in very good agreement with the measured depth of a primitive etch figure. It is also well within the magnitude of the critical sizes of the CDm of fine powders (see Part A, Section 1).[9–12]

An *isomorphous* atom (Sb) causes a much smaller disturbance because of its similarity with A. The small dissimilarity will also for small concentrations cause a higher stability in a plane than in the volume, though the difference of stability for different planes is probably exceedingly small which is a satisfactory reason for the statement in Section 5.4.

For $N > N_c$ one has to assume that gradually other planes with lower affinities are filled which destroy the increase gained by blocking the paths also in this direction. Thus the gain of CDm will be lost and α becomes negative. If admixtures are added even after all planes are filled (indicated probably by $\alpha_\perp = \alpha_{||}$ (Fig. 27)) they distribute themselves over the volume until also this is saturated (limit of the metallographic solubility). For this region a general decrease of the CDm and small values for α should be expected which agrees with the observations.

Analogous to similar hypotheses the authors have given in an earlier paper,[48] one should expect that at higher temperatures the boundaries become less sharp and the effect of the B atoms becomes much smaller: the difference between the stabilities of the B atom in the volume and in the plane becomes less.

Very little can be said about the nature of the concentration N_c' as long as the theoretical analysis of the CDm is as little developed.

The above hypothesis leads one to postulate similar effects though smaller in magnitude ($\sim\lambda$) for the conductivity and the thermal e.m.f. in Bi crystals containing B atoms. One has to realize though that these phenomena must be affected in the *opposite* direction within the crystal. One of us (F) has measured an *increase* of the conductivity *parallel* to [111] for small concentrations of Te and a *decrease* in the *same* direction for Sn admixtures. Dr. M. F. Hasler could prove a similar relation for the thermal e.m.f.'s.

In case of a macroscopic solubility (Ag) (see Part C, Section 1), the dissimilarity between A and B atoms is so large that their insertion will work completely at random, i.e., increasing or decreasing the anisotropy (Fig. 9).

Finally something remains to be said about the pseudoallotropic transformation point at 75°C. The question of its existence has been discussed by many authors, though no definite interpretation of its nature has yet been obtained. Goetz and Hergenrother[31] proved by x-ray analysis that the lattice structure does not undergo a change, whereas the observation of a Peltier heat[28] as well as of a change in the macroscopic thermal dilation[45] seems to prove the existence of a discontinuous change in the electron configuration over crystal complexes too large to be seen by x-rays (mosaic structure). Recently J. A. Hedvall and his collaborators[46] have confirmed the existence of a discontinuity of the macroscopic expansionof pure Bi and in addition to this they have found a distinct change in the tendency of chemical reaction (*chemische Reaktionsfähigkeit*) between 74° and 76°C.* For the CDm this point is characterized by a negative discontinuity normal and a positive discontinuity parallel to [111], being absent for pure Bi and for high concentrations (Section 6.3). One is probably not far from reality by assuming that the plane structure above this point becomes unstable, which breakdown of the walls causes the surface effect to disappear in a volume effect. Hence the existence of the point is only marked for a large surface effect, i.e., not for large concentrations and not for pure metal. Furthermore

* Through the kindness of Professor Hedvall the senior of the authors had a chance of a discussion on this subject by letter before the article appeared, for which courtesy he wishes to express his sincere obligation.

the influence of admixtures is small above this point and exists practically only parallel to [111], suggesting the possibility of the disappearance of only one type of plane.

A more detailed discussion of the possible nature of this transformation point in connection with this hypothesis will be published soon.

It is a pleasant duty to thank a number of persons for their contributions to this paper: Professor L. M. Dennis of Cornell University for donating the Ge metal, Professor S. J. Barnett of the University of California for the loan of the electromagnet, Dr. M. F. Hasler for the spectroscopic analysis of the metals, Dr. R. C. Hergenrother for its distillation, Mrs. S. Scott-Korff for help in the computation and Mr. J. H. Darlington for general assistance during the later phase of the experiments.

Bibliography

[1] A. B. Focke, Phys. Rev. **36**, 319 (1930).
[2] A. Goetz and A. B. Focke, Science **74**, 603 (1931).
[3] A. Goetz and A. B. Focke, Phys. Rev. **38**, 1569 (1931).
[4] K. Honda, Ann. d. Physik **32**, 1027 (1910).
[5] K. Honda, Sc. Rep. Tohoku Univ. I **1**, 1 (1912).
[6] F. Bitter, Phys. Rev. **36**, 978 (1930).
[7] F. E. Lowance and F. W. Constant, Phys. Rev. **38**, 1547 (1931).
[8] G. Borelius, C. H. Johansson, J. O. Linde, Ann. d. Physik **86**, 291 (1928).
[9] V. J. Vaidyanathan, Ind. J. Phys. **5**, 559 (1930).
[10] S. R. Rao, Ind. J. Phys. **6**, 241 (1931).
[11] R. N. Mathur and M. R. Varma, Ind. J. Phys. **6**, 181 (1931).
[12] S. Paramasivan, Ind. J. Phys. **4**, 139 (1929).
[13] J. H. Van Vleck, Electr. and Magn. Susceptb. XII, 359.
[14] P. Ehrenfest, Physica **5**, 388 (1925).
[15] P. Ehrenfest, Zeits. f. Physik **58**, 719 (1929).
[16] C. V. Raman, Nature **123**, 945; **124**, 412 (1929).
[17] C. H. Johansson and J. O. Linde, Ann. d. Physik **5**, 762 (1930).
[18] H. Endo, Sc. Rep. Tohoku Univ. **14**, 479 (1925); **16**, 201 (1927).
[19] J. F. Spencer and M. E. John, Proc. Roy. Soc. **A116**, 61 (1927).
[20] Y. Shimizu, Sc. Rep. Tohoku Univ. **21**, 826 (1932).
[21] B. Otani, Sc. Rep. Tohoku Univ. **13**, 293 (1925).
[22] P. Barlow, Zeits. f. Anorg. Chemie **70**, 183 (1911).
[23] A. Bucher, Zeits. f. Anorg. Chemie **98**, 117 (1916).
[24] B. Monkemeyer, Zeits. f. Anorg. Chemie **46**, 419 (1905).
[25] K. Honda and T. Sone, Sc. Rep. Tohoku Univ. **2**, 1 (1913).
[26] A. Goetz, Proc. Nat. Acad. Sci. **16**, 99 (1930).
[27] A. Goetz, Phys. Rev. **35**, 193 (1930).
[28] A. Goetz and M. F. Hasler, Phys. Rev. **36**, 1752 (1930).
[29] R. C. Hergenrother, Physics **2**, 63 (1932).
[30] A. Goetz and R. Jacobs, still unpublished.
[31] A. Goetz and R. C. Hergenrother, Phys. Rev. **40**, 643 (1932).
[32] A. B. Focke, Thesis, Cal. Inst. Tech. 1932.
[33] C. Nusbaum, Phys. Rev. **29**, 905 (1927).
[34] P. Kapitza, Proc. Roy. Soc. **A131**, 224 (1931).
[35] Int. Crit. Tabl. **VI**, 365.
[36] L. Schubnikow and W. J. de Haas, Comm. Phys. Lab, Leyden. No. 207 a. 1930.
[37] Jeriomin, Zeits. f. anorg. u. angew. Chemie **55**, 412 (1907).
[38] G. T. Petrenko, Zeits. f. anorg. u. angew. Chemie **50**, 133 (1906).
[39] Cook, J. Inst. of Metals (London) **28**, 421 (1911).
[40] Parravano, Gaz. Chim. Ital. **43**, 293 (1915).
[41] N. Tomashige, Mem. Coll. Sci, Kyoto Univ. **4**, 55 (1919).
[42] N. Agreew, M. Hansen, G. Sachs, Zeits. f. Physik **63**, 293; **66**, 350 (1930).
[43] P. Wiest, Zeits. f. Physik **74**, 225 (1932).
[44] U. Dehlinger, Metallw. **9**, 589 (1930).
[45] A. Goetz and T. L. Ho, still unpublished.
[46] J. A. Hedvall, R. Hedin, E. Anderson, Zeits. f. Anorg. Chemie **212**, 84 (1933).
[47] P. W. Bridgman, Proc. Am. Acad. **63**, 351 (1929).
[48] A. Goetz and A. B. Focke, Phys. Rev. **37**, 1054 (1931).

Precise Measurements of Dispersion in Nitrogen

CLARENCE E. BENNETT, *Eastman Laboratory, Massachusetts Institute of Technology*

(Received December 9, 1933)

A new and much improved displacement interferometer has been built after the general plan of the one previously described to measure simultaneously refractive index and dispersion constants for a gas over a range of pressures above atmospheric. It is constructed as a single unit on a steel I-beam framework 10 feet long and 2 feet wide. The whole apparatus is supported on automobile inner tubes which very effectively eliminate vibration. The features also include a G.E. S-1 sunlamp light source, aluminum mirrors, a carefully calibrated micrometer screw of high quality and an improved temperature control.

Observations made on nitrogen at four wave-lengths, 5780A, 5461A, 4359A and 4047A, corresponding to pressure runs up to 14 atmospheres measured by a Keyes dead-weight gauge, at temperatures of 50°C, 30°C and 0°C, give readings that are linear with pressure to such a degree that the Cauchy dispersion constants can be expressed to four significant figures. The results for N.T.P. conditions are: $A_0-1=0.0002932$ and $B_0=1.637\times10^{-14}$. Since A_0-1 is the extrapolated infinite wave-length refractive index, a dielectric constant $\epsilon=1.0005864$ is thus predicted. This agrees with published determinations. The refractive index at any wave-length can be computed from these results and values so calculated are found to agree with values found by other methods, which are not suitable for direct extrapolation to infinite wave-length and which are not likely to be so accurate.

INTRODUCTION

IN a previous paper[1] a method was presented for measuring the refractive index and dispersion constants for a gas over a range of pressures above atmospheric by displacement interferometry. Since that time many changes have been made in the experimental procedure which have finally resulted in the construction of an entirely new apparatus. The essential features of this new interferometer are much like those of the former one but improvements have been made in practically every important detail. Better methods have also been employed in the control and measurement of the temperature and pressure, as well as in the purification of the gas under observation. These latter changes alone have made possible a considerable extension in the range of pressures that can be used. Moreover, the manner of reducing the observations has been somewhat modified so that the results take on added significance. As a consequence of all these improvements, experimental results are obtained which are not only remarkably self-consistent and therefore precise in a relative way but also precise in an absolute sense.

[1] C. E. Bennett, Phys. Rev. **37**, 263 (1931).

THEORY

The general arrangement of the mirrors and miscellaneous optical apparatus included in the set-up of the displacement interferometer as well as the manner in which the interference pattern is established has been adequately discussed.[1] It will suffice to recall here that with this arrangement one deals with the displacements of an unsymmetrical oval dark-fringe interference pattern across a continuous spectrum in which certain wave-lengths are indicated by superposed bright or dark spectral lines, depending upon the nature of the light source used. Theory developed in the former paper[1] shows that so far as displacements of the central spot of the interference pattern are concerned,

$$\mu-1=\Delta x/e+\lambda\partial\mu/\partial\lambda, \qquad (1)$$

where μ is the refractive index of any transparent substance of length e which, upon being introduced into one path of the interferometer to replace a vacuum path of the same length, produces a shift of the central fringe which requires a displacement of the movable mirror of the instrument equal to Δx to restore the fringe pattern to its original position in the spectrum.

Eq. (1) shows that the displacement is not only

a function of the refractive index and path length of the substance in question but also depends upon the manner in which the refractive index changes with wave-length. By assuming a Cauchy dispersion relation

$$\mu = A + B/\lambda^2 + C/\lambda^4 + \cdots, \tag{2}$$

from which $\partial\mu/\partial\lambda$ can be calculated, one gets by substitution in Eq. (1) the following result:

$$\Delta x/e = (A-1) + 3B/\lambda^2 + 5C/\lambda^4 + \cdots. \tag{3}$$

Here A is of course the value of μ corresponding to infinite wave-length, a quantity which takes on physical significance as the square root of the dielectric constant of the substance.

If Δx is determined experimentally for as many wave-lengths in the spectrum as the number of arbitrary constants assumed in (2) then the same number of simultaneous equations can be set up so that values of A, B, C, etc., can be determined. Experiments show that for nitrogen gas just two constants A and B suffice to describe the dispersion to a high degree of accuracy. Therefore, under these circumstances, observations at two wave-lengths give two equations in A and B which, when solved, give

$$B = \frac{\Delta x_1 - \Delta x_2}{3e(1/\lambda_1^2 - 1/\lambda_2^2)}; \quad A - 1 = \frac{\Delta x_1/\lambda_2^2 - \Delta x_2/\lambda_1^2}{e(1/\lambda_1^2 - 1/\lambda_2^2)}. \tag{4}$$

Once the values of A and B are known (A being μ for infinite wave-length) the value of the refractive index can be calculated for any wave-length by the relation

$$(\mu - 1) = (A-1) + B/\lambda^2. \tag{5}$$

It will be noted that these results (Eqs. (4) and (5)) hold only for a given value of the density of the gas, since Δx is measured by comparison with an exhausted tube in which the gas density is zero. Experimentally it is found, however, that for nitrogen, Δx increases linearly with pressure, at constant temperature to an extremely high degree. No deviation from linearity can be detected for the observed values up to the limiting pressure of 14 atmospheres thus far attained and accurately measured. This is interpreted to mean that A and B increase linearly with density as theory suggests, because the density of nitrogen is known to depart but slightly from linearity with pressure over this restricted range. Therefore, the values of A, B and also $(\mu-1)$ can be reduced to N.T.P. conditions by means of an equation of state if they are not measured under those conditions. It is hoped that, in the near future, calculations involving the use of an accurate equation of state for nitrogen will be completed, so that a direct accurate experimental determination of the validity of the Lorentz-Lorenz relation can be made. As will be pointed out, however, the results of this paper are in no way dependent upon this determination.

The fact that Δx is linear to such a high degree with pressure in the case of nitrogen indicates that for such a gas the dispersion constants can be determined with a greater accuracy than is obtainable in a single measurement of Δx, by considering the quantity $\Delta x/p$. The determination of this quantity can be based upon any number of observations of Δx over a wide range of pressures. Furthermore, the accuracy with which Δx can be measured also increases with pressure, so that with an interferometer of this type adapted for work at high pressures it is reasonable to suppose that the dispersion constants of nitrogen for N.T.P. conditions can be determined with an accuracy not attained thus far by other observers. Under these circumstances Eqs. (4) are modified to read as follows: Where the subscript zero refers to N.T.P. conditions

$$B_0 = \frac{76.0\tau}{3e273.1}\left(\frac{\Delta x_1/p - \Delta x_2/p}{1/\lambda_1^2 - 1/\lambda_2^2}\right); \quad A_0 - 1 = \frac{76.0\tau}{e273.1}\left(\frac{(1/\lambda_2^2)(\Delta x_1/p) - (1/\lambda_1^2)(\Delta x_2/p)}{1/\lambda_1^2 - 1/\lambda_2^2}\right). \tag{6}$$

Of course, if it so happens that more than two spectral lines are available for these measurements the more appropriate procedure to obtain the highest accuracy is as follows: determine the best values of $\Delta x/p$ at each wave-length; multiply by $(\tau/273.1)(76.00/e)$ to get $\Delta x/e$; then set up as many equations like Eq. (3) as the data allow; and determine the coefficients A_0 and B_0

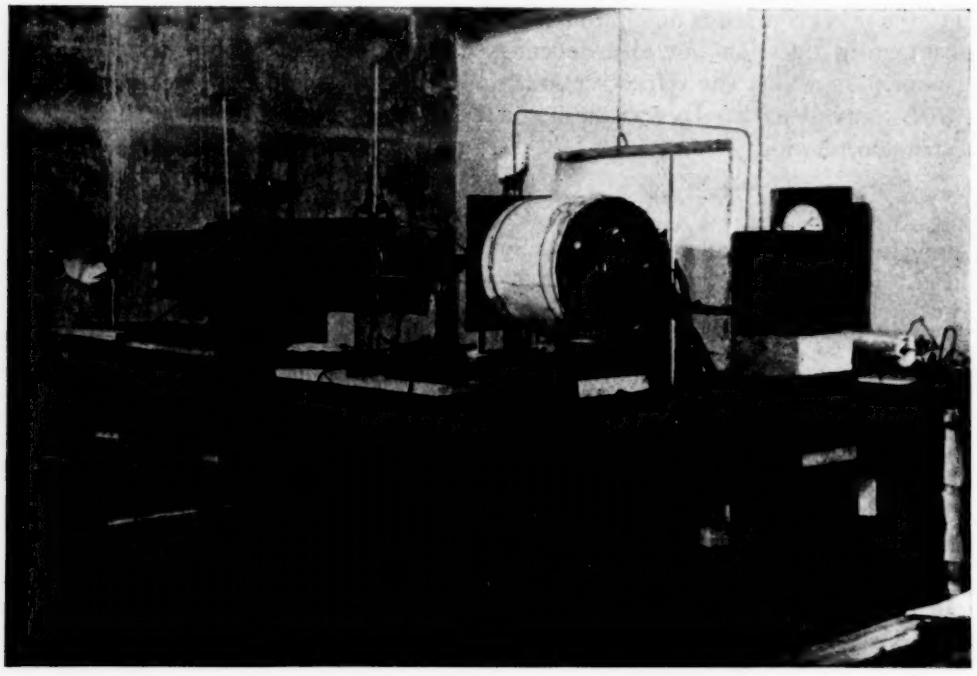

FIG. 1.

by methods of least squares. With more than two constants, however, this procedure is not feasible.

APPARATUS

In the accompanying photograph, Fig. 1, the new apparatus is shown as it is set up on a rectangular table 10 feet long and 30 inches wide with the following pieces of apparatus mounted at a fixed elevation: at the center, enclosed in a dust-proof container, a vertical semi-reflecting mirror with its face parallel to the short side of the table; at the corner of the table in the foreground the source of light; diagonally across from it, a movable vertical mirror; in the corner adjacent to the light source, a fixed vertical mirror; and diagonally across from it, adjacent to the movable mirror, a telescope with a diffraction grating mounted in front of it. The diagonal light paths, which thus lie in a plane parallel to, and at a fixed distance above the table, intersect at the surface of the semi-reflecting mirror and enclose an angle of about 20°.

The new apparatus was designed with every possible consideration given to reduce vibration to a minimum. Whereas in the former apparatus the three mirrors, separated by paths of approximately 130 cm, were mounted on independent cement piers, in the present assembly every unit was fastened to a single steel frame consisting of two I-beams 5 inches deep by 10 ft. long held parallel by cross members 2 ft. long rigidly bolted to them. This whole frame, supported on a wooden platform with a flat bottom to distribute the load uniformly, was then floated on three partially inflated automobile inner tubes uniformly spaced side by side on a specially built rigid pipe-leg table, itself resting on sponge rubber squares under each of its eight legs. The mirrors were fastened to short sturdy rods projecting out of specially constructed cement blocks approximately $11\times11\times6$ inches, constructed so as to slide in steel channel-iron frames 2 ft. long $\times11$ inches wide laid across the I-beams at the ends and in the center, as shown. Slight accidental relative displacements of the heavy cement blocks, channels and I-beams, after the final optical adjustments were made, were prevented by applying soft wax to all regions of contact. The steel frame was loaded with slabs of soapstone and other miscellaneous heavy materials and the

inner tubes pumped up until optimum anti-vibration conditions were realized. This air cushion method of mounting was found to be far superior to any of a number of other methods tried and resulted in a suspension, vibrationless to such an extent that the ever present traffic tremors, made visible by reflections in a dish of mercury placed almost anywhere in the laboratory, even on a table already mounted on sponge rubber, were completely eliminated. With this support, interference fringes formed by mirrors at the extremities of the steel frame work were observed to be stationary for periods as long as several seconds at a time, even with heavy machinery in operation on the same floor only a few doors away.

As a source of light a General Electric S-1 Sunlamp was used.[2] This lamp is ideally suited for this sort of work by virtue of the fact that it gives a continuous spectrum on which the ordinary mercury spectrum, in the visible region, is superposed as bright lines. Furthermore, it requires no attention whatever. In its use an image of one of the tungsten electrodes is formed on the slit of the interferometer.

Other improvements in the optical system included the use of aluminum mirrors[3] which extended the spectral range so as to include the mercury 4047A line. These mirrors also have the valuable property of not tarnishing readily. The intensity of the continuous spectrum was also improved by the use of a diffraction grating specially ruled so as to throw most of the light into the first order spectrum on one side only of the normal beam.[4]

To measure the displacements of the fringes, the movable mirror was mounted on the carriage of a small laboratory Michelson interferometer, the screw of which was carefully calibrated in advance by interferometric methods over several millimeters of its length. This screw was found to be more uniform than the one formerly used. No variation in pitch exceeding one part in four hundred was observed in any whole turn. The actual pitch was found to be 1.040 percent greater than 0.5 mm.

In addition to the optical aspects of this problem, considerable attention was also given to the purity of the gas used, as well as to the constancy and precise measurement of pressures and temperatures. The nitrogen used in this work was commercial water pumped nitrogen which was passed under pressure through a 30-inch steel tower of silica gel to remove traces of water vapor and through a furnace consisting of a steel tube one inch in diameter and 12 inches long, packed tightly with crumpled 100-mesh copper screening maintained at a temperature of about 600°C to remove possible traces of oxygen.

The temperature of the gas was regulated by a mercury-switch thermostat to variations of less than 0.01°C measured by two calibrated mercury thermometers, one at each end of the bath of paraffin oil, which completely surrounded the experimental tube except for the glass windows at the ends. The bath, described before except for minor improvements, is 100 cm long with a square cross section 20 cm to a side.

Pressures were measured to one millimeter of mercury over the whole range from vacuum to nearly 11,000 mm (approx. 14 atmos.) by a Keyes type dead-weight piston gauge.[5] Variations in pressure from the measured value never exceeded a few millimeters in any run and in some cases were less than one millimeter throughout a set of readings made at a given pressure over a period of 15 to 30 minutes.

The same gas refraction tube was used in these experiments as before, the only difference being a slight modification in the method of fastening on the glass windows. The film of De Khotinsky cement used in the former packing, which was described in some detail, was replaced by a cement consisting of litharge and glycerine to facilitate the use of higher temperatures than were formerly possible. Also, a very thin gasket of lead foil was used to replace the one of dental

---

[2] The author is grateful to the General Electric Company for the sunlamp unit placed at his disposal for this work.

[3] These mirrors were made by Dr. J. C. Wulff by evaporation of aluminum on glass.

[4] The replica grating used was loaned by Dr. H. M. O'Bryan.

[5] This pressure gauge was kindly loaned by Dr. F. G. Keyes, Director of the Laboratory of Physical Chemistry, to whom the author is also greatly indebted for the opportunities offered to discuss with him high pressure technique and matters pertaining to the purification of gases.

rubber formerly used. The tube is made of $\frac{1}{8}$-inch steel and is 100.30 cm long by 2.5 cm in diameter. The windows are $\frac{1}{4}$ inch thick.

Steel tubing was used throughout to connect the various parts of the apparatus and steel stopcocks of improved design replaced those used in the former set-up. These specially constructed stopcocks were necessary to insure against leakage in the packings, because in some cases they are used as open rather than as closed valves.

Results

Observations were made in a manner similar to that previously described[1] at four wave-lengths, namely: 5780, 5461, 4359, 4047A. Pressure runs were made corresponding to constant temperatures of 50, 30 and 0°C. The 0°C observations were obtained with a constant temperature bath of cracked ice and water. Readings of the micrometer screw in centimeters corresponding to absolute pressures and wave-lengths at the various temperatures are given in Table I.

The readings in Set III at 30° were made several months after all the others for purposes of checking the constancy of the apparatus over a period of time. As a result of many hours of continuous operation, the sunlamp bulb had become blackened and the mirrors had become slightly tarnished so that it was impracticable to attempt accurate observations on the 4047A line. In Table I the readings of the micrometer screw are recorded rather than values of Δx as was the former procedure, because instead of actually calculating the values of $\Delta x/p$ it is more accurate to calculate what corresponds to the same thing, namely, the slope of the readings themselves *vs.* pressure. In the former work the values of Δx were computed by subtracting the readings at zero pressure from the readings at the various pressures which, of course, gives a greater weight to all the readings corresponding to zero pressure (vacuum) than to the others, thereby increasing the probable error.

The above micrometer readings were first plotted against pressure on a very large scale and showed not the slightest departure from linearity. They were then analyzed by the standard method of averaging by splitting the data into groups and solving the linear equations so obtained. Table II gives the values of $\Delta x/p$ so obtained, with the corresponding values reduced to 0°C by multiplying the former by $\tau/273.1$ (τ = absolute temperature). These values have been corrected for micrometer screw error.

Table I. *Micrometer readings vs. pressure.*

Temp. °C	Pressure (cm Hg)	Wave-length 5780A	5461A	4359A	4047A
30° (I)	0.00	0.5995	0.6680	1.0530	1.2260
	356.04	3.1855	3.2630	3.7230	3.9445
	497.49	4.2120	4.2930	4.7825	5.0100
	626.23	5.1515	5.2345	5.7525	5.9885
	803.64	6.4365	6.5260	7.0850	7.3250
(II)	0.00	0.6235	0.6925	1.0700	1.2460
	331.22	3.0350	3.1155	3.5600	3.7710
	566.56	4.7325	4.8175	5.3160	5.5510
	800.59	6.4170	6.5175	7.0750	7.3280
	1075.36	8.4160	8.5250	9.1385	9.4140
(III)	0.00	0.5145	0.5830	0.9660	
	309.80	2.7650	2.8475	3.2920	
	566.60	4.6220	4.7135	5.2230	
50°	0.00	0.6210	0.6875	1.0660	1.2400
	309.75	2.7335	2.8140	3.2585	3.4500
	582.91	4.5860	4.6780	5.1810	5.4120
	1022.20	7.5775	7.6880	8.2835	8.5600
0°	0.00	0.6160	0.6830	1.0615	1.2290
	321.09	3.1860	3.2655	3.7270	3.9405
	437.68	4.1225	4.2050	4.6935	4.9215
	549.42	5.0250	5.1155	5.6265	5.8740
	662.69	5.9430	6.0385	6.5740	6.8300
	791.48	6.9825	7.0830	7.6565	7.9160
	1000.57	8.6570	8.7745	9.3960	9.6935

Table II. *Values of $\Delta x/p$ (cm/cm Hg).*

Temp.	5780A	5461A	4359A	4047A
	Results obtained by analysis of data			
30°C				
(I)	.00036695	.00036820	.00037911	.00038333
(II)	.00036532	.00036728	.00037868	.00038330
(III)	.00036604	.00036807	.00037943	
50°C	.00034342	.00034325?	.00035633	.00036186
0°C	.00040661	.00041006	.00042194	.00042725
	Preceding values reduced to 0°C			
30°C				
(I)	.00040731	.00040870	.00042081	.00042550
(II)	.00040550	.00040768	.00042033	.00042546
(III)	.00040630	.00040856	.00042117	
50°C	.00040627	.00040606?	.00042154	.00042808
0°C	.00040661	.00041006	.00042194	.00042725
Mean	.00040640	.00040875	.00042116	.00042657
Pr. error mean	±.00000020	±.00000040	±.00000022	±.00000050

It will be observed that the values of $\Delta x/p$ reduced to 0°C as given in Table II are very nearly constant for each wave-length. The probable error of the mean in each case is less than one part in a thousand on the average. The greatest deviation is observed for the values at wave-length 4047A. This is due to the relatively poor visibility in this region. As was pointed out before, only the use of aluminum mirrors made these observations possible at all. On the other hand, the probable error here is only five parts in four thousand.

The fact that $\Delta x/p$ shows no detectable temperature variation other than that associated with density from 0°C to 50°C is interpreted to mean that these results, over this limited temperature range, are in accord with the accepted view that the refractive index of nitrogen does not vary with temperature except through its dependence on density. This latter view is based upon the fact that no successful attempt to measure such a coefficient has ever been reported.

On the basis of these data, the values of A_0 and B_0 were determined by the alternative method suggested in the preceding theoretical discussion, whereby least square calculations were carried out on four equations patterned after Eq. (3). These results are tabulated in Table III, where values of $\Delta x/e$ have been calculated from the computed A_0 and B_0, for purposes of comparison with the observed values of the same quantity.

TABLE III. *Cauchy dispersion constants A and B for nitrogen (0°C, 76.0 cm Hg).*

λ	$\frac{\Delta x}{p}$	$\frac{3}{\lambda^2}\times 10^{-8}$	$\frac{\Delta x}{e}$ (obs.)	$\frac{\Delta x}{e}$ (calc.)
5780A	0.00040640	8.9799	0.00030793	0.00030792
5461	.00040875	10.0596	.00030971	.00030969
4359	.00042116	15.7887	.00031911	.00031907
4047	.00042657	18.3174	.00032321	.00032321
	$(A_0-1)=0.00029322$		$B_0=1.637\times 10^{-14}$	

The accuracy with which A_0-1 and B_0 are here determined can be appreciated by noting that the average deviation between the last two columns of Table III is only two parts in thirty thousand. This high relative accuracy led the writer to check the numerical calculations by carrying out the detailed computations indicated by Eq. (6), considering all six possible ways of combining the four sets of data taken two at a time. In only one case did the resulting value of A_0-1 differ from that given above by more than one part in three thousand. A check to one part in sixteen hundred was also obtained in this manner for B_0. Of course, the least square values are considered the more accurate.

TABLE IV. *Cauchy dispersion constants for nitrogen (0°C, 76.0 cm Hg).* (Three-constant formula.)

Wave-length range	B_0 $\times 10^{-14}$	C_0 $\times 10^{-24}$	A_0-1
5780A–5461A–4359A	1.672	−0.21	0.0002929 (5780A)
5461 –4359 –4047	1.705	− .44	.0002929 (5461A)
5780 –5461 –4047	1.677	− .25	.0002929 (4359A)
5780 –4359 –4047	1.700	− .38	.0002929 (4047A)
Mean	1.689	− .32	.0002929

SUFFICIENCY OF TWO CAUCHY CONSTANTS

All the foregoing calculations have been based on the assumption that the refractive index of nitrogen can be adequately expressed by Eq. (2) limited to the λ^2 term. In the former paper[1] the author cited his graphical analysis of the work of Meggers and Peters on air[6] to justify this procedure. The high precision obtained with the new apparatus, however, has warranted the carrying out of calculations on the basis of a three-constant formula to check this point. The simple least square method used in the two-constant case is not applicable here, so that only an extension of the other method is feasible. This calls for a consideration of the four possible ways of combining the four sets of data taken three at a time. The equations for determining B_0, C_0 and (A_0-1) corresponding to Eq. (6) become considerably more involved, as follows:

[6] Meggers and Peters, Bull. 372, Bureau of Standards, 1918.

$$B_0=\frac{76.0\tau}{3e273.1}\left\{\frac{\left(\frac{\Delta x_2}{p}-\frac{\Delta x_1}{p}\right)\left(\frac{1}{\lambda_3^4}-\frac{1}{\lambda_1^4}\right)-\left(\frac{\Delta x_3}{p}-\frac{\Delta x_1}{p}\right)\left(\frac{1}{\lambda_2^4}-\frac{1}{\lambda_1^4}\right)}{\left(\frac{1}{\lambda_2^2}-\frac{1}{\lambda_1^2}\right)\left(\frac{1}{\lambda_3^4}-\frac{1}{\lambda_1^4}\right)-\left(\frac{1}{\lambda_3^2}-\frac{1}{\lambda_1^2}\right)\left(\frac{1}{\lambda_2^4}-\frac{1}{\lambda_1^4}\right)}\right\},$$

$$C_0=\frac{76.0\tau}{5e273.1}\left\{\frac{\left(\frac{\Delta x_3}{p}-\frac{\Delta x_1}{p}\right)\left(\frac{1}{\lambda_2^2}-\frac{1}{\lambda_1^2}\right)-\left(\frac{\Delta x_2}{p}-\frac{\Delta x_1}{p}\right)\left(\frac{1}{\lambda_3^2}-\frac{1}{\lambda_1^2}\right)}{\left(\frac{1}{\lambda_2^2}-\frac{1}{\lambda_1^2}\right)\left(\frac{1}{\lambda_3^4}-\frac{1}{\lambda_1^4}\right)-\left(\frac{1}{\lambda_3^2}-\frac{1}{\lambda_1^2}\right)\left(\frac{1}{\lambda_2^4}-\frac{1}{\lambda_1^4}\right)}\right\}. \tag{7}$$

(A_0-1) is then obtained by Eq. (3) for the value of $\Delta x/p$ at each wave-length, by using the mean values of B_0 and C_0 thus obtained. The results of these calculations are given in Table IV.

It must be pointed out that this procedure is a very severe test of the data, and the consistency of the (A_0-1) values is very remarkable. The spread of the B_0 and the C_0 values can be easily attributed to the relative inaccuracy of the 4047A data previously pointed out. A three-constant calculation would require data at six wave-lengths for the same accuracy as a two-constant calculation gives from data at four wave-lengths. Furthermore, the C_0 values in Table IV, although reasonably consistent, are relatively extremely small (0.32×10^{-24}). Besides, the value obtained for (A_0-1) by these less accurate calculations differs from the two constant value by only one part in one thousand, which is, after all, just about the accuracy of the absolute value of this quantity as based on the figures of Table II. These considerations, therefore, indicate that no necessity exists for considering the C_0 constant in the Cauchy formula, even though dispersion data are customarily so expressed in the literature even when based upon data known to be less accurate than the above.

Comparison of Results with Other Published Values

The conclusion drawn from this work is that for nitrogen A_0-1 is 0.0002932 to better than one-tenth of one percent and that B_0 is 1.64 to better than one part in one hundred and fifty, certainly. It is of some interest to compare these results with other published values. A value for the dielectric constant of nitrogen has recently been published[7] giving $\epsilon=1.000589$ with a probable error of three figures in the last place. The above value of A_0-1 gives $\epsilon-1=0.0005864$ to one-fifth of one percent.

As for published values of $\mu-1$, the results obtained by other methods are usually not extrapolated to infinite wave-length (this not being generally possible from determinations at isolated wave-lengths) but expressed for specific wave-lengths. Displacement interferometry, however, yielding the B constant as well as the A constant, provides the means of directly calculating $\mu-1$ for any wave-length by Eq. (5). Cheney[8] reported values of μ_0-1 for nitrogen at wave-lengths 6678A, 6143A and 5852A, of 0.0002969, 0.0002977 and 0.0002985, respectively. The above values of A_0-1 and B_0 give 0.0002971, 0.0002975, and 0.0002980, respectively, which are in close agreement. In the opinion of the writer, however, the values of refractive index given in this paper are more accurate than previously published values for the reasons already presented. Furthermore, since it is generally believed that nitrogen possesses no absorption bands in the infrared, the extrapolated A_0-1 value predicts a value for the dielectric constant probably more accurate than has previously been determined.

Summary

An improved displacement interferometer has been built which has definitely established the fact that methods of displacement interferometry are suitable for precise absolute as well as relative determinations of dispersion in gases.

[7] H. L. Andrews, Physics **1**, 366 (1931).

[8] E. W. Cheney, Phys. Rev. **29**, 292 (1927).

For a gas like nitrogen for which the displacements are linear with pressure to a high degree, the dispersion constants have been determined with extremely high accuracy. It is also shown that two Cauchy constants are quite sufficient to express the dispersion to one part in a thousand for nitrogen up to pressures of 14 atmospheres, at least. Furthermore, within this pressure range and within a temperature range of 0° to 50°C the Lorentz-Lorenz relation $[(\mu^2-1)/(\mu^2+2)](1/\rho)$ is shown to be probably constant, where ρ is the density. It must be pointed out, however, that the accuracy with which this relation is shown to hold is not necessarily the accuracy claimed for A_0-1 in the preceding work, because in this paper the results are based on the experimentally observed linearity of the displacements as functions of pressure, not density. Calculations involving accurate knowledge of p.v.t. data are under way at present to ascertain the precise validity of the Lorentz-Lorenz relation within this density range.

The value of A_0-1 given by this work is 0.0002932 to better than one-tenth of one percent. This value is in accord with other published results determined at atmospheric pressure but is in all probability more accurate than these by virtue of the fact that it is obtained by averaging a great many observations over a range of pressures. The result is also consistent with dielectric constant measurements of others.

In conclusion it seems proper to emphasize by restating that displacement interferometry yields not only refractive index values but gives simultaneously the manner in which they vary with wave-length. It is the lack of the latter information, of course, that has made previous isolated determinations of refractive index at particular wave-lengths less useful than they might otherwise have been in molecular refraction considerations.

The results of this paper have been critically reviewed by Professor A. deF. Palmer, of Brown University, with whom the writer has had the pleasure of discussing the work from time to time throughout its progress.

Absorption of Supersonic Waves in Mixtures of Air and Carbon Dioxide at Different Relative Humidities*

HENRY H. ROGERS, *Department of Physics, Pennsylvania State College*

(Received June 3, 1933)

The absorption of supersonic waves of frequency 409.6 kc/sec. in mixtures of air and CO_2 at eight relative humidities ranging from 10 percent to 75 percent was measured. The source of the radiation was a quartz crystal oscillator. The receiver was an acoustic radiometer of the torsion vane type. Curves of the logarithm of the radiometer readings as a function of distance between radiometer and crystal face were straight lines the slopes of which gave the absorption constant k. The values of k are given in the table. The absorption constant k is a linear function of the percent of CO_2. For a given mixture of air and CO_2 it is a nonlinear function of the relative humidity increasing to a maximum at 45 percent and then dropping off rapidly.

	Relative humidity							
	10%	15%	35%	45%	55%	65%	70%	75%
10% CO_2	0.096	0.13	0.17	0.19	0.17	0.16	0.11	0.08
40% CO_2	.40	.46	.56	.61	.59	.51	.43	.33
80% CO_2	.81	.89	1.07	1.17	1.10	.99	.84	.66

INTRODUCTION AND HISTORY OF ABSORPTION OF SUPERSONIC WAVES IN CO_2

IN the past few years data relating to absorption of high frequency sound in gases and gas mixtures have been notably meager in comparison with velocity measurements. G. W. Pierce[1] in 1925 noted an excessive absorption of supersonic waves by carbon dioxide and also mentioned an unpublished investigation of D. L. Rich and G. E. Raeburn in 1917. Their initial attempt to obtain absorption data for carbon dioxide was made with a modified form of Neklapajev's apparatus fitted with pressure vane detectors. With a beam of supersonic waves T. P. Abello[2] noticed a logarithmic decrease in transmitted energy with increase in percentage of carbon dioxide in the mixture. This increase in absorption coefficient at 612 kc/sec. for 1 percent by volume of carbon dioxide in air was found to be 0.029, where his formula was of the form $I_x = I_0 f(t,x) e^{-kx}$. W. H. Pielemeier[3] has used a torsion vane for absorption measurements in air, oxygen and carbon dioxide. A careful determination at 645.8 kc/sec. with this type of apparatus gave 0.0032 as a value of A for carbon dioxide where the absorption coefficient is of the form $k = A/\lambda^2$. An excessive absorption at high frequencies was verified by him with both the radiometer method and the interferometer method. He also commented on the marked effect of humidity on absorption in carbon dioxide in his paper published in 1929. Grossmann[4] in 1932 found that the absorption coefficient, A, was a function of the frequency, having a maximum at 100 kc/sec. for carbon dioxide. Hubbard[5] in 1932 using an acoustic resonator interferometer found values for the absorption constant of carbon dioxide that checked the value of Pielemeier already given in this paper.

Work was begun by the author on this problem in 1930 who used a modified form of a torsion vane radiometer of the type previously employed by Pielemeier. The purposes of this research were to determine the relation between the absorption coefficient k and the relative humidity of a mixture of air and carbon dioxide as well as the relation between the absorption coefficient k and the percent by volume of carbon dioxide in the mixture. This work together with similar investigations of the effect of relative humidity on air,

* Presented by Henry H. Rogers in partial fulfilment of the requirements for the degree of Ph.D. at the Pennsylvania State College.

[1] G. W. Pierce, Proc. Am. Acad. Arts and Sci. **60**, 271 (1925).

[2] T. P. Abello, Proc. Nat. Acad. Sci. **13**, 699 (1927); Phys. Rev. **31**, 1083 (1928).

[3] W. H. Pielemeier, Phys. Rev. **34**, 1184 (1929); **36**, 1005 (1930); **38**, 1236 (1931).

[4] Grossmann, Ann. d. Physik (5) **13**, 681 (1932).

[5] J. C. Hubbard, Phys. Rev. **41**, 523 (1932).

hydrogen, oxygen and helium to be carried out in the next few years by the author may shed some light on molecular structure.

Apparatus and Procedure

The apparatus was arranged in a dark room kept at a temperature of about 25°C. The absorption tube (glass cylinder, 35 cm long, 15 cm diam.) was mounted in a vertical position with the oscillating crystal (the source of the ultrasonic radiation) near the bottom. The top of the absorption tube was of brass through which passed a sliding brass tube which carried the radiometer box shown in Fig. 1. The fine quartz suspension

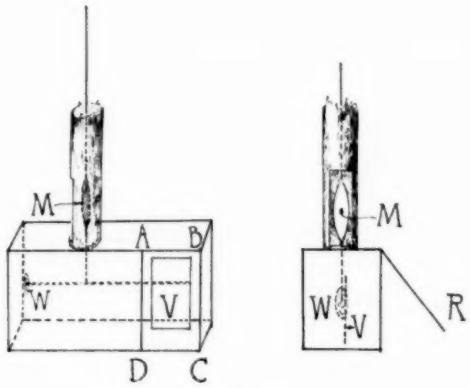

Fig. 1. Diagram of radiometer.

for the radiometer vane was attached at the upper end of the brass tube to a torsion head. By sliding the tube up and down the distance between radiometer and source could be varied from 0.5 cm to 5 cm. The inside of the brass top was padded to prevent sound reflection. The outside of the absorption tube was covered with heat insulation except for a strip in front for passage of a light beam to and from the radiometer mirror. The absorption tube also contained a sensitive hygrometer, thermometer and a dish for chemicals which controlled the humidity. A square iron box with a glass front but otherwise similar to the glass absorption tube was used to check all observations and to obtain observations in the higher humidity ranges. Carbon dioxide entered the absorption tube through a valve at the bottom and passed out through a valve at the top. An Orsat apparatus was used to determine the percentage of CO_2 at the end of each run.

Radiometer detector

Fig. 1 shows the radiometer which consisted of a small cardboard box with an opening $ABCD$ on one side and containing a torsion vane V made of a very thin sheet of mica fastened by amberoid glue to a small quartz rod at the other end of which a counterweight W was fastened. Another quartz rod was glued at right angles to this rod and to it was fastened a very small ovoid mirror, m, with the plane of the mirror at right angles to the plane of the vane. A thin aluminum reflector R making an angle of 45° with the vertical was fastened to the top edge AB. The image of a single straight filament from a hooded lamp 135 cm from the radiometer mirror was reflected on a scale 370 cm from the mirror.

Crystal oscillator and circuit

A piezoelectric quartz crystal sputtered on both faces with platinum and having two natural frequencies 389.3 and 409.6 kc/sec. served as the source of supersonic waves. The crystal was connected by twisted short wire leads to an oscillating circuit through an air tight valve in the bottom of the tube. The oscillating circuit was a modification of the one used by Pierce and is sketched in Fig. 1 of Pielemeier's[3] paper. The oscillation frequency is determined by the natural frequency of the crystal and not by the electrical constants of the circuit. The frequency of the crystal was checked by standard crystals at WPSC, the college broadcasting station.

Procedure

After adjusting the CO_2 content of the tube to the desired value, the mixture was allowed to stand for twelve hours to come to equilibrium. For each position of the radiometer box the deflection of the radiometer was measured with the sound beam off and on. The sound beam was cut off by opening the plate circuit of the oscillating tube. The filament circuit remained closed throughout the run. Temperature readings were taken at regular intervals both inside and outside the absorption tube and were not allowed to vary from 25°C by more than one degree. The relative humidity of the mixture was controlled by the presence of a saturated solution of some chemical such as phosphoric pentoxide, calcium chloride, chromium oxide, potassium nitrate or sodium bromide.

The position x in centimeters of the radiometer from the crystal was plotted against the logarithm of the average deflection ($\log_{10} D_x$). The slopes of the straight lines thus obtained gave the values for the absorption constant $k = A/\lambda^2$. For each of the eight relative humidities used k was obtained for at least five different mixtures of air and CO_2. All of these runs were repeated to check values obtained for k except in case of 75 percent CO_2. In Fig. 2 the values of k are plotted against percent of carbon dioxide in the sample for each relative humidity from 10 percent to 75 percent. Fig. 3 represents the values of k plotted against the relative humidity for 10, 40 and 80 percent CO_2 respectively.

Discussion of Results

The data as plotted in Fig. 2 show that the absorption constant k is a linear function of the

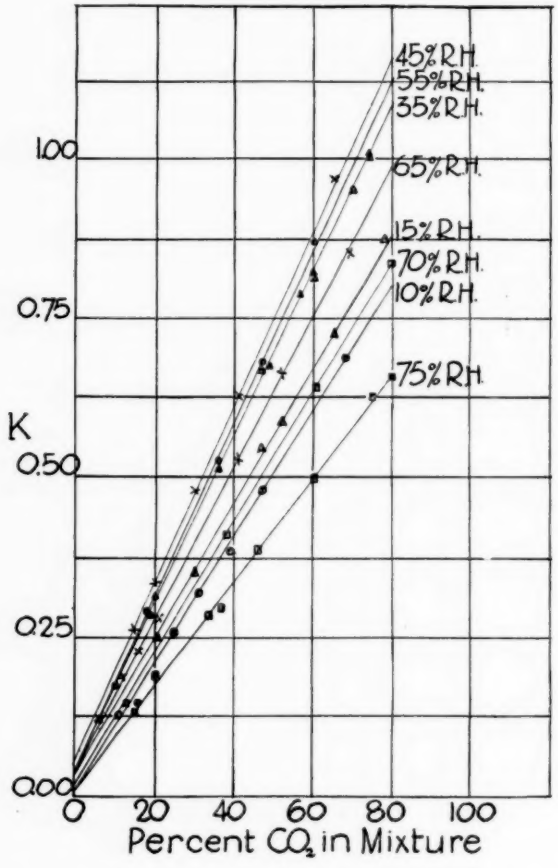

Fig. 2. The absorption coefficient as a function of percent of carbon dioxide for various relative humidities.

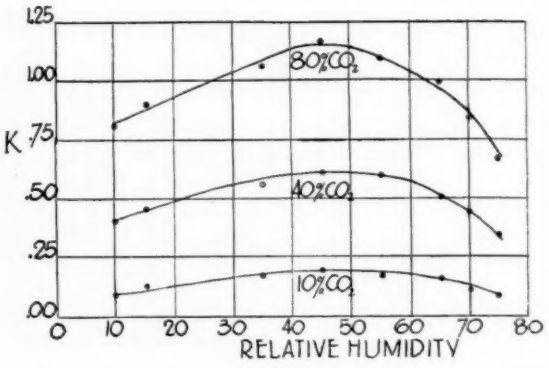

Fig. 3. Absorption coefficient as a function of relative humidity for various percentages of carbon dioxide.

percent of carbon dioxide in the air. These data in turn plotted in Fig. 3 relating the absorption constant to the percent relative humidity of the mixture of air and carbon dioxide give a series of curves with a maximum at 45 percent R.H. These results have a probable explanation in the consideration of energy transfer at molecular collisions. Sound absorption in gas mixtures is due to the conversion of sound energy into heat energy by means of a thermal equilibrium adjustment between the vibrational energy and the rotational-translational energies of the molecules.

H. O. Kneser[6] in explaining the maximum for absorption in air when the frequency is varied, states that "the rate of thermal adjustment depends directly on the number (N) of water molecules present." The probability of transition from one vibrational state to another for a carbon dioxide molecule at collision is many times greater if one colliding particle is an H_2O molecule than if it were a CO_2 molecule. This assumption explains readily the rising part of the curve. Referring to the square wave form representing volume variation in Kneser's[7] paper, it is evident that if the compression stroke takes place in zero time there would be no explanation for the falling off in absorption with increase in the number (N) of the water molecules present. Physically there must be a finite time for this compression in the actual passage of the sound wave through the gas.

This finite time is represented graphically in Fig. 4 by Δt_c, the vectors Δp represent the change

[6] H. O. Kneser, Bull. Am. Phy. Soc. Vol. 8, No. 2.
[7] H. O. Kneser, Ann. d. Physik **16**, 337 (1933).

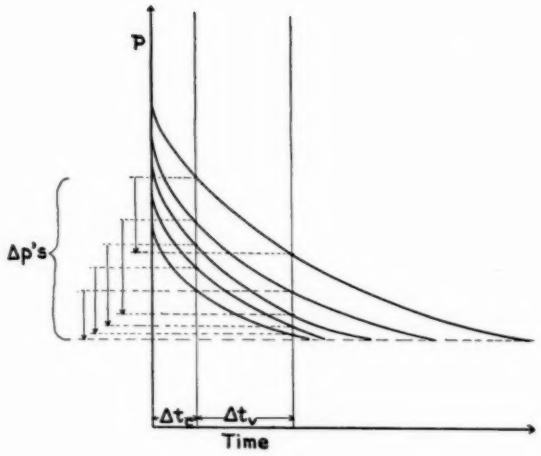

FIG. 4.

in pressure only in the PV diagram and Δt_v gives the time of constant volume. The successive curves represent increasing adjustment rates because of increasing water vapor concentration, and because of the greater slope of the curves at the upper end, the intercept cut off at this end by Δt_c is at first less than the increase at the lower end of the curves, but finally becomes greater than with higher humidities. Thus the vectors representing pressure change at first increase with increasing (N) and then decrease. The square wave form curves of Kneser are ideal representations, while actually the specific volume varies sinusoidally and the PV area instead of being a parallelogram is elliptical in form.

The author wishes to express his thanks and appreciation to Dr. W. H. Pielemeier, of the Department of Physics of the Pennsylvania State College, for his helpful advice and supervision of this work.

LETTERS TO THE EDITOR

Prompt publication of brief reports of important discoveries in physics may be secured by addressing them to this department. Closing dates for this department are, for the first issue of the month, the twentieth of the preceding month; for the second issue, the fifth of the month. The Board of Editors does not hold itself responsible for the opinions expressed by the correspondents.

Directional Measurements on the Cosmic Rays Near the Geomagnetic Equator

In a letter to the Physical Review of July 3, 1930 I pointed out that, if the primary cosmic rays are electrically charged particles, the deflection of their paths in the earth's magnetic field should be noticeable by an unsymmetrical directional distribution of the intensity with respect to the geomagnetic meridian.[1] More precisely I showed that at a point on the earth of geomagnetic latitude λ no particles with an energy less than V (if $V<61.5\times10^9$ e.v.) can reach the observer in a direction the angle ϑ of which, to the geomagnetic meridian satisfies the following equation:

$$\sin\vartheta=\frac{300M}{R^2V}\cos\lambda-\left(\frac{300M}{R^2V}\right)^{\frac{1}{3}}\frac{2}{\cos\lambda}. \qquad (1)$$

Here M is the magnetic moment of the earth (8.33×10^{25} c.g.s.), R its radius (6.38×10^8 cm); the energy V of the particles is given in electron-volts, ϑ is positive towards the east for negative particles, positive towards the west for positive particles. This involves the existence, at any point of the earth and for each monoenergetic component of the cosmic radiation, of a cone, defined by Eq. (1), which separates the allowed directions from the forbidden ones. The region "in shadow" is west of this cone for negative particles, east for positive particles.

In the above equation the rest mass of the particles was neglected as compared with their relativistic mass. This is permissible, as a first approximation and for the energies under consideration, even in the case of particles as heavy as protons. It is further to be noted that Eq. (1) does not give the exact value of the minimum energy of the particles coming in a given direction, but a lower limit for this energy. A better approximation is obtainable by a more complex theory recently developed by Lemaitre and Vallarta;[2] but the differences are insignificant for the discussion of our results.

A first attempt to detect the expected azimuthal effect was performed by the writer in Florence in 1931[3] with a coincidence method, but the experiments gave a negative result. This negative result may be due (as E. Fermi and the writer pointed out in a more detailed discussion on the influence of the earth's magnetic field on the cosmic rays presented in February, 1933)[4] to the atmospheric absorption, that cuts off just the softer component of the cosmic radiation for which, at the geomagnetic latitude of Florence, an azimuthal effect should be expected.

As the energy of the particles which are excluded from a cone of a given opening increases on approaching the geomagnetic equator, a new set of directional measurements was planned, to be made at a lower geomagnetic latitude and at a greater elevation. Shortly before the beginning of these measurements, the results of which are to be presented, Johnson[5] and Alvarez and Compton[6] gave an account on similar experiments performed at the Mexico City (elevation 2310 m, geomagnetic latitude 29°) which shows clearly the expected azimuthal effect.[7]

The present experiments were made in Asmara (Colonia Eritrea, East Africa) at a geomagnetic latitude of 11° 30′ and an elevation of 2370 m (mean barometric pressure: 577 mm Hg). As in the earlier experiments, the double-coincidence method was adopted. The Geiger-Müller counters had an internal diameter of 2.4 cm and an effective length of 16 cm; their axes were parallel to one another and horizontal. The frame carrying the counters could rotate about both horizontal and vertical axes. In some experiments the counters were surrounded by a cylindrical lead shield. Between the counters lead screens of various thickness could be interposed. The coincidences were recorded by the method already described.[8] We shall denote by "direction of the counter system" the direction of the straight line joining their centers; z will be the zenith angle of this line, d the distance between the axes of the counters, x the thickness of the absorbing screen (if any); N, W, S, E indicate that the counter system is directed respectively towards the geomagnetic North, West, South, East.

---

[1] B. Rossi, Phys. Rev. **36**, 606 (1930).

[2] G. Lemaitre and M. S. Vallarta, Phys. Rev. **43**, 87 (1933); M. S. Vallarta, Phys. Rev. **44**, 1 (1933).

[3] B. Rossi, Rend. Lincei **13**, 47 (1931) and Nuovo Cim. **8**, 85 (1931).

[4] E. Fermi and B. Rossi, Rend. Lincei **17**, 346 (1933).

[5] T. H. Johnson, Phys. Rev. **43**, 834 (1933).

[6] L. Alvarez and A. H. Compton, Phys. Rev. **43**, 835 (1933).

[7] Previous experiments of T. H. Johnson and J. C. Street (Phys. Rev. **43**, 381A, 1933), on Mount Washington (55° geom. lat., 1900 m height) seem also to indicate a small azimuthal effect.

[8] B. Rossi, Nature **125**, 636 (1930).

The results are presented in Tables I, II and III. All experiments agree in showing remarkably greater intensity from the west than from the east for the same zenith angle;

TABLE I. *Measurement of the azimuthal effect at different zenith angles.*

z	Direction	Total counts	Rate (min.$^{-1}$)	W/E ratio
(a) counters unshielded. $d=6.5$ cm[9]				
45°	W	4734	5.01±0.052	
45°	E	4078	4.32±0.049	1.161±0.017
(b) counters shielded, 16 mm lead+2 mm brass. $d=12$ cm				
45°	N	2516	1.39±0.02	
45°	W	2669	1.47±0.02	
45°	S	2446	1.35±0.02	
45°	E	2246	1.24±0.02	1.188±0.022
30°	W	4290	2.08±0.022	
30°	E	3710	1.80±0.021	1.157±0.018
15°	W	3962	2.48±0.028	
15°	E	3570	2.23±0.026	1.11±0.018

TABLE II. *Variation of intensity with zenith angle in western direction; counters surrounded by a cylindrical shield of 17 mm lead+1 mm brass. $d=25$ cm.*

z	Total counts	Rate (min.$^{-1}$)
0°	1760	0.845±0.015
15°	1708	0.818±0.015
30°	1228	0.588±0.013
45°	924	0.443±0.012
60°	467	0.224±0.009

TABLE III. *Absorption measurements in 4 and 8 cm lead; counters unshielded. $d=12$ cm.*

z	x cm	Total counts	Rate (min.$^{-1}$)
0°	0	4758	3.70±0.038
0°	4	2867	2.23±0.029
0°	8	2447	1.90±0.028
45°W	0	3156	1.87±0.024
45°W	4	2016	1.19±0.02
45°W	8	1815	1.08±0.018
45°E	0	2653	1.57±0.022
45°E	4	1647	0.98±0.017
45°E	8	1378	0.82±0.016

whilst the intensities from the northern and southern directions are the same within the limits of experimental error. We conclude therefore, in agreement with the results of Johnson and of Alvarez and Compton, that a portion at least of the cosmic radiation consists of positively charged particles. Compton has suggested, however, that the main body of the cosmic radiation is due to rays which are not affected by the earth's magnetic field (particles of very great energy or electrically neutral rays); whilst the charged component should form a rather narrow band with a mean energy of about 7×10^9 e.v.[10] My results do not confirm this view. The greater portion of Compton's band should vanish at the geomagnetic latitude of Asmara both in the eastern and in the western directions; one would therefore expect to find in this place no azimuthal effect at all, or, at most, but a very small one. The west-east differences which I have found at the different inclinations to the geomagnetic meridian are, on the contrary, much greater than the differences found by Johnson and by Alvarez and Compton at Mexico City under the same conditions.

It follows from equation (1), for $\lambda=11°\ 30'$, that at an angle of 45° to the geomagnetic meridian; no positive particles with an energy less than about 2.3×10^{10} e.v. can reach the observer in the eastern direction, whereas the minimum energy in the western direction is about 1.1×10^{10} e.v. The remarkable difference found in experiments (I) and (III) at $z=45°$ indicates therefore the existence of a considerable number of particles with an energy between 1.1 and 2.3×10^{10} e.v. The results of these experiments, in connection with the data obtained by Johnson and by Alvarez and Compton at $\lambda=29°$, confirm the view, supported by the early experiments of the writer,[11] that cosmic rays consist chiefly of a charged corpuscular radiation with a continuous energy spectrum extending to very great energies. Moreover the new results on the azimuthal effect show that the charge is predominantly positive.

It is however possible that, in addition to the positive particles, a smaller amount of other kinds of rays (negative particles, photons, neutrons) is contained in the cosmic radiation. In fact, some results are rather difficult to explain by supposing that the cosmic radiation consists merely of positive particles. Experiment II shows that the intensity of the cosmic rays decreases very rapidly as the zenith angle increases. Since in these measurements the counter system was directed towards the west, the earth's magnetic field should give rise to a precisely opposite variation of the intensity with zenith angle. Thus if the assumption of a pure positive radiation were true, the observed zenith effect could only be due to atmospheric absorption. But here we meet again with a difficulty. The thickness of the atmosphere, which is equivalent to 785 g/cm² (at the elevation of Asmara) in the vertical direction, increases to $785/\cos 30°=906$ g/cm² for the rays coming at an angle of 30° to the vertical. It is hardly conceivable that the large diminution of the intensity, which is observed by going from $z=0°$ to $z=30°$ can be due to the greater absorption of the atmosphere in the inclined direction, since the minimum energy of the cosmic particles in the vertical direction is (from Eq. (1)) about 1.4×10^{10} e.v. and

[9] From these figures the chance coincidences have been deduced; the probable statistical errors are calculated from the number of counts.

[10] A. H. Compton, Phys. Rev. **43**, 387 (1933).

[11] B. Rossi, Zeits. f. Physik **82**, 151 (1933).

the range of particles of this energy is supposed to be much greater than the thickness of the atmosphere at $z=30°$.[12]

The experimental results would be more easily accounted for by supposing that the cosmic radiation has a complex nature. In the case, for instance, that this radiation contains a γ-component, we may expect to find the greater portion of its secondary particles in directions close to the vertical line if we assume that the absorption of the atmosphere on the primary γ-radiation itself is large enough to produce a very sharp maximum of its intensity in the vertical direction. Also it is possible that a portion of the cosmic radiation may consist of negatively charged particles, the intensity of which would be reduced in the western direction by the earth's magnetic field.

In connection with the hypothetical γ-component of the cosmic radiation the results of the absorption measurements (III) are of interest. They show the existence of a great number of particles with a mean range of a few cm lead, which are, without any doubt, to be regarded as a secondary radiation generated in the superincumbent atmosphere. In Florence, at an elevation of only 150 m, I have also found a secondary radiation due to an interaction between the primary cosmic particles and matter,[11] and it is certain that a portion at least of the now observed secondary radiation has the same origin. It seems however that in Asmara this secondary radiation is relatively more abundant and shows a greater zenith effect than in Florence. This would support the view that at a great elevation a portion of the softer corpuscular rays consists of secondary particles of a γ-radiation; this radiation should vanish at sea level because of its small penetrating power.

The funds for the African expedition were supplied by the Consiglio Nazionale delle Ricerche and by the Ministero delle Colonie; I am also very indebted to the Government of the Colonia Eritrea for the many facilities placed at my disposal. Finally I wish to thank warmly Professor I. Ranzi and Dr. S. De Benedetti for their valuable assistance in this work.

BRUNO ROSSI

Asmara, Eritrea,
November 25, 1933.

[12] As long as the thickness of the absorbing layer is smaller than the range of the softest particles, one would expect to find no diminution at all, if the range of the cosmic corpuscular rays is supposed to be quite definite. This would be the case for particles which lose in every elementary process but a very small portion of their energy. We know, on the contrary, that the cosmic particles sometimes produce secondary processes which involve the loss of a considerable amount of their energy (see B. Rossi, Nature **132**, 173 (1933)). These processes should give rise to a kind of "quantum absorption." We may therefore expect that a certain number of cosmic particles will be stopped before reaching the normal range, but it seems very unlikely that this quantum absorption may be so important to produce by itself the observed zenith effect.

Absorption Measurements on the Cosmic Rays at 11° 30′ Geomagnetic Latitude and 2370 Meters Elevation

Experiments performed by Professor Rossi in Asmara[1] show that the intensity of the cosmic rays decreases with increasing zenith angle more rapidly than we should expect to result from the atmospheric absorption if the primary cosmic radiation consists merely of positively charged particles (since the softest particles are cut off by the earth's magnetic field). It follows either that we have undervalued the absorption of the cosmic particles or that the cosmic radiation has a complex nature.

In order to test these hypotheses I have measured the absorption of the cosmic corpuscular radiation in lead by the double coincidence method. The experiments were performed under the same conditions as in Rossi's experiments and with a similar apparatus. The counters were 16 cm long and 2.4 cm in diameter. They were surrounded by a cylindrical shield of 17 mm lead+1 mm brass and were arranged one above the other at a distance of 25 cm from axis to axis. The axes were horizontal and parallel to the geomagnetic meridian. The coincidences were alternately counted with no screen and with lead screens of 4, 10, 16 cm between the counters. The results are given in Table I.

TABLE I. *Effect of lead screens on coincidences.*

Screen (cm)	Total counts	Counting rate (min.$^{-1}$)
0	2474	0.805 ± 0.012
4	1868	0.608 ± 0.011
10	1814	0.591 ± 0.011
16	1782	0.581 ± 0.011

The considerable diminution of coincidences from 0 to 4 cm lead is due to the absorption of secondary particles (generated by the primary particles or having some other origin) which are not stopped by the lead cylinders surrounding the counters. From 4 to 16 cm lead we have on the contrary but a very small diminution of coincidences. Presumably this diminution corresponds to the absorption of the primary particles themselves.

A layer of 12 cm lead is approximately equivalent, as far as the absorption of cosmic rays is concerned, to the difference between the thickness of the atmosphere at a zenith angle z of 30° and in vertical direction. Now by going from $z=0°$ to $z=30°$, Rossi finds that the intensity is reduced by (30 ± 2) percent. By interposing a lead screen of 12 cm, after eliminating the secondary rays with 4 cm lead, I find, however a diminution of only (4.6 ± 2.5) percent. The observed zenith effect therefore cannot be due merely to the absorption of the atmosphere on the primary cosmic particles.

This effect may be explained, as Rossi has pointed out, by assuming that the cosmic radiation includes, in addition to

[1] B. Rossi. *Directional Measurements on the Cosmic Rays Near the Geomagnetic Equator*, Phys. Rev. **45**, 212 (1934).

the positive particles, a γ-component, the secondary radiation of which decreases rapidly in number as zenith angle increases. In this case the diminution of the total intensity between 0° and 30° in the western direction should be chiefly due to the decrease of the secondary rays which are not eliminated in Rossi's experiments. By interposing a screen of 4 cm lead, which is sufficient to cut off the whole secondary radiation, we should therefore expect to find only the small zenith effect corresponding to the absorption of the primary positive particles. In other words we should expect to find (with 4 cm lead between the counters) the same diminution of coincidences by going from $z=0°$ to $z=30°$ as by increasing the lead screen from 4 to 16 cm lead.

In order to test these conclusions the number of coincidences was counted under the following conditions: (1) The plane of counters' axes parallel to the geomagnetic meridian and 4 cm lead between the counters; (2) The plane of the axes parallel to the geomagnetic meridian and 16 cm lead between the counters; (3) The plane of the axes at 30° to the geomagnetic meridian and 4 cm lead between the counters.

The counters were surrounded by the cylindrical lead shields.

The results obtained are given in Table II.

TABLE II.

Experimental condition	Total counts	Counting rate (min.$^{-1}$)
(1)	2324	0.627±0.010
(2)	2138	0.575±0.009
(3)	1916	0.516±0.009

It is seen that under these conditions also, by inclining the counter system at 30° toward the west the number of coincidences shows a greater diminution than by introducing a layer of 12 cm lead between the counters. The existence of a hypothetical γ-radiation in addition to the positively charged particles seems therefore insufficient to account for the observed zenith effect.[2] Provisionally the simplest hypothesis to explain this behavior would be to suppose that a portion of the cosmic radiation consists of negatively charged particles.

By putting together the results of both experiments we find that the portion of the cosmic particles which are absorbed between 4 and 16 cm lead is (6.5±1.6) percent. Now at the geomagnetic latitude of Asmara the minimum energy of cosmic particles coming vertically (whether positively or negatively charged) is about 14×10^9 electron-volts. Particles of this energy should have a normal range much greater than the total thickness of matter traversed by the rays, even with the lead screen of 16 cm between the counters (*viz.*, 1027 g/cm², of which 785 are due to the superincumbent atmosphere, 60 to the lead cylinders and 182 to the absorbing screen). We may therefore assume that the decrease of coincidences observed by increasing the lead screen from 4 to 16 cm is due to some kind of "quantum absorption."[1] The expected magnitude of this absorption (as it may be roughly estimated from the frequency of the secondary phenomena produced by the cosmic particles) is large enough to explain the experimental result.

It is a pleasure to acknowledge my indebtedness to Professor Rossi for his valuable advice in the discussion of these experiments.

SERGIO DE BENEDETTI

Asmara, Eritrea,
November 25, 1933.

[2] The measurements nevertheless do not exclude the existence of a γ-radiation. Moreover such a radiation would explain the greater zenith effect found by Rossi with no lead screen between the counters.

Adsorption of Hydrogen

Benton and White, from work on adsorption of hydrogen by certain metals, proposed[1] that physical adsorption consists in the formation of concentric rows of adsorbed molecules.

In the adsorption of hydrogen by charcoal the present writer has obtained experimental results which agree with this hypothesis. The rate of adsorption of hydrogen by charcoal at liquid oxygen temperature depends upon the time that elapses between the outgassing and the start of the adsorption process. If this time is made as short as three minutes, the sorption is small when the hydrogen is first admitted to the charcoal; the rate of sorption increases markedly, reaching a maximum after about thirty seconds.

If we propose that "permanent" adsorption occurs most readily at the boundary of a "puddle" of already adsorbed gas, the effect can be explained. When the charcoal is allowed to stand for a considerable time after being outgassed the residual gas forms small puddles of adsorbed gas, and thus when the hydrogen is admitted it finds considerable lengths of boundary along which adsorption can take place. If, however, the charcoal stands only long enough to cool to liquid oxygen temperature, puddles of residual gas do not have time to form.

Since boundaries along which gas can condense are short, adsorption proceeds slowly at first. As adsorption continues, the lengths of boundaries of these expanding puddles increases, and with them the rate of adsorption. Later, as these puddles run into each other, the length of boundary decreases so that the rate of adsorption decreases with the greater lapse of time.

THOMAS D. PHILLIPS

Marietta College,
Marietta, Ohio,
December 12, 1933.

[1] Benton and White, J. Am. Chem. Soc. **53**, 2807–8 (1933).

Pleochroic Haloes and the Age of Minerals

In collaboration with S. Bateson, L. G. Turnbull and C. M. Mushkat I have been engaged in a quantitative study of pleochroic haloes in biotite with the aid of a special microphotometer, which measures the intensity of blackening in the actual halo. Reports on the progress of this work have been given and published in abstract at the last two annual meetings of the Royal Society of Canada and a full account will be published shortly. It is the purpose of this letter to summarize some of the results obtained.

A typical record obtained with this instrument is shown in the upper half of Fig. 1 and a photomicrograph of the

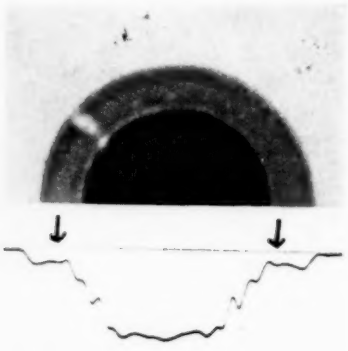

FIG. 1.

halo from which it was taken is shown below. Six rings or humps are to be seen, five of which completely account for the eight α-particles of the uranium family. The values of the ring radii are in better agreement with calculation from the α-particle ranges, than were previous measurements with the micrometer microscope. There is no evidence of an increase in the ring radii with increasing age of the mineral. Two other small rings have also been found on the records with radii corresponding to α-particles of 1.74 and 1.05 cm range.

With the aid of artificial blackening curves for biotite obtained by exposure to radon, it has been possible to calculate the shape of a number of these photometer curves. They are in good agreement with the actual records. In the formation of haloes the biotite shows characteristics very like those of a photographic plate, including the Eberhard effect.

The sixth ring, indicated by arrows, has not hitherto been known and is undoubtedly due to the actinium family. By comparing the height of this hump with that due to Ra C′ just outside it, it is possible to calculate the age of the mica. This has been done for three biotites which have been studied in detail and the results are in agreement with the geological evidence. The accuracy is at present limited by uncertainties in the constants of the actinium series. The method is free from the error due to leaching which may creep into other methods of age determination.

This work is being continued. I am anxious to secure more micas containing haloes and I would be obliged if any reader of this letter would furnish me with samples, preferably of crystals greater than 5 mm in size.

G. H. HENDERSON

Dalhousie University,
Halifax, Canada,
December 21, 1933.

On the Relativistic Photoelectric Effect

The relativistic quantum electrodynamics provides a formal expression for the photoelectric cross section of a Dirac electron in the field of a nucleus. The evaluation of this cross section is of considerable theoretical interest, while a comparison of the strict result with experiment is highly desirable.

In this theory the cross section per electron, σ, may be written as a sum over the angular momentum of the photoelectron.

$$\sigma=\sum_{1}^{\infty}{}_k I_k^2(\kappa^1, \alpha). \tag{1}$$

I_k is an integral over radial functions. It involves the light quantum energy $\kappa^1=h\nu/mc^2$; and also the electron binding through $\alpha(=Z/137)$. It has been pointed out[1] that the main contribution to the sum in Eq. (1) comes for $k\gg 1$ when $h\nu/mc^2\gg 1$. Since a direct attempt to evaluate the terms in the sum meets serious analytical difficulties, the following method has been used.

It is possible to transform I_k to the form

$$I_k=\int_0^1 f(k, u)du \tag{2}$$

in such a way that the sum over k of $f(k, u)f(k, v)$ converges absolutely for all (u, v) in the square $0\leq u, v\leq 1$. With the use of Eq. (2) it is possible to perform the sum (1) strictly, and the resulting double integral is a convenient form for the study of σ when $\kappa^1\gg 1$.

An evaluation good to within a fractional error of about $\alpha^2/2$ gives

$$\sigma=\sigma_0/\left[\alpha^{2\alpha^2}e^{\alpha(\pi-2\alpha)}\right] \tag{3}$$

where σ_0 is the cross section obtained by neglecting α consistently.[2]

$$\sigma_0=0.58\times 10^{-23}Z^5\lambda\cdot R$$
$$R=1+\left[4(1-\alpha^2)^{\frac{1}{2}}-5/3\right]/\kappa^1+\cdots.$$

The total absorption from the K-shell is $\tau_K=2\sigma$. For $Z=82$, (Pb), and $\lambda=4.7$ X.U. (Th C″), Eq. (3) gives $\tau_K=1.1\times 10^{-24}$ cm². This result is compared with other data in Table I.

In the light of this result experiment and theory appear

[1] Harvey Hall and J. R. Oppenheimer, Phys. Rev. **38**, 57 (1931).

[2] F. Sauter, Ann. d. Physik **11**, 454 (1931).

TABLE I.

Pb $\lambda=4.7$ X.U.

Z	A_{Chao}	A_{Tarrant}	σ_{KN}	τ_K
82	14.1×10^{-24}	13.4×10^{-24}	10.2×10^{-24}	1.1×10^{-24}

A = total absorption observed

σ_{KN} = Klein-Nishina scattering

to be in excellent agreement. The surplus, $A-\sigma_{KN}-\tau_K$, agrees qualitatively with the theoretical absorption for the formation of positron-electron pairs.[3]

Details of the calculation, and more complete results will soon be submitted for publication.

HARVEY HALL

Department of Physics,
Columbia University,
New York, New York,
December 25, 1933.

[3] J. R. Oppenheimer and M. S. Plesset, Phys. Rev. **44**, 53 (1933).

On Collisions Between Photons

In the November, 1933 issue of the *Journal of the Optical Society*, Dr. F. L. Mohler describes an experiment in which two conical beams of light were made to intersect each other in such a way that the axes of the cones made an angle of 180° with each other. This experiment is similar to one described three years previously by us.[1] In our experiment the axes of the conical beams made an angle of 120° with each other. In both experiments evidence for the scattering of light by light was sought in a direction bisecting the re-entrant angle between the axes of the two cones. A superficial difference between the two experiments seems to be that Dr. Mohler looked for scattering without, while we looked for scattering with, change of wave-length. However, according to the theory given in our paper the wave-length of the light scattered in the direction of the bisector of the re-entrant angle is

$$\lambda_1=\lambda/(1+\cos\theta),$$

where λ is the wave-length of the light in the original beams and 2θ is the angle between the beams. In Dr. Mohler's experiment $\cos\theta=0$ while in our experiment $\cos\theta=0.5$. Thus on our theory no change of wave-length was to be expected in Dr. Mohler's experiment and his experiment is just a repetition of ours, the only difference being the value of the angle between the two beams of light.

Further, Dr. Mohler's remark that:

"The effect looked for by Hughes and Jauncey can also be ruled out on the evidence that the converse process, the spontaneous creation of two photons from one, is not observed. The radiation from distant stars maintains its spectral characteristics (apart from red shift) for periods of more than 10^8 years"

has no point. If the theory underlying Eqs. (1) and (2) of our paper is examined, it will be seen that we certainly did *not* contemplate the possibility of *two* photons coalescing to form *one* photon. We considered the case where *two* colliding photons gave rise to *two* other photons. Hence the question as to the creation of *two* photons from *one* and *vice versa* has no relation to our work. Conservation of both momentum and energy can be satisfied in the process we contemplated, but not in the process incorrectly ascribed to us by Dr. Mohler. It is believed that, in order to conserve both momentum and energy in photon-photon collisions, the number of photons must be conserved; certainly a process resulting in one photon will not do.

A. L. HUGHES
G. E. M. JAUNCEY

Washington University,
St. Louis, Missouri,
December 27, 1933.

[1] A. L. Hughes and G. E. M. Jauncey, Phys. Rev. **36**, 773 (1930).

Radiation from the Mutual Annihilation of Protons and Electrons

Sir Arthur Eddington on pages 78 and 79 of *The Expanding Universe* (Macmillan, 1933) says

"So long as they (i.e., free protons and free electrons) are not combined in complex nuclei, protons and electrons are immune from annihilation. The reason for this security is that the photon or quantum of radiation, which results from the annihilation of a proton and electron has to be provided with momentum, which must be balanced by a recoil momentum. But in hydrogen there is nothing left to recoil. Annihilation of a proton and electron (if it ever occurs) can happen only when they form part of a complex system which will leave a residuum to carry the recoil."

Eddington ascribes this argument as to why protons and electrons cannot annihilate each other to Sir Alfred Ewing. The matter was first discussed, however, by Hughes and Jauncey in a letter dated January 4, 1926. This letter appeared in the February 6, 1926 issue of *Nature* and was in criticism of the annihilation hypothesis put forward by J. H. Jeans in a letter in the December 12, 1925 issue of *Nature*. Jeans had calculated the energy of the photon

resulting from a proton-electron collision using the conservation of energy, but disregarding the conservation of momentum. Hughes and Jauncey stated in their letter that any annihilation process must satisfy the following conditions:

(1) Conservation of energy,
(2) Conservation of momentum,
(3) Conservation of charge,
(4) Reversibility of process considered,
(5) Velocities never to exceed that of light.

It was shown that with these conditions to be satisfied it is impossible for a photon to be formed by the mutual annihilation of a proton and an electron, no matter what their velocities or directions of motion may be. In the same letter it was also pointed out that, if we assume microscopic reversibility to hold, there is considerable difficulty in accounting for the reverse of Jeans' process, *viz.*, the disappearance of a photon and the appearance of a proton and an electron. As an alternative to Jeans' suggestion, it was shown that in a collision of two electrons and one proton (or two protons and one electron) giving rise to a photon and an electron (or proton) the above conditions are satisfied. Further comments by Hughes and Jauncey on this matter appeared in an article in the March 15, 1926 issue of the *Proceedings of the National Academy of Sciences* and in an abstract in the April, 1926 issue of the *Physical Review*.

Although our letter calling attention to the difficulties of the simple electron-proton annihilation hypothesis appeared within a few weeks of Jeans' announcement of the hypothesis in 1925, no attention whatever has been paid to it. Various writers discussing the annihilation theory of the origin of high-energy photons have continued to ignore the difficulty of the conservation of momentum until recently, and those who have recently paid attention to the point have completely ignored the fact that the question was raised and discussed rather fully eight years ago by us.

It is interesting to note that just recently Blackett and Occhialini have suggested that a high-energy photon on collision with the nucleus of an atom may give rise to an electron and a positron and a nucleus. This process can be made to satisfy all the conditions listed above.

A. L. HUGHES
G. E. M. JAUNCEY

Washington University,
St. Louis Missouri,
December 27, 1933.

Indications of a Simple Rule Relating Nuclear Resonance Levels with Atomic Number

A study of the entry of alpha-particles into a nucleus which they disintegrate has shown that it occurs in general by two processes: first by penetration through the nuclear potential wall and, second by resonance with a "virtual" energy level inside. In an analysis of the experimental results on the minimum energies which will penetrate by the former process[1] I suggested that this energy, which is directly related to the height of the potential barrier, is a linear function of atomic number for light elements. It appears that a similar rule may hold for the resonance levels. Results are available for Be, B, N, F, Mg, Al[2] which are plotted in Fig. 1 together with the results on minimum penetration level. It will be seen that for the two highest resonance levels the energy rises linearly with the atomic number and that the lines are parallel to the line relating minimum penetration level with the same quantity. It thus appears likely that *the energies of the resonance levels are a linear function of the atomic number*. The experimental accuracy is not as yet very high.

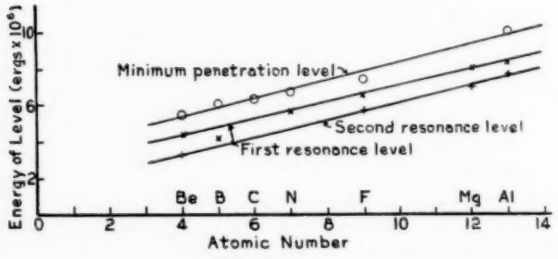

FIG. 1.

Both sodium and phosphorus disintegrate under alpha-particle bombardment with a release of energy. The protons so produced have therefore ranges sufficiently great to permit analysis into groups. Examination of these protons should show the existence of resonance levels at 7.4×10^6 and 6.6×10^6 ergs for sodium and 9.3×10^6 and 8.4×10^6 ergs for phosphorus.

An approximate explanation is suggested as follows: The light nuclei contain equal numbers of neutrons and protons. This can be used to explain the linear relation for the penetration level and it is found that if the attractive force between neutron and proton is represented by a potential of the form

$$V = ke^2/r^p,$$

where r is the distance between them, k is a constant and p is an unknown index, we have an expression

$$V = (2Ze^2/r)\left[1-(2k/r^{p-1})\right].$$

This is the equation representing the potential barrier around the nucleus. The potential V for a given r is proportional to Z, the atomic number. Now the resonance level is one for which the alpha-particle forms a standing wave within the potential barrier of the nucleus. If this

[1] E. Pollard, Phil. Mag. **16**, 1131 (1931).

[2] G. Bernadini, Zeits. f. Physik **85**, 555 (1933); J. Chadwick, Proc. Roy. Soc. **A142**, 5 (1933); E. Pollard, Proc. Roy. Soc. **A141**, 385 (1933); J. Chadwick and J. E. R. Constable, Proc. Roy. Soc. **A135**, 48 (1932); W. Bothe and H. Klarmann, Naturwiss. **35**, 639 (1933).

occurred at a constant radius for all light nuclei then the potential at which it did so would vary with the atomic number as found experimentally. For this to be so, the wave-length of the alpha-particle inside must be, approximately at least, a constant. If E is the potential energy of the alpha-particle inside and V is its kinetic energy of approach, its wave-length is $h/[2m(E+V)]^{\frac{1}{2}}$. Now an inspection of the change of the binding energy of light nuclei as an alpha-particle is added shows that the energy increases in equal increments, of the order of 10^{-7} ergs per alpha-particle.[3] Then, the wave-length of the alpha-particle will change slowly with V and so can be treated as constant for a first analysis, which means that the potential of the level of the standing wave is a linear function of the atomic number.

ERNEST POLLARD

Sloane Laboratory,
Yale University,
January 3, 1934.

[3] See Gamow, *Atomic Nuclei & Radio Activity*, p. 112.

Segregation of Polonium in a Bismuth Crystal

The magnetic properties of bismuth crystals and their variation with amount and kind of impurity are explained by Goetz and Focke[1] on the following assumptions: (1) That the abnormal ("crystal") diamagnetism of Bi is due to electrons which move in very large orbits $d \leqq 1\mu$ as suggested by Raman.[2] (2) That a secondary structure, characterized by equidistant π planes, postulated by Zwicky[3] for heteropolar crystals is also present in metals. (3) That those impurities which form limited solid solutions in bismuth enter only these π planes when the impurity is present in very small amounts. Two cases may be distinguished in Bi: (a) Metals of sub-group IV b which have one valency electron less than Bi (sub-group V b), such as Pb, Sn, Ge, enter a set of π planes which are steeply inclined to the (111) planes. (b) Metals of sub-group VI b which have one valency electron more than Bi, such as Te, Se, enter (111) π planes.

While these three assumptions explain the results very well, not one of them has been accepted as anything better than a questionable hypothesis. A very fortunate set of coincidences permits an excellent test of assumptions 2 and 3(b). The last member of the sub-group VI b is polonium, a radioactive element which disintegrates to lead with the emission of an α-particle of range 3.8 cm (air) or 13μ (Bi). According to Goetz[4] the distance between the (111) π planes of Bi is 0.4μ, thus if a crystal containing Po is cleaved on (111) and the Po is confined to (111) π planes, α-particles from some 30 planes should be able to emerge from the cleavage surface. After leaving the surface the α-particle would travel a distance in air dependent upon the depth of the layer from which it came. If then the number of α-particles per unit of time can be determined as a function of the distance from the point of observation to the crystal face, this number should be a discontinuous function. It should increase suddenly whenever the distance from point to crystal is decreased by the air equivalent of one Zwicky block.

To test this prediction a crystal infected with Po while molten, was cleaved parallel to the (111) planes. The cleavage face was then placed in a closed chamber 3.8 cm from a mica window (2.5 cm air equivalent). By varying the air pressure in the chamber the effective distance from the crystal to the counting device outside the window could be varied. One millimeter air equivalent corresponded to a change of pressure of 2 cm Hg. A Geiger counter placed before the window provided the means of counting the α-particles which came through. Counts were taken for pressure steps of one cm Hg and the curve given in Fig. 1

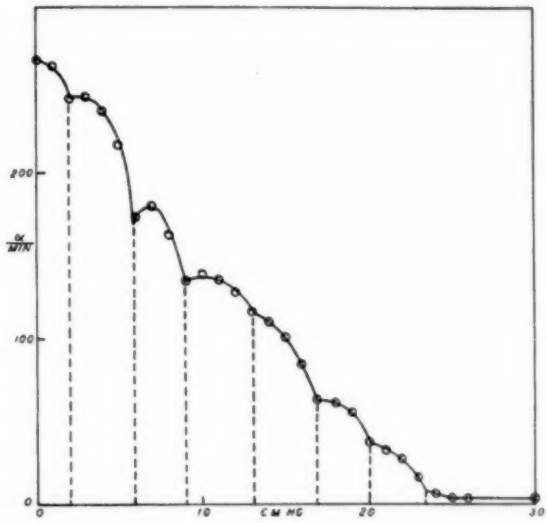

FIG. 1.

was obtained. The rounding of the steps may be explained in either or both of two ways; first, the α-particles straggle to some extent so that all do not have exactly the same range, and second, some Ra E may have been introduced into the bismuth along with the polonium. As Ra E is an isotope of Bi it would be free to occupy any point of the Bi lattice whence it could not depart at room temperature after disintegration to polonium. This uniformly distributed polonium would contribute a linear component to the observed number-distance curve.

In spite of these two difficulties the curve gives good evidence for the existence of relatively thin layers of polonium parallel to the (111) plane separated by a distance

[1] A. Goetz and A. B. Focke, Phys. Rev. **45**, 170 (1934).
[2] C. V. Raman, Nature **123**, 945; **124**, 412 (1929).
[3] F. Zwicky, Proc. Nat. Acad. Sci. **16**, 211 (1930).
[4] A. Goetz, Proc. Nat. Acad. Sci. **16**, 99 (1930).

of $0.6\pm0.1\mu$. This spacing is in good agreement with the spacing 0.4μ, quoted above. Thus this experiment gives independent support for assumptions 2 and 3(b). The work is being continued in an effort to get deeper into the crystal and to find out whether the spacing depends upon conditions of preparation.

I wish to express my thanks to Professor A. F. Kovarik for supplying the polonium; to Dr. E. C. Pollard for his many helpful suggestions; and to Dr. D. Cooksey for the use of the amplifier used with the Geiger counter.

ALFRED B. FOCKE*

Sloane Physics Laboratory,
Yale University,
January 3, 1934.

* National Research Fellow.

The Emission of Protons and Neutrons from Various Targets Bombarded by Three Million Volt Deutons

Continuing experiments reported in these columns,[1, 2] we have found that many substances under bombardment by 3 million volt deutons emit large numbers of neutrons and protons. We had found earlier[2] in confirmation of the observations of Lauritsen, Crane and Soltan,[3] that with 1.3 million volt deutons the yield of neutrons from Be and Li was far greater than that from other elements: for example, a hundred times as many from Be as from NH_4NO_3. Although at 3 million volts the neutron yields are higher for the lighter elements, the variation with atomic number is now very much less. Thus the observed yields from various targets on a relative scale are roughly:

Be—100	NH_4NO_3—10
Li—62	Al—10
B_2O_3—34	$Ca(OH)_2$—8
CaF_2—18	Pt—1

In the case of Be we counted about 5000 recoil protons per minute, corresponding presumably, as estimated from the geometry of the apparatus, to the emission of about 10^7 neutrons per second. Even the neutron emission from Pt, the least of all, was great enough to produce 40 observable recoil protons in the ionization chamber per minute. These very high neutron yields obtained with a deuton current of only $3(10^{-8})$ amp. indicate that it is quite possible to produce neutron radiation in the laboratory with an intensity comparable with that of x-rays.

We have observed also from these targets the emission of protons in large numbers. In most cases the majority of the protons have a continuous distribution in range extending to about 40 centimeters air equivalent.*

The proton yields from the various targets were found to be roughly proportional to the neutron yields, suggesting that the neutrons and protons were involved in the same nuclear reaction. Again it seems that the process is the disintegration of the deuton itself. The observed ranges of the protons agree well with this hypothesis, if the mass of the neutron is about unity.

We have obtained evidence of groups of protons of definite range from some of the substances bombarded. Al, for example, emits, in addition to protons that we ascribe to deuton disintegration, a group having a range of about 68 cm. These might well be the result of the reaction of the deutons with Al nuclei wherein neutrons are added to the Al nuclei and protons are emitted.

Oliphant, Kinsey and Rutherford[4] have shown that alpha-particles distributed in range continuously to 8.3 cm are emitted from Li under deuton bombardment. They attribute them to the reaction of the deuton with Li^7 to form two alpha-particles and a neutron. We investigated the possibility that an appreciable portion of the neutrons observed from Li in the present experiments resulted from this reaction, by comparing the number of recoil protons (produced by the neutrons) with the number of long range alpha-particles. We observed 1/6 as many recoil protons as long range alphas, a ratio so large as, it would seem, to rule out this reaction as accountable for the neutrons observed.

This investigation has been aided by a grant from the Josiah Macy, Jr., Foundation. We wish to thank also Professor G. N. Lewis for furnishing deuterium and Commander T. Lucci for his invaluable assistance.

ERNEST O. LAWRENCE
M. STANLEY LIVINGSTON

Radiation Laboratory,
Department of Physics,
University of California,
January 3, 1934.

[1] Lawrence, Livingston and Lewis, Phys. Rev. **44**, 56 (1933).

[2] Livingston, Henderson and Lawrence, Phys. Rev. **44**, 782 (1933).

[3] Lauritsen, Crane and Soltan, Comptes Rendus **197**, 639 (1933).

* In the earlier communication we reported protons with ranges of 33 cm, but with higher bombarding currents we find that the continuous range distribution extends somewhat beyond this value.

[4] Oliphant, Kinsey and Rutherford, Proc. Roy. Soc. **A141**, 722 (1933).

A High-Intensity Mass-Spectrometer

For the last eight years experiments have been going on in this laboratory to perfect a magnetic lens by which all positive ions of one mass emitted from a source of large area can be brought to a focus on a narrow slit. In 1932 a satisfactory lens of this type was completed. In this arrangement the parallel beam of ions, previously accelerated in an electric field and having a cross section 6 mm wide and 20 cm long, passes through the uniform

magnetic field existing between the plane faces, 6 mm apart, of the pole pieces of an electromagnet. The incident edge of the pole pieces was given a convex circular curvature and the emergent edge a concave circular curvature. The circles contained correction for the bulging of the magnetic field at the edges. The abberation at the focus due to defects in the lens is less than the spread due to other causes, such as the thermal velocities normal to the electric field.

The objective being great intensity of positive ion current, a source of ions was developed to this end. To attain a high accelerating field so that space charge should not limit emission, a source, without grids, was designed to concentrate, in the absence of space charge, the whole emission from a concave surface 3 cm wide into a parallel beam 6 mm wide. Appreciable space charge diverges the beam from this source, but it has been possible partially to remedy this defect by empirical modifications.

By last summer it was possible to bring to the receiving slit a current of 0.1 milliampere of K^{39} ions. This current was space charge limited, represented nearly 20 percent of the total emission, and could be maintained for about 20 hours. The resolving power is adequate for elements such as lithium, but is susceptible to some improvement.

References to this apparatus will probably be appearing in the literature shortly since we have already supplied one-microgram samples of Li^6 and Li^7 to several workers on atomic disintegration, for which reason it seems advisable to publish this note. A complete description of the apparatus should appear in the next six months. A similar instrument embodying some refinements is under construction at the Bartol Research Foundation.

W. R. SMYTHE
L. H. RUMBAUGH*
S. S. WEST

California Institute of Technology,
January 6, 1934.

* Now National Research Fellow, Bartol Research Foundation of the Franklin Institute.

"Doublet" Intervals for $H^1\alpha$ and $H^2\alpha$

The "doublet" structure of $H^1\alpha$ and $H^2\alpha$ has been examined by use of large-scale microphotometer records of interferometer patterns photographed on very fine-grained plates.[1, 2] The interval between *intensity peaks* of each "doublet" has been measured, and for this interval an average value of 0.304 cm^{-1} for $H^1\alpha$ and 0.317 cm^{-1} for $H^2\alpha$ has been obtained. With the half-line-width found from our analysis of the complex structure, theory predicts a value of about 0.323 cm^{-1} for this interval in the case of $H^1\alpha$, thus indicating a discrepancy between experiment and theory of about 6 percent. Similar theory applied to $H^2\alpha$ shows a discrepancy of about 2 percent. Unequal shifts of the $2s\,^2S_{1/2}$ levels for the two isotopes probably accounts chiefly for these differential discrepancies with theory, and these results support our reasons for choosing only the $2p\,^2P_{3/2}-3d\,^2D_{5/2}$ transition in the e/m computation.[2] The spread of the $H^2\alpha$ measurements was somewhat less than that for $H^1\alpha$. These preliminary results will be checked by further measurements.

Houston and Hsieh[3] have reported similar discrepancies for the first five members of the Balmer series of H^1. Spedding, Shane and Grace,[4] according to the interpretation of their report by Kemble and Present,[5] found somewhat smaller discrepancies between their measurements and theory for both $H^1\alpha$ and $H^2\alpha$. However, since they do not explicitly state that their findings in this connection apply to both isotopes, we think they may have given fine-structure-constant results for $H^2\alpha$ only. If so, there would be no serious disagreement between their results and ours.

Fine-structure analyses of the intensity curves indicate that the difference between the $H^1\alpha$ and $H^2\alpha$ "doublet" intervals cannot be ascribed merely to differences in the relative intensities of the components of the "doublets." A more detailed discussion of the general subject of $H^1\alpha$ and $H^2\alpha$ fine-structure will be reported in a later paper.

R. C. GIBBS
R. C. WILLIAMS

Department of Physics,
Cornell University,
January 6, 1934.

[1] Williams and Gibbs, Phys. Rev. **44**, 325 (1933).
[2] Gibbs and Williams, Phys. Rev. **44**, 1029 (1933).
[3] Houston and Hsieh, Bull. Am. Phys. Soc. **8**, 5 (1933).
[4] Spedding, Shane and Grace, Phys. Rev. **44**, 58 (1933).
[5] Kemble and Present, Phys. Rev. **44**, 1031 (1933).

The Infrared Absorption Spectrum of Water, Containing Protium and Deuterium

It has been shown[1] that absorption bands of ordinary distilled water occur at the approximate wave-lengths 1.5μ, 2μ, 3μ, 4.8μ and 6.2μ. Of these, the 3μ and 6.2μ bands are very pronounced. The 4.8μ band is weak.

When water of deuterium content 56 percent (manufacturer's value) was used as the absorbing material, the bands at 3μ and 6.2μ were reduced considerably, and the band at 4.8μ practically disappeared. New strong absorption bands appeared at approximately 4.2μ and 6.9μ. The absorption curves in Fig. 1 show the results of readings taken at intervals of 30 seconds on a Leiss spectrometer.

The band at 4.2μ is due, probably, to the combinations

[1] Schaefer and Matossi; Coblentz; Lecomte.

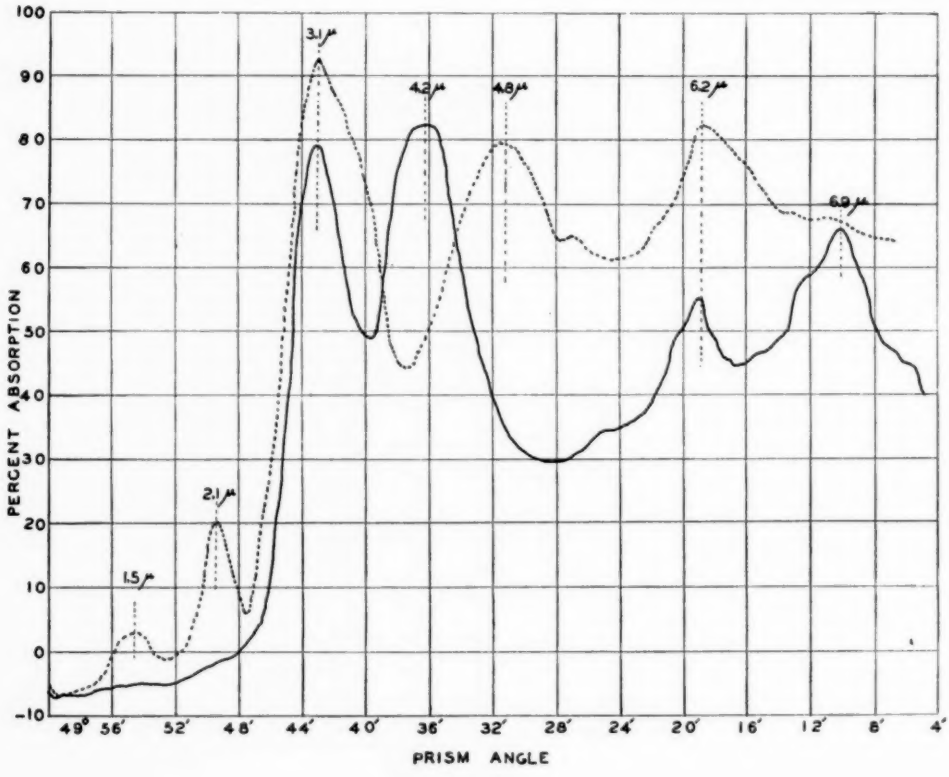

FIG. 1.

$H^2 \longleftrightarrow H^2$ and $O^{16} \longleftrightarrow H^2$. The band at 6.9$\mu$ should be due to a $H^1 \longleftrightarrow H^2$ combination and the indication of a band on the short wave-length side of the 6.9μ band should be due to a $H^2 \longleftrightarrow H^2$ combination, which, preliminary computations show, should produce absorption at about 6.76μ.

The absorption cell used for the heavy water (solid curve) was considerably thinner than the cell used for the ordinary water (dotted curve). This may account for the apparent absence of the 4.8μ band in the heavy water curve.

Further intensive study of this work is being made at this University. A full report will be given in the near future.

A. L. CASSELMAN

University of Cincinnati,
Department of Physics,
Cincinnati, Ohio,
January 11, 1934.

Ultraviolet Bands of Beryllium Chloride

A band system lying in the near ultraviolet region of the spectrum (3468–3700A) has been obtained by using a beryllium arc in an atmosphere of chlorine. The spectrum is quite intense and plates have been obtained in the first four orders of the twenty-one foot grating at Ryerson Physical Laboratory, University of Chicago.

The bands degrade to the red and follow a very narrow Condon parabola as do the beryllium fluoride bands. Only the -1, 0, $+1$ sequences show measurable heads but the $+2$ and -2 sequences are present but are too weak for measuring.

The system is undoubtedly due to a $^2\Pi \rightarrow {}^2\Sigma$ electronic transition. Four heads, ${}^sR_{21}$, R_2, R_1 and Q_1, are located in each band but it is quite impossible to calculate the vibrational constants from the heads because of their large distance from the origin. The electronic separation is about the same order of magnitude as the distance between, ${}^sR_{21} - R_2$, heads. Since this causes the heads of the various branches to overlap, there may be some uncertainty in our present assignments.

The isotope effect, however, appears to be the guide in making the correct selection of heads. On the second and third order plates, the isotope shift of the various heads in the $+1$ sequence shows that they may be separated into two groups with isotope shifts of about 4.3 and 3.8 cm^{-1}. This difference can be interpreted as due to the rotational isotope effect of a head turning somewhat near the origin and one turning at a high J value. The difference of 0.5 cm^{-1} corresponds roughly to rotational displacements of 50 cm^{-1} which is approximately the spacing between the R_1

and the Q_1 heads. The spacing between the R_2 and Q_1 heads is about 72 cm^{-1} and since the R_2 should turn at a greater distance from the origin than the Q_1 (since $B_2 > B_1$), it can be assumed that the electronic transition cannot be greater than 70 cm^{-1}.

We are making a rotational analysis of the bands from our third and fourth order plates. Where there is not too much overlapping, the lines are very well resolved and the various series of lines can easily be selected. A complete analysis of the rotational structure will be reported later.

W. R. FREDRICKSON
MARTIN E. HOGAN, JR.

Syracuse University,
January 13, 1934.

The Constant in the Compton Equation

At a recent meeting of the Physical Society the writers[1] reported the results of an attempt to make a precision determination of the constant in the Compton equation specifying the wave-length modification of scattered x-rays. According to the simple Compton equation this constant should have the value h/mc. Birge's[2] most probable values of e, h, and e/m lead to the value 0.02415×10^{-8} cm for this constant. The mean experimental value in our investigation using tin $K\beta$ radiation and a graphite scattering block and assuming the simple Compton equation to apply was $(0.02380\pm0.00003)\times10^{-8}$ cm.

It seems to the writers that this discrepancy in values may, to a first approximation, be accounted for by the following simple theory expressible harmoniously with Compton's original corpuscular derivation. Assume that the interaction between the impinging quantum and the scattering electron extends over a time interval Δt and that the electron is held to an atom by a Coulomb binding force whose mean effective value is F during the interaction. If the scattering process is to result in modified radiation the electron must be removed from the atom during the interaction interval Δt. Let mv be the momentum of the electron *after escape* from the atom and let φ be the angle between that momentum and the momentum $F\Delta t$ acquired by the nucleus during the escape of the electron. Then the final momentum relations may be expressed by:

$$(F\Delta t)^2+(mv)^2+2mvF\Delta t\cos\varphi = (h\nu/c)^2+(h\nu'/c)^2-2(h\nu\cdot h\nu'/c^2)\cos\theta, \quad (1)$$

$$(mv)^2+2mvF\Delta t\cos\varphi = 2(h\nu/c)^2(1-\cos\theta). \quad (2)$$

The energy relations may be expressed by:

$$mv^2/2+nF\nu\Delta t\cos\varphi = h\nu-h\nu'. \quad (3)$$

In this equation the relatively very small kinetic energy acquired by the nucleus has been neglected. The second term on the left-hand side represents the binding energy, E, of the scattering electron and n is a numerical term depending upon the manner of variation of v with respect to t.

From Eq. (2) we have:

$$2m(mv^2/2+F\nu\Delta t\cos\varphi) = 2(h\nu/c)^2(1-\cos\theta),$$

$$2m(mv^2/2+nF\nu\Delta t\cos\varphi) = 2(h\nu/c)^2(1-\cos\theta)-(1-n)2mF\nu\Delta t\cos\varphi.$$

Substituting from Eq. (3) we obtain:

$$2m(h\nu-h\nu') = 2(h\nu/c)^2(1-\cos\theta)-(1-n)2mF\nu\Delta t\cos\varphi,$$

$$\frac{\nu-\nu'}{\nu^2} = \frac{h}{mc^2}(1-\cos\theta)-\frac{F\nu\Delta t\cos\varphi}{h\nu^2}(1-n),$$

$$\Delta\lambda = \frac{h}{mc}(1-\cos\theta)-\frac{\lambda^2}{hc}(nF\nu\Delta t\cos\varphi)\frac{1-n}{n},$$

$$\Delta\lambda = \frac{h}{mc}(1-\cos\theta)-\frac{\lambda^2}{hc}\cdot\frac{1-n}{n}\cdot E. \quad (4)$$

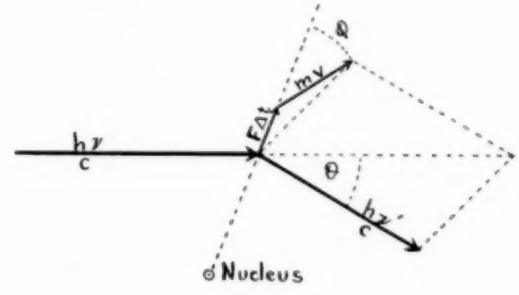

FIG. 1.

To test this equation we might *assume* a uniform acceleration of the scattering electron during expulsion, giving $n=\frac{1}{2}$. By taking E for carbon L as 19.9 volts[3] and by considering 90° scattering of Sn $K\beta$ Eq. (4) gives $\Delta\lambda = 0.02415\times10^{-8}-0.00031\times10^{-8} = 0.02384\times10^{-8}$ cm in good agreement with our experimental value of 0.02380×10^{-8} cm.

Although the adoption of $\frac{1}{2}$ as the value of n is somewhat arbitrary, any value which could reasonably be assumed leads to a departure from the original Compton shift which is of the proper order of magnitude to agree with that which we have observed. We are proceeding to test Eq. (4) for other values of λ and E.

P. A. ROSS
PAUL KIRKPATRICK

Stanford University,
January 13, 1934.

[1] Ross and Kirkpatrick, Bull. Am. Phys. Soc. **8**, No. 6 (1933).
[2] Birge, Phys. Rev. **40**, 319 (1932).
[3] I.C.T. **6**, 68.

The Mass of the Neutron and the Stability of Heavy Hydrogen

The different calculations of the mass of the neutron (n^1) show rather large discrepancies. Chadwick's value[1] 1.0067 was based on the assumed process

$$_5B^{11}+{}_2He^4\rightarrow{}_7N^{14}+{}_0n^1.$$

Curie and Joliot,[2] by bombarding boron with α-particles from polonium, discovered that positive electrons (positrons) were produced in this process, besides neutrons, protons and γ-rays. They assume that not B^{11}, but B^{10}, is transformed and that either a proton or a neutron plus a positron (ϵ^+) are produced.[3] In combining these two possible processes, they find 1.012 for the neutron mass without making use of the different atomic masses besides the proton. They take as mass of the positive electron the same as that of the negative electron (0.0005_5), 0.0045 as the sum of the kinetic energies (k.e.) of neutrons and positrons (in mass units), and 0.0094 as that of the protons. This value corresponds to the largest range (74 cm) of protons observed in this process. If one uses the shorter range (33 cm) corresponding to 0.0054, one gets 1.0076 as neutron mass. An upper limit for this mass, namely 1.0093, can be calculated according to Chadwick[4] from the process

$$_3Li^7+{}_2He^4\rightarrow{}_5B^{10}+{}_0n^1,$$

assuming that the k.e. of the neutrons be zero; it is known to be small (of the order of 0.0005). Dunning and Pegram[5] calculate this mass from the maximum k.e. of the neutrons emitted from a very strong radon-Be source. Assuming that the process is

$$_4Be^9+{}_2He^4\rightarrow{}_6C^{12}+{}_0n^1$$

and that these neutrons are produced by the α-rays of Ra C′, they get 1.0066 as the neutron mass.

Further values can be calculated from the transformation of Li and other nuclei by artificially accelerated H-nuclei, especially in combining the two processes (according to reports from the Cavendish Laboratory):

$$_3Li^7+{}_1H^1\rightarrow 2{}_2He^4+T_1;\quad {}_3Li^7+{}_1H^2\rightarrow 2{}_2He^4+{}_0n^1+T_2.$$

The k.e. of the α-particles produced in the first process T_1 is accurately known:[6] 0.0184. The k.e. of the particles produced in the second process is a little doubtful. According to the assumption of Oliphant, Kinsey and Rutherford,[7] the fastest α-particles observed correspond to the mode that the two α-particles are emitted in opposite directions, the neutron getting no energy. Then $T_2 = 0.01775$, and the neutron mass comes out to be[8] 1.0066, the mass of H^1 and of H^2 being respectively 1.0072 and 2.0131. But the fastest α-particle would be produced if one of them goes off in a direction opposite to that in which the other α-particle and the neutron are emitted, although this mode has a rather small probability. From the equations of conservation of momentum and energy it is easily calculated that in this case T_2 is only nine-tenths of the value mentioned above.[8] The corresponding neutron mass is 1.0083.

A totally different value is calculated by Lawrence, Livingston and Lewis[9] and by Livingston, Henderson and Lawrence[10] from the assumption that the heavy hydrogen isotope H^2, called deuton, when hitting various targets, breaks up into a proton and a neutron. By accelerating the deutons with 1.2 million volts (MV) they always find protons of 18 cm range corresponding to a k.e. of 3.6 MV. They assume that the deuton was disintegrated as a result of nuclear collision with atoms of the various targets and that the proton and the neutron each acquire 2.4 MV from inner energy. They confirm their result in different ways, especially by observing neutrons of the expected yield. From these experiments they calculate the neutron mass as the difference between the masses of the deuton and the proton minus the energy of 4.8 MV released in the disintegration process, and get the value 1.0006, i.e., very near to unity.

So we have the following values today:

1^a 1.0067; 1^b 1.012; 1^c 1.0076 (transformation of B by α-particles
2 1.0093 (upper limit; transformation of Li)
3 1.0066 (transformation of Be)
4^a 1.0066; 4^b 1.0083 (disintegration of Li by H^1 and H^2)
5 1.0006 (disintegration of H^2)

The first four values lie very near to the proton mass, whereas the last one is about 0.006 unit smaller. If it was the right value, one could obviously expect the H^2 nucleus to be unstable, although the natural lifetime was difficult to foresee. Then one could also suppose that the Be nucleus was unstable assuming that it consists of two He-nuclei and one neutron—but it seems to be very stable.[11]

Quite independently of such theoretical considerations, it is rather interesting to see if any radioactivity of the heavy hydrogen can be detected or rather to determine the lower limit of its natural lifetime.

---

[1] Chadwick, Proc. Roy. Soc. **A136**, 692 (1932).

[2] Curie and Joliot, Comptes Rendus **196**, 1885; **197**, 237 (1933).

[3] But it should not be overlooked that the positron could, in this case, also be produced, together with an electron, by internal conversion of a γ-ray emitted by the B-nucleus.

[4] Chadwick, Proc. Roy. Soc. **A142**, 1 (1933) gives the value 1.0070; but the data he uses lead to the value given above. If γ-rays were involved in this process, the neutron mass would come out correspondingly lower.

[5] Dunning and Pegram, Bull. Am. Phys. Soc. Boston Meeting, 1933, No. 54.

[6] Cockcroft and Walton, Proc. Roy. Soc. **A137**, 229 (1932).

[7] Oliphant, Kinsey and Rutherford, Proc. Roy. Soc. **A141**, 722 (1933).

[8] Provided that no γ-rays are involved in this process.

[9] Lawrence, Livingston and Lewis, Phys. Rev. **44**, 56 (1933).

[10] Livingston, Henderson and Lawrence, Phys. Rev. **44**, 781 (1933).

[11] Compare Evans and Henderson, Phys. Rev. **44**, 59 (1933) and others.

For the first experiments I used a Geiger point counter which gave only about 1 stray count in 5 minutes. It was controlled by use of a very weak polonium source of known activity. Recoil protons of a few centimeters range in air could easily be counted. Heavy water (80 percent) in a cup of about 1 cm² surface did certainly not give 0.05 count per minute more than ordinary water.[12] For instance, the mean value of counts per minute over 6 hours was $0.20_5 \pm 0.02$ for heavy and $0.19_4 \pm 0.02$ for ordinary distilled water. If protons of 2.4 MV, corresponding to a range of about 11 cm in air, were given off from H^2, they could penetrate a layer of about 90 microns of water. Then the experiments show that the constant of transformation of H^2 would be: $\lambda < 2 \cdot 10^{-23}$ and its "period" $T > \cdot 10^{15}$ years.[13] An ionization chamber with linear amplifier which can probably detect a hundred times smaller yield will be used in the near future.

Of course such experiments cannot prove that the neutron mass is not so small as Livingston, Henderson and Lawrence assume, but it appears now more improbable that it is so small. Perhaps another explanation for their experiments can be found.

I am much indebted to Professor Hugh S. Taylor and Dr. T. N. Selwood for providing the heavy water and to Mr. J. B. Kuper and Mr. M. B. Sampson for their valuable help in these experiments.

RUDOLF LADENBURG

Palmer Physical Laboratory,
Princeton University,
January 15, 1934.

[12] Professor H. C. Urey and Dr. J. R. Dunning have kindly informed me that they have carried out similar experiments; it is probable that such experiments have also been done elsewhere.

[13] Such a lifetime for a nucleus which emits spontaneously a proton would only be possible, if the potential barrier of a reasonable thickness (5×10^{-13} cm) had a height of some billion volts—provided that the Gurney-Condon-Gamow theory of α-ray disintegration is applicable.

On the Interior Magnetic Field in Iron

In an effort to determine the magnitude of the deflecting field in magnetized iron, the following experiment was recently performed: Beta-rays from radium C ($H\rho = 5900$) were focussed in a field of 1900 gauss, and after passing through 0.36 mm of transformer iron, were registered on a photographic film, 1.53 mm from the latter. Both the iron sheet and the film were parallel to the direction of the field, and normal to the incident beta-rays. To prevent darkening of the film due to the continuous spectrum, and to secondary and scattered beta-rays from the walls of the spectrograph, a sheet of brass 2 mm thick was placed 1.88 mm above the film. A 1 mm slit in this sheet allowed the beta-rays to strike the iron, which was waxed to its lower side, only in a definite line, parallel to the radon tube which was used as the source of beta-rays. The brass sheet was soldered to two pieces of brass, which rested directly on the film. One of these supporting pieces was pierced with a thin slit, through which some of the beta-rays passed to darken the plate in a line parallel to the source. The sharp edge of this line served as a fiducial mark.

Photographs were taken with the apparatus as described, and with an equal thickness of copper in place of the iron. The field was kept constant to within less than one percent with the aid of a ballast lamp. Small variations in the field could not shift the line on the plate, since its position was determined by the stationary slit. Exposures of 110 millicurie hours gave maximum contrast as measured by a Mohl microphotometer. The shape of the microphotometer traces was very nearly the same for the copper and iron photographs, and agreed very well with a curve calculated on the basis of the theory of beta-ray scattering.[1]

If the field in the iron were assumed to be equal to the induction B, which in this case was 17,000 gauss, the point of maximum density on an iron photograph should have been 0.15 mm further from the fiducial mark than the corresponding point on a copper photograph. (The induction was calculated from the magnetization curve of the iron used, after allowing for the demagnetizing effect of the free poles developed at the ends of the sheet,[2] and was later measured with a fluxmeter.) Since it was difficult to locate the maximum point with precision, the shift could be more easily detected at a point 1/3 of the distance down from the peak of the microphotometer trace. Here the trace was quite smooth, and in addition, the expected shift was considerably increased because of the greater distance from iron to film, the inclination of the film to the beta-rays, and the greater path in the iron. 1/3 down on the trace (corresponding to a point on the film 1.2 mm from the center of the line), the expected shift was 0.27 mm. The traces were measured on a comparator equipped with micrometer screws at right angles, and similar curves were plotted with the aid of the readings obtained in this manner. All measurements were made on these enlarged traces ($\times 5$); the shift 1/3 down should have been 0.92 cm. Points on these curves could be reproduced to within 1 mm.

Fig. 1 shows the distance from the mean abscissa of a trace to the fiducial mark, as a function of the half width of the curve at the corresponding ordinate. The curves in this figure are essentially the center lines of the microphotometer traces, corrected for variations in exposure time. Their inclination is due to the "straggling" of the beta-rays by the metal sheets. The dotted lines show the calculated positions of iron curves for various values of the interior field.

The data obtained so far are in definite disagreement with the classical theory of magnetism, which postulates an interior field $= B$. The experimental results indicate that the deflecting field in iron is less than 1/3 of B. This is

[1] Rutherford, Chadwick and Ellis, *Radiations from Radioactive Substances*, 219 (1930).

[2] DuBois, *The Magnetic Circuit*, 34, 41 (1896).

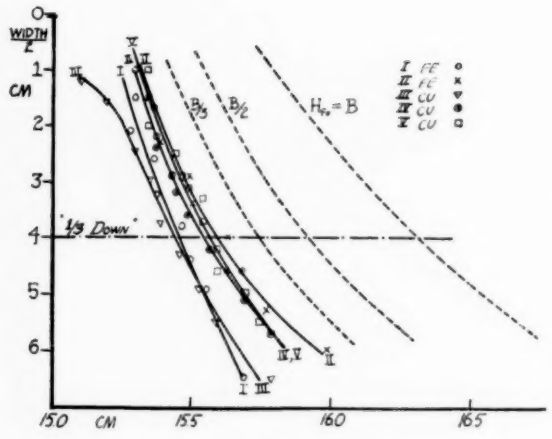

FIG. 1.

consistent with the findings of Mott-Smith,[3] and Rossi,[4] in conjunction with the later work of Curtiss.[5] The data are also in accord with the view that the interior field is equal to the field in a spherical cavity, and not to that in the usually assumed, pill-box shaped cavity. In this case, the equation is $H_{Fe}=(2+\mu)H_{air}/3$.

In the hope of evaluating H_{Fe}, the experiments are being continued, by using a piece of cobalt iron ($B=25{,}000$) and a greater distance from iron to film. The expected shift could also be tripled, and the scattering reduced, by using the beta-rays of thorium C″, a thicker sheet of iron, and a reversal of the induction. In this case, no focussing field would be necessary, since the iron sheet would filter out a nearly homogeneous beam of beta-rays of initial $H\rho=10^4$.

The author expresses with pleasure, his indebtedness to Dr. James Thompson for the loan of several radon tubes, and to Professors A. H. Compton and J. B. Hoag for suggestions and encouragement during the course of the experiment.

LUIS ALVAREZ

University of Chicago,
January 16, 1934.

[3] L. M. Mott-Smith, Phys. Rev. **39**, 403 (1932).
[4] B. Rossi, Nature **128**, 300 (1931).
[5] L. F. Curtiss, Bur. Standards J. Research **9**, 815 (1932).

Disintegration of Beryllium by Deutons

We reported recently[1] that neutrons were produced in large numbers when beryllium was bombarded with deutons having energies between 400,000 and 800,000 electron-volts. This has since been confirmed by Livingston, Henderson and Lawrence,[2] by using deutons of considerably higher energy. In our early measurements of neutrons the ionization chamber was protected by a lead armor 5 cm thick, in order to minimize the effect of other types of radiation. Realizing that nuclear γ-radiation might be produced in the disintegration, we later made provision for reducing the thickness of lead in the direct path of the radiation to $\frac{1}{4}$ inch. With this arrangement we have measured the absorption of the beryllium radiation in lead and in paraffin, using in each case a lead and a paraffin lined ionization chamber. The paraffin lined chamber is more than twice as sensitive to neutrons as the lead lined chamber, and only 0.6 times as sensitive to γ-radiation as the lead lined chamber. Thus by comparing the absorption curves obtained with the two chambers, a mixture of neutrons and γ-rays can be to some extent analyzed.

Four absorption curves, obtained by using the two kinds of absorber and the two chambers, are shown in Fig. 1. Consider first the curves (II and IV) for the lead absorber, at thicknesses greater than 4 cm. The slope is the same for the lead and the paraffin chambers, indicating that the radiation is of a single type, either entirely neutrons or entirely γ-rays. The large displacement of curve II (paraffin chamber) above curve IV (lead chamber) shows clearly that this radiation is neutrons. The slope of curves II and IV, beyond 4 cm absorption is therefore taken to be the absorption coefficient for the neutrons in lead. At thicknesses of absorber less than 4 cm, curve IV shows a steep rise, which clearly indicates the presence of a component of

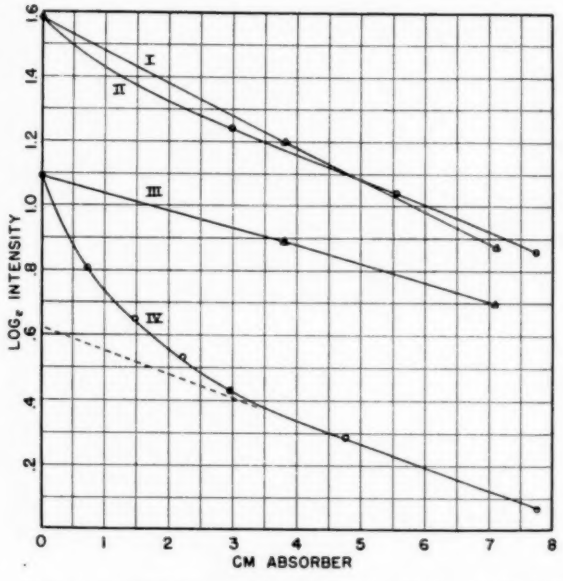

FIG. 1. Absorption of the beryllium radiation. I. Paraffin lined chamber, paraffin absorber; II. Paraffin lined chamber, lead absorber; III. Lead lined chamber, paraffin absorber; IV. Lead lined chamber, lead absorber.

radiation which is much more absorbable than the neutrons, and which is almost entirely screened out by 4 cm of lead. That this component is γ-radiation is indicated by the fact

[1] Crane, Lauritsen and Soltan, Phys. Rev. **44**, 692 (1933).
[2] Livingston, Henderson and Lawrence, Phys. Rev. **44**, 782 (1933).

that it shows up very much more in the lead chamber curve than in the corresponding paraffin chamber curve. By extending the straight part of curve IV backward, as indicated by the dotted line in Fig. 1, we can determine the intensity contributed by neutrons alone, for absorbers less than 4 cm. The difference between the total intensity and the intensity represented by the dotted line should then be just the intensity due to the γ-rays. Since all the curves are on a log scale, the intensity of γ-rays will be the difference between the antilogs of corresponding points on curve IV and the dotted line. The intensity of γ-rays thus obtained, as a function of thickness of absorber, is plotted on a log scale in Fig. 2. An absorption curve for the γ-rays from a radium source made under the same experimental conditions is shown for comparison. The γ-rays from beryllium appear to be monochromatic, and their absorption coefficient is the same as that of radium γ-rays after 1 or 2 cm lead filtration.* Since the strength of the radium source is known, the number of γ-rays emitted from beryllium can be calculated, and it turns out to be equal to the number of neutrons, to well within the accuracy with which we are able to determine the number of neutrons. It is therefore supposed that the neutrons and the γ-rays are produced in the same reaction, namely

$$Be^9+H^2\rightarrow B^{10}+n^1+\gamma.$$

The above measurements were made at 800,000 volts and 2 microamperes deuton current, and under these conditions we find that the number of γ-rays produced is approximately equal to the number emitted by 0.15 milligram of radium. It is interesting to note that the γ-rays observed in the present experiment are, as closely as we can determine, of identical hardness with those produced in the disintegration of lithium by protons.[3]

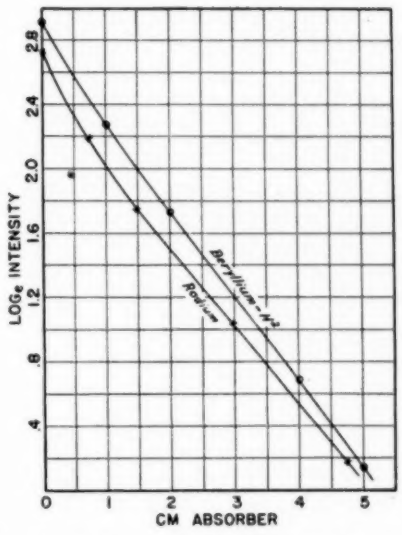

FIG. 2. Absorption curve of the beryllium γ-rays, with an absorption curve of radium γ-rays for comparison.*

We wish again to express our gratitude for support received from the Seeley W. Mudd Fund, which has made this, as our previous experiments, possible.

H. R. CRANE
C. C. LAURITSEN

Kellogg Radiation Laboratory,
California Institute of Technology,
January 17, 1934.

* A telegram from the authors informs me that the ordinate scale for the beryllium curve in Fig. 2 is wrong by a factor of 2. The gamma rays correspond therefore more nearly to 100 million volts than to the gamma rays from radium as stated.—EDITOR.

[3] Lauritsen and Crane, Phys. Rev. **45**, 63 (1934).